[All Theses and Dissertations (ETDs)](#)

January 2009

Coordinate Interstitial Deletions Of Retinoblastoma (Rb1) And Neurobeachin (Nbea) Genes On Chromosome 13 In Mgus And Multiple Myeloma

Julie O'Neal
Washington University in St. Louis

Follow this and additional works at: https://openscholarship.wustl.edu/etd

WASHINGTON UNIVERSITY IN SAINT LOUIS

Division of Biology and Biomedical Sciences
(Molecular and Cellular Biology)

Dissertation Examination Committee:
Michael H. Tomasson (chair)
J. William Harbour
James J. Hsieh
Timothy J. Ley
Daniel C. Link
Anthony J. Muslin
Matthew Walter

COORDINATE INTERSTITIAL DELETIONS OF RETINOBLASTOMA (*RB1)*
AND NEUROBEACHIN (*NBEA)* GENES ON CHROMOSOME 13 IN MGUS AND
MULTIPLE MYELOMA

by

Julie O'Neal

A dissertation presented to the
Graduate School of Arts and Sciences
of Washington University in
partial fulfillment of the
requirements for the degree
of Doctor of Philosophy

August, 2009
Saint Louis, Missouri

My family is amazing. My parents have always promoted education, and without that being instilled in me, I wouldn't be here. The older I get, the luckier I realize I am to have them. In addition to my parents, older bro Tim, older sis Leslie, and twin Linda (Noodle) are great friends, sources of inspiration and support. They have all cooked *many* great meals for us, enjoyed much (probably too much, ha) great wine, and have made our time here so great. I also have great in-laws (lucky me!) who are always encouraging. Luke, my wonderful husband has completely supported and encouraged me during my grad career at WashU, even during these past couple of months from Glasgow, Scotland. There is truly no way I would have made it though graduate school without him.

Table of Contents

Chapter 2- Identification of chromosome 13 genes affected by DNA copy number decrease in plasma cell dyscrasias

Chapter 3- Characterization of Retinoblastoma (*RB1)* in Multiple Myeloma

Figures

Chapter 4

Tables

ABSTRACT OF THE DISSERTATION

Coordinate interstitial deletions of Retinoblastoma (*RB1*) and Neurobeachin
(*NBEA*) genes on chromosome 13 in monoclonal gammopathy of undetermined
significance (MGUS) and multiple myeloma

By

Julie O'Neal

Doctor of Philosophy in Biology and Biomedical Sciences (Molecular and Cellular
Biology)

Washington University in Saint Louis, 2009
Assistant Professor Michael H. Tomasson, Chair

Numeric or structural chromosomal abnormalities are detected in nearly all
patients with plasma cell dyscrasias, including primary amyloidosis, monoclonal
gammopathy of undetermined significance (MGUS) and multiple myeloma (MM).
Chromosome 13 deletions, most frequently monosomy 13, are detected in 10-
20% of MM cases by routine cytogenetics or metaphase fluorescent in situ
hybridization (FISH) and are a significant predictor of shortened survival.
Previous efforts to map somatically acquired DNA copy number losses on
chromosome 13 have been limited by their low resolution. To identify DNA copy
number losses on chromosome 13 at high resolution, we used genomic DNA
isolated from CD138 enriched bone marrow cells (tumor) from twenty patients

with MM, monoclonal gammopathy of undetermined significance (MGUS) or amyloidosis. We used matched skin biopsy (normal) genomic DNA to control for copy number polymorphisms and a novel aCGH array dedicated to chromosome 13 to map somatic DNA gains and losses at unprecedented resolution (>385,000 probes; median probe spacing 60bp). We identified *RB1* and *NBEA* as being coordinately affected by copy number loss in MGUS and MM. To characterize these genes in the context of myeloma biology, we performed sequence and expression analysis on *RB1* and found exonic mutations affecting *RB1* were extremely rare, RB1 levels were decreased in patient samples harboring monosomy 13, and RB1 protein phosphorylation was not common. Expression analysis of NBEA revealed most patient samples harboring monosomy 13 had reduced NBEA, but to our surprise, a subset harbored high levels. Analysis of Nbea in hematopoietic tissues revealed although it was detected in thymus and spleen, using a fetal liver transplantation assay, Nbea was dispensable for hematopoietic development. Future studies investigating cooperation of *RB1* and *NBEA* in plasma cell dyscrasias are warranted.

Chapter 1

Introduction

1.1 Plasma cells are terminally differentiated B cells responsible for antibody production

Plasma cells are terminally differentiated B cells whose function is to produce and secrete antibodies in response to antigen exposure. Their development in adults begins in the bone marrow stemming from the common lymphoid precursor (CLP) that gives rise to mixed B, T and natural killer cell progeny. Primitive B cells undergo regulated changes as they differentiate into mature B cells ready to exit the bone marrow. These changes are marked by cell surface expression of specific proteins representing successful recombination events required for formation of the B cell receptor (BCR).

Antibodies are comprised of two identical heavy chain subunits and two identical light chain subunits. There are two different parts of an antibody that help it function effectively. First, the variable region, comprised of both heavy and light chains, is responsible for antigen recognition. Multiple mechanisms exist to increase the diversity of this region, ensuring maximal affinity for antigen targets. These include introduced mutations during VDJ end joining that occurs early in B cell development, and later, during somatic hypermutation that occurs in germinal centers (discussed below). The second part of an antibody molecule is the constant region, comprised of heavy chains, of which there are five isotypes: $\mu,\alpha,\gamma,\varepsilon,\delta$. These are each responsible for activation of different downstream pathways best suited to trigger effective immune responses.

Antibody production involves DNA rearrangements affecting both heavy and light chain molecules. Their formation marks the different stages of early B cell development in the bone marrow that all occur *before* these cells have 'seen' antigen. Pre/pro-B cells, distinguished from CLPs by expression of B220, have not yet begun DNA rearrangements required for antibody formation. Heavy chains are formed first by recombination of diversity (D) to junction (J) segments, and then the variable (V) segments are recombined to DJ segments. Pro B cells have begun to rearrange their heavy chain loci and upon completion of successful formation of VDJ segments, are now termed early Pre-B cells. Late Pre-B cells are defined by detection of light chain rearrangement. Finally, upon completion of a functional cell surface expressed antibody (the BCR), these cells are now mature B cells ready to exit the bone marrow and home to the secondary lymphoid organs, lymph node and spleen.

There are multiple types of B cells in the spleen including follicular (B2), marginal zone (MZ), and B1, each with different cell surface markers but all with the ability to mature into plasma cells. B2 cells predominate in number compared to the minor types MZ and B1 B cells. The latter two types contribute the first line of antibody-mediated defense, which is rapid, short-lived, and results in production and secretion of low-affinity antibodies. Long-lived plasma cells are mainly derived from the B2 cells [1] that respond to antigens presented by splenic dendritic cells and require CD4 T cells.

B2 cells migrate into Germinal Centers, a zone in the spleen comprised of rapid proliferation, where they mature into centroblasts. They will undergo two DNA modifying events including Somatic hypermutation (SHM) and class-switch recombination (CSR). Both events involve activation-induced cytidine deaminase (AID), the enzyme responsible for deaminating a cytosine residue resulting in a uridine:guanosine (U:G) mismatch. In SHM, this mismatch can be repaired by a variety of mechanisms. First, the uridine can be interpreted as a deoxythymidine, leading to an adenine-thymidine base pair. Alternatively, uracil DNA glycosylase can recognize the uracil, remove it, and then it can be fixed by short patch base excision repair or mismatch repair. The involvement of low fidelity DNA polymerases enhances the chance for mistakes. These events occur within the variable region of antibody only, ultimately leading to generation of B cells with the ability to generate antibody with high affinity for antigen.

CSR also involves AID, which generates double stranded breaks within the 'switch regions' located between the sequences encoding for the different subtypes of heavy chain locus on human chromosome 14. This leads to intrachromosomal deletion recombination and production of transcripts encoding one type of heavy chain. Long lived, post germinal center plasma cells ultimately leave secondary lymphoid organs and home back to bone marrow. Mistakes occurring in the germinal center DNA modifying processes are believed to be responsible for chromosomal abnormalities found in PC diseases, since if breaks are not repaired properly, translocations and mutations occur.

1.2 Multiple Myeloma (MM)

Multiple myeloma (MM) is a malignancy of terminally differentiated bone marrow plasma cells. It is the second most common hematological cancer in the United States, responsible for 2% of all cancer deaths. It accounts for approximately 12,000 deaths a year and remains incurable in most patients. MM (and MGUS-see below) prevalence is twice as high in African Americans than Caucasians [2]. Myeloma incidence progressively increases with age and rarely affects persons under the age of 30 (less than 0.3%) [3]. During the period 2000-2004, in the US the median age of diagnosis of MM was 71 years based on US Surveillance Epidemiology and End Results Programme (SEER).

Myeloma is a progressive tumor with multiple defined stages. Smoldering (asymptomatic) multiple myeloma (SMM) is slow growing and may not progress for months or years. SMM is defined by greater than 10% PCs in the bone marrow and monoclonal protein greater than 3g/dl without end stage damage such as osteolytic bone lesions (**Table 1**). Also asymptomatic, indolent myeloma is similar to SMM, but patients may have mild anemia or a few bone lesions.

Increased numbers of PCs in the bone marrow, renal failure, osteolytic lesions and anemia characterize advanced (symptomatic) myeloma (**Table 1**). These patients are treated immediately with high dose chemotherapy, stem cell transplants and/or other drugs including Thalidomide, Bortezomib, Pamidronate or Zoledronic acid (www.mmrc.com). Myeloma remains an incurable disease,

although patients are living longer due to newer therapies. Identification of MM cells outside the bone marrow cavity (extramedullary) defines aggressive MM (called primary or secondary plasmacytoma depending if prior MM was diagnosed). During this advanced disease, myeloma cells have high rates of proliferation, and it is only during this advanced disease where cell lines have been isolated.

1.3 Monoclonal Gammopathy of Undetermined Significance (MGUS)

Like MM, MGUS is a disease associated with age. It is found in 2% of persons in the general population 50 years of age or older, and ~3% of patients age 70 and older [4]. MGUS is clinically defined by plasma cell percentages within normal range (<10%), but detection of monoclonal antibody in the serum or urine (levels less than 3g/dl; **Table 1**). The risk of developing MM from prior MGUS is ~1%, per year of having MGUS, and most patients die of other causes before ever developing overt MM [4]. Although the total numbers of plasma cells are in the normal range, it is reported that in order to actually detect monoclonal antibody, at least $5X10^9$ clonal cells are required, representing at least 30 cell doublings [5]. MGUS cells therefore at some point undergo cell division, in addition to not being eliminated via apoptosis.

1.4 MGUS likely always precedes MM

MGUS can be (but is not always) detected prior to development of overt myeloma, and, although controversial, is posited to be a "premalignant" tumor. It

is a current interest in the field to determine whether all MM has a prior MGUS phase, since if so, myeloma prevention could ultimately become a reality. The difficulty in determining whether MGUS precedes all MM is the lack of patient data prior to MM diagnosis. Two recent studies provide evidence that MM is always preceded by an MGUS. First, a study presented at the American Society of Hematology Meeting (San Francisco, 2008) [6] analyzed retrospectively, serum samples from active duty service members and found most MM patients had a detected plasma cell serum abnormality up to 2.5 years prior to MM diagnosis. Additionally, a very recent paper [7] examined patients for 1-8+ years via the prostate, lung, colorectal and ovarian screening trial, and found essentially all patients diagnosed with MM had a prior detection of monoclonal antibody. These data suggest MGUS is a preclinical stage and studies to elucidate ways to prevent MM are warranted.

There is much interest in identifying risk factors associated with progression from MGUS to MM. It is known MGUS patients with higher amounts of monoclonal protein at diagnosis, or monoclonal antibody of IgA or IgM (versus IgG) subtype have an increased risk of progression to MM [4]. Abnormal serum kappa/lambda ratio also confers higher risk for MGUS patients [8].

1.5 Primary Amyloidosis

Primary Amyloidosis is a PC disorder characterized by overproduction of immunoglobulin light chains that form insoluble fibril deposits in a variety of organs including heart, kidney, liver, nerves, and/or bowel. This leads to organ

dysfunction and if not treated, median survival of 10-14 months. Amyloidosis PCs have many of the same chromosomal abnormalities detected in MGUS and MM patient samples (discussed below) [9].

1.6 Chromosomal abnormalities in plasma cell dyscrasias

Numeric or structural chromosomal abnormalities are detected in nearly all MGUS and MM patients [10] and can be divided into groups (**Figure 1**) based on chromosome number. About half of MM is hyperdiploid (48-75 chromosomes), characterized by trisomies usually involving chromosomes 3, 5, 7, 9, 11, 15, 19 and 21. Non-hyperdiploid myeloma is comprised of hypodiploid, (<45 chromosomes), pseudodiploid (44-47 chromosomes), or near tetradiploid (75 or more). Near tetraploid appears to be 4N duplications of pseudodiploid or hypodiploid. Therefore, these three groups are usually grouped together as non-hyperdiploid (<45 chromosomes or >75 chromosomes) [11]. This group is distinguished by lack of trisomies, and presence of primary translocations that juxtapose the strong heavy chain enhancers (IgH) located on chromosome 14 with variant partner chromosomes. These translocations are found in a higher percentage of non-hyperdiploid cells (>70%) vs. of hyperdiploid (<40%) of hyperdiploid MM [12]. The breakpoints within the IgH locus occur mostly at switch regions, but can also occur within VDJ sequences. These are thought to be mediated either by errors in switch recombination or somatic hypermutation. Additionally, since these mistakes occur during normal processes during B cell maturation within a germinal center, they are believed to be tumor-initiating events.

Within primary IgH translocations, the IgH locus is translocated to a variety of partner chromosomes at different frequencies (**Table 2**). The two most common translocations are the t(11;14)(q13;q32) and the t(4;14)(q32q23). The t(11;14) correlates with good prognosis, [13, 14] while the t(4;14) predicts poor prognosis [15]. Secondary translocations are detected in patient samples with advanced disease. In contrast to primary translocations, secondary translocations involve the IgH locus less and are structurally complex [12]. One of the common targets of secondary translocations is the *c-MYC* oncogene. In addition to secondary translocations, late-stage MM samples harbor mutations affecting *Ras*, *FGFR3*, and/or *P53*.

1.7 Monoallelic deletion of chromosome 13 is associated with poor prognosis

Monoallelic deletion of chromosome 13 is detected in 30-50% of MGUS and MM. It is associated with reduced patient survival and decreased time to relapse, [11, 15-18] although this association has been complicated by its method of detection. Analysis of monosomy 13 in PC dyscrasias is performed by cytogenetics, metaphase-fluorescent in situ hybridization (M-FISH), interphase FISH (I-FISH), or comparative genomic hybridization (GCH). Cytogenetics and M-FISH require cell proliferation in culture, which is not needed for the latter two analyses. Because of this, up to one third of cytogenetic analyses fail and are uninformative. Consistent with this, higher percentages of chromosomal

abnormalities are found in I-FISH [11].

Multiple reports (using either interphase or metaphase methods) report monosomy 13 is associated with poor survival [11, 15-18]. However, it has become clear that only metaphase (cytogenetics or M-FISH) detected del 13 associates with poor survival [15,16]. This becomes apparent if samples with del 13 by I-FISH *and* M-FISH (or cytogenetics) are separated from those detected by I-FISH only. If the deletion is detected only by I-FISH, the poor survival association goes away [15,16]. These analyses highlight that there is a currently unknown abnormality/factor that confers the ability of these cells to grow in culture, which is contributes to the poor prognosis of those patients.

Monosomy 13 is found both hyperdiploid and non-hyperdiploid samples, but is found in a higher percentage of hypodiploid tumors [16]. Hypodiploid status is associated with reduced patient survival compared to non-hyperdiploid tumors [19]. Cytogenetically detected del 13 confers poor outcome to both hyperdiploid and non- hyperdiploid patients, [20] but the reverse analysis revealed that dividing del 13 patients by ploidy status does not worsen patient outcome [15, 20]. This suggests poor prognosis is determined by monosomy 13.

Monosomy 13 is highly associated with the t(4;14)(q32;q23) translocation, also a predictor of poor patient prognosis [15]. Since almost all t(4;14) positive samples harbor monosomy 13, it is difficult to distinguish which abnormality is the cause

of the poor patient outcome. Monosomy 13 samples that do not have t(4;14) still predict poor outcome.

If monosomy chromosome 13 were directly involved in the progression from MGUS to MM, then one would predict detection of monosomy 13 would be present in a lower percentage of MGUS samples vs. myeloma samples, representing MGUS patients progressing faster to MM. Although reported in limited studies [21], more reports have found this not to be true [17,22]. Instead, the detection of monosomy 13 in MGUS at similar levels to MM supports the conclusion that monosomy 13 is an initiating event in PC transformation.

1.8 Chromosome 13 Mapping Studies

Previous efforts have been made to identify the important tumor- promoting regions on chromosome 13. Mapping studies using comparative genomic hybridization (CGH) analysis with 10Mb resolution identified 13q14-q21 and 13q32-34 as regions on chromosome 13 commonly lost [23-25]. Fluorescent In Situ Hybridization (FISH), which probes for the presence or absence of known sequences, but with better resolution (1Mb) has highlighted similar regions [26-29]. Whole genome array CGH (0.73Mb resolution) combined with gene expression analysis identified *CUL4A* (13q34) as a potentially relevant gene located within a 0.77Mb deletion on chromosome 13 [30]. Single nucleotide polymorphism (SNP) analysis (10Kb resolution) revealed a 1.9Mb minimally deleted region (MDR) in one patient spanning 13q13.3 to q21.3 [31].

The relatively low resolution of these studies has precluded identification of specific genes targeted by chromosome 13 deletions. The focus of this thesis was to indentify genes on chromosome 13 affected by copy number loss in MGUS, amyloidosis and myeloma patient samples. To this end, we employed high resolution aCGH using a novel, custom designed chromosome 13 focused array (Nimblegen) with median probe spacing of 60bp, on DNA isolated from primary CD138 selected cells with patient matched normal controls. We found the retinoblastoma (*RB1*) and neurobeachin (*NBEA*) genes were coordinately affected by copy number decrease in multiple patient samples. The focus of the thesis based on this result has been to characterize these two genes in PC diseases.

1.9 Retinoblastoma (*RB1*) tumor suppressor

Our aCGH analysis (**Chapter 2,** below) identified *RB1* as being coordinately deleted with Neurobeachin (*NBEA)* in multiple patient samples taken from patients with MGUS or MM. *RB1* was the first identified tumor suppressor gene, and is highly studied, as disabling the "RB1 pathway" is believed to be essential for virtually all tumor formation [32]. Mutations in, or deletions of, both copies are causative for development of retinoblastoma tumors in humans. Observations of retinoblastomas led to Knudson's famous "two hit" model of tumor suppressor genes. Knudson observed patients with inherited predisposition to retinoblastoma

and correctly predicted that one defective tumor allele was inherited, and the other was somatically mutated [33].

RB1 is a nuclear phosphoprotein that functions in multiple cellular processes including cell cycle, apoptosis, differentiation, and senescence. Its most well studied function is to inhibit cell cycle, which is regulated by phosphorylation. Hypo-phosphorylated is the "active" form of RB1 that represses transcription of cell cycle-promoting genes in two ways. First, RB1 can directly to bind to the transactivation domain of the E2F transcription factor [34, 35]. Second, while RB1/E2F complexes bind DNA, RB1 can recruit chromatin remodeling enzymes that downregulate gene expression [36-39]. Both events prevent transcription of E2F targets including genes required for replication, DNA metabolism and synthesis, cyclin E, and cyclin A [32, 40].

RB1 has 16 serine/threonine phosphorylation sites whose phosphorylation status changes throughout cell cycle. RB1 gets partially phosphorylated during the cell cycle by cyclin dependent kinase (CDK, CDK4/CDK6) - Cyclin D (and then E) complexes. CDKs require cyclins for active kinase activity. There are two protein families that act to inhibit cyclin/CDK complexes from phosphorylating RB1. First, the INK family (P16^{INK4a}, P15^{INK4b}, P18^{Ink4C}, P19^{Ink4D}) can specifically block the kinase activity of CDKs. Second, the "Cip/Kip" family (p27^{KIP1}, P21^{CIP1} and p57^{Kip2}) can bind to and sequester cyclins from CDKs. Both of these negative

regulators, when intact, prevent phosphorylation (and therefore inactivation) of RB1. Together, these proteins comprise the "RB1 pathway".

1.10 Inactivation of RB1 pathway occurs via mutation, deletion, methylation, or phosphorylation

Inactivation of the RB1 pathway occurs in different ways in a different tumor types. Deletion or mutation of *RB1* is found in retinoblastoma, breast, bone, brain, bladder, and some lung cancers. However, genetic inactivation of *RB1* is not universal to all cancers, including those with heterozygous *RB1* mutations [41]. In many tumors, the remaining RB1 is inactivated post-translationally by phosphorylation. This occurs via deletion, mutation or methylation of the INK4a locus (*CDKN2A*) affecting p16. Alternatively, over-expression of Cyclin D, (which can activate CDK4/6) also results in hyper-phosphorylated RB1. Together, multiple mechanisms inactivate RB1.

1.11 Neurobeachin *(NBEA)* is a BEACH domain containing protein implicated in vesicle trafficking

Neurobeachin (*NBEA, BCL8B*) was identified in our study as being affected by copy number decrease by high-resolution aCGH analysis in plasma cell dyscrasias (**Chapter 2,** below). *NBEA* is a large gene whose genomic sequence spans 730Kb that produces a 9.5Kb transcript encoding a 327KDa protein. It is the largest member of the *BCL8* gene family containing *BCL8A-E* [42]. All members of the family except *NBEA* are pseudogenes or produce sterile

transcripts [42]. It has homologs in mice (*Nbea*), *C elegans* (*Sel-2*), which is shared with *LRBA* [43] and *drosophila* *(rugose*, DAKAP550). NBEA protein encodes multiple domains (**Figure 1),** including a Pleckstrin Homology (PH), BEACH, WD40 and a PKA binding.

NBEA is one of a group of five known mammalian genes containing a highly conserved BEACH (beige and Chediak-Higashi) domain. BEACH domain containing proteins are found in Drosophila melanogaster (six), Caenorhabditis elegans (three), Arabidopsis thaliana (five), Dictyostelium discoideum (six) and Saccharomyces cerevisiae (one).

Homozygous deletions within or upstream of the BEACH domain (leading to truncated proteins) in the Lysosomal Trafficking Regulator gene (*LYST,CHS1*) are found in patients with Chediak-Higashi Syndrome (CHS) [44-46]. This is a rare, autosomal recessive disorder characterized by variable albinism, bleeding tendency, progressive neurologic abnormalities and severe immunodeficiency with lack of natural killer cell activity. The cellular hallmark of CHS is enlarged lysosomal and lysosomal related organelles in almost all granulated cells, [47-49] (suggesting the BEACH domain regulates vesicle size, structure or function [47,49].

Other mammalian BEACH encoding proteins are implicated aspects of vesicle function. LPS-Responsive Vesicle Trafficking, Beach and Anchor containing

15

(*LRBA, BGL, CDC4L*), which like *NBEA*, encodes a Protein kinase A (PKA) binding domain (discussed below) is implicated in vesicle release in polarized cells [50]. Neutral Spingomyelinase Activation Associated Factor (*NSMAF, FAN*) encoding the protein FAN is implicated in TNF signaling and activation of neutral sphingomyelinase. *Nsmaf* deficient mice have slightly enlarged lysosomes [51]. The protein encoded by the WD Repeat and FVYE Domain-containing 3 (*WDFY3, ALFY*) gene binds Phosphoinositol 3 phosphate that regulates endocytic and autophagic trafficking [52]. Finally, *NBEA* is implicated in induced vesicular release at the neuromuscular junction [53, 54].

Crystal structure analysis of the BEACH domain and the 130amino acids N-terminal to it revealed it lies C-terminal to a Pleckstrin Homology domain that is not conserved by sequence, but by structure [55]. The BEACH domain physically interacts with the PH domain, suggesting these two domains function as a single unit [55]. Although PH domains can bind either to fatty acids or proteins, the interaction of the PH domain with the BEACH domain physically blocks the alpha helix known to mediate fatty acid binding, suggesting the PH domain of NBEA mediates protein-protein interactions [55].

1.12 NBEA is a Protein Kinase A (PKA) Anchoring Protein (AKAP)

In addition to the domains discussed above, *NBEA* encodes a PKA binding site. PKA the term used to describe its enzyme complex composed of four regulatory subunits (RIα, RIβ ,RIIα and RIIβ) and two catalytic subunits (Cα and Cβ) with

16

serine/threonine kinase activity that is activated in response to increases in cAMP. Murine Nbea binds to PKA regulatory subunits RIIα (Kd 10nM) and RIIβ (Kd: 30nM) [53]. Mouse and human NBEA are highly conserved within the PKA binding region, and therefore human NBEA is predicted to bind PKA, although this has not yet been shown. Neurobeachin is therefore characterized as an AKAP thought to localize PKA to correct cellular locations. When levels of cAMP increase, PKA signaling only occurs at correct locations, which facilitates appropriate phosphorylation of downstream targets.

1.13 NBEA expression is highest in brain

NBEA transcripts and protein are detected at very high levels in both mouse and human brain [42, 53, 54, our own data]. Lower, but relatively robust transcripts are found in uterus, adrenal gland, ovary, testes, lung and kidney with even lower expression in heart, spleen, stomach, and small intestine [42, 54]. Mice that lack *Nbea* die immediately after birth due to a block in synaptic transmission at the neuromuscular junction, supporting a functional role in the nervous system [54].

1.14 *NBEA* spans the common fragile site, FRA13A

Fragile sites are nonrandom, weak regions of the genome that have mostly been identified *in vitro* by culturing cells in the presence of agents that delay or inhibit replication, such as aphidicolin and then examining metaphase spreads. They have received considerable attention since breaks that result from fragile sites can result in translocations, deletion or gene amplification that may contribute to

cancer development. Common fragile sites are present in virtually all individuals while rare fragile sites are found in less than 5% of the population. There are over 80 common and at least 27 rare common fragile sites in the human genome [56]. Rare fragile sites occur due to mutation of di- or tri-nucleotide repeats and are detected at very low frequency [57], while the specifics of common fragile sites are not completely understood.

NBEA spans the 650Kb common fragile site FRA13A [58]. FISH mapping revealed breaks within 650Kb of NBEA and were detected from intron one to 41, although most breaks (74%) were located in a 245Kb region spanning NBEA exons 34 to 40 [59]. Consistent with other common fragile sites, sequence analysis of the 345Kb region revealed that it is AT rich (65%) and lack the di or tri-nucleotide repeats found in rare fragile sites [58].

The main goal of this thesis project was to identify genes with copy number loss in DNA isolated from purified tumor cells from patient samples with PC dyscrasias. We identified *RB1* and *NBEA* as being coordinately affected by copy number loss (**Chapter 2**). Since we were interested in further characterizing these genes in the context of myeloma biology, we performed sequence and expression analysis on *RB1* (**Chapter 3**), and expression and hematopoietic analysis on *NBEA* (**Chapter 4**). The work presented in this dissertation, as with most scientific endeavors, leaves many questions and avenues to pursue. These are discussed in **Chapter 5**.

1.15 References

1. Fairfax KA, Kallies A, Nutt SL et al. Plasma cell development: from B-cell subsets to long-term survival niches. Seminars in Immunology. 2008; 20:49-58.

2. Landgren O, Gridley G, Turesson I, et al. Risk of monoclonal gammopathy of undetermined significance (MGUS) and subsequent multiple myeloma among African American and white veterans in the United States. Blood. 2006; 107: 904-906.

3. Sirohi B, and Powles R, Epidemiology and outcomes research for MGUS, myeloma and amyloidosis. Eur. J of Cancer. 2006; 42: 1671-83.

4. Kyle RA, Therneau TM, Rajkumar VS. et al. A Long-Term Study of Prognosis in Monoclonal Gammopathy of Undetermined Significance. New England Journal of Medicine 2002; 346: 564-69.

5. Fonseca R., Barlogie B., Bataille R. et al Genetics and Cytogenetics of Multiple Myeloma: A Workshop Report. Cancer Research. 2004; 64: 1546-58.

6. Weiss BM, Verma P, Abadie J, et al. A Pre-Existing Plasma Cell Disorder Occurs in Most Patients with Multiple Myeloma. *Blood* (ASH Annual Meeting Abstracts). 2008; 112: Abstract 1693.

7. Landgren O, Kyle RA, Pfeiffer RM, et al. Monoclonal gammopathy of undetermined significance (MGUS) precedes multiple myeloma: a prospective study.Blood. 2009; epub. Ahead of print.

8. Rajkumar SV, Kyle RA, Terry M, et al. Serum free light chain ratio is an independent risk factor for progression in monoclonal gammopathy of undetermined significance (MGUS). Blood. 2005; 106: 812-817.

9. Harrison, CJ., Mazzullo H., Ross, FM., et al. Translocations of 14q32 and deletions of 13q14 are common chromosomal abnormalities in systemic amyloidosis. British Journal of Haematology. 2002; 117: 427-435.

10. Zandecki M. Multiple Myeloma: Almost all patients are cytogenetically abnormal. British Journal of Hematology. 1996; 94: 217-227.

11. Fonseca R, Barlogie B, Bataille R. et al. Genetics and Cytogenetics of Multiple Myeloma: A Workshop Report. Cancer Research. 2004; 64: 1546-1558.

12. Liebisch P, and Döhner H. Cytogenetics and molecular cytogenetics in multiple myeloma. European Journal of Cancer. 2006; 42: 1520-29.

13. Fonseca R, Blood EA, Oken MM, et al. Myeloma and the t(11;140(q13;q32); evidence for a biologically defined unique subset of patients. Blood 2002, 99:3735-41.

14. Moreau P, Facon T, Leleu X, et al. Recurrent 14q32 translocations determine the prognosis of multiple myeloma, especially in patients receiving intensive chemotherapy. Blood. 2002, 100: 1579-83.

15. Chiecchio L, Protheror RKM, Ibrahim AH. et al. Deletion of chromosome 13 detected by conventional cytogenetics is a critical prognostic factor in myeloma. Leukemia. 2006; 1-8.

16. Shaughnessy J, Jr, Tian E, Sawyer J, et al. Prognostic impact of cytogenetic and interphase fluorescence in situ hybridization-defined chromosome 13 deletion in multiple myeloma: early results of total therapy II. Britosh Journal of Haematology. 2003;120: 44-52.

17. Zojer N, Konisburg R, Ackerman J, et al. Deletion of 13q14 remains an independent adverse prognostic variable in multiple myeloma despite its frequent detection by interphase fluorescence in situ hybridization. Blood. 2000; 95: 1925-30.

18. Shaughnessy J, Jacobson J, and McCoy J. Continuous absence of metaphase-defined cytogenetic abnormalities, especially of chromosome 13 and hypodiploidy, ensures long-term survival in multiple myeloma treated with Total Therapy I: interpretation in the context of global gene expression. Blood. 2003; 101: 3849-56.

19. Chng WJ, Santana-Dávila R, Van Wier SA. et al. Prognostic factors for hyperdiploid-myeloma: effects of chromosome 13 deletions and IgH translocations. Leukemia. 2006; 20: 807-13.

20. Fassas ABT, Spencer T, Sawyer J, et al. Both hypodiploidy and deletion of chromosome 13 independently confer poor prognosis in multiple myeloma. British Journal of Hematology. 2002;118: 1041-47.

21. Avet-Loiseau H, Li JY, Morineau N, Facon T, et al. Monosomy 13 is associated with the transition of monoclonal gammopathy of undetermined significance to multiple myeloma. Blood. 1999; 94: 2583-2589.

22. Konigsberg R, Ackermann J, Kaufmann H, et al. Deletions of chromosome 13q in monoclonal gammopathy of undetermined significance. Leukemia. 2000;14:1975-79.

23. Aalto Y, Nordling S, Kivioja AH, Karaharju et al. Among numerous DNA copy number changes, losses of chromosome 13 are highly recurrent in plasmacytoma. Genes, Chromosomes and Cancer. 1999; 25:104-107.

24. Avet-Loiseau H, Andree-Ashley LE, Moore D, 2nd, et al. Molecular cytogenetic abnormalities in multiple myeloma and plasma cell leukemia measured using comparative genomic hybridization. Genes, Chromosomes and Cancer. 1997;19:124-133.

25. Nomdedeu JF, Lasa A, Ubeda J, et al. Interstitial deletions at the long arm of chromosome 13 may be as common as monosomies in multiple myeloma. A genotypic study. Haematologica. 2002; 87:828-835.

26. Fonseca R, Oken MM, Harrington D, et al. Deletions of chromosome 13 in multiple myeloma identified by interphase FISH usually denote large deletions of the q arm or monosomy. Leukemia. 2001; 15: 981-986.

27. Shaughnessy J, Tian E, Sawyer J, et al. High incidence of chromosome 13 deletion inmultiple myeloma detected by multiprobe interphase FISH. Blood. 2000; 96:1505-11.

28. Elnenaei MO., Hamoudi RA., Swansbury J., et al. Delineation of the minimal region of loss at 13q14 in multiple myeloma. Genes, Chromosomes and Cancer. 2003: 36:99-106.

29. Agnelli L, Bicciato, S, Fabris S, et al. Integrative genomic analysis reveals distinct transcriptional and genetic features associated with chromosome 13 deletion in multiple myeloma. Haematologica. 2007; 92: 56-65.

30. Carrasco DR, Tonon G, Huang Y, et al. High-resolution genomic profiles define distinct clinico-pathogenetic subgroups of multiple myeloma patients. Cancer Cell. 2006; 9: 313-25.

31. Walker BA, Leone PE, Jenner MW, et al. Integration of global SNP-based mapping and expression arrays reveals key regions, mechanisms, and genes important in the pathogenesis of multiple myeloma Blood. 2006; 108: 1733-43.

32. Sherr CJ and McCormick F The RB and P53 pathways in cancer. Cancer Cell. 2002; 2: 103-12.

33. Knudson A. Mutation and cancer: statistical study of retinoblastoma. PNAS. 1971; 68: 820–23.

34. Flemington EK, Speck SH, and Kaelin WJ. E2F-1-mediated transactivation is inhibited by complex formation with the retinoblastoma susceptibility gene product. PNAS. 1993; 90: 6914-18.

35. Helin K, Wu C, Fattaey AR, et al. Heterodimerization of the transcription factors E2F-1 and DP-1 leads to cooperative *trans*-activation. MCB. 1993; 7: 1850-61

36. Weintraub SJ, Chow KNB, Luo RX et al. Mechanisn of active transcriptional repression by the retinoblastoma protein. Nature. 1995; 375: 812-15.

37. Sellers WR, Rodgers JW and Kaelin WG. A potent transrepression domain in the retinoblastoma protein induces a cell cycle arrest when bound to E2F sites. PNAS.1995; 92: 11544-48.

38. Bremner R, Cohen BL, Sopta M et al. Direct Transcriptional repression by pRB and its reversal by specific cyclins. MCB. 1995; 15: 3256-65.

39. Adnane J, Shao Z, and Robbins PD. The retinoblastoma susceptibility gene product represses transcription when directly bound to the promoter. JBC. 1995; 270: 8837-43.

40. Johnson DG. Schwartz JK, Cress WD. et al. Expression of transcription factor E2F1 induces quiescent cells to enter S phase. Nature. 1993; 365: 349-52.

41. Horowitz JM, Park SH, Bogenmann E, et al. Frequent inactivation of the retinoblastoma anti-oncogene is restricted to a subset of human tumor cells. PNAS. 1990; 87: 2775-79.

42. Dyomin V, Chaganti SR, Dyomina K, et al. *BCL8* Is a Novel, Evolutionarily Conserved Human Gene Family Encoding Proteins with Presumptive Protein Kinase A Anchoring Function. Genomics. 2002; 80: 158-65.

43. DeSouza N, Vallier LG, Fares H, et al. SEL-2 SEL-2, the *C. elegans* neurobeachin/LRBA homolog, is a negative regulator of *lin-12/Notch* activity and affects endosomal traffic in polarized epithelial cells. Development. 2007; 134: 691-702.

44. Perou CM, Moore KJ, Nagle DL et al. Identification of the murine *beige* gene by YAC complementation and positional cloning. Nature Genetics. 1996; 13: 303-08.

45. Nagle DL, Karim MA, Woolf EA et al. Identification and mutation analysis of the complete gene for Chediak-Higashi syndrome. Nature Genetics. 1996; 14: 307-11.

46. Certain S, Barrat, F, Pastural E et al. Protein truncation test of LYST reveals heterogeneous mutations in patients with Chediak-Higashi syndrome. Blood. 2000; 95: 979-83.

47. Kaplan J, De Domenico I and Ward DM. Chediak-Higashi syndrome. Current Opinion in Hematology. 2008; 15: 22-29.

48. Westbroek W, Adams D, Huizing M, et al. Cellular defects in Chediak-Higashi Syndrome correlate with the molecular genotype and clinical phenotype. Journal of Investigative Dermatology. 2007; 127: 2674-77.

49. Karim M, Nagle DL, Kandil HH et al. Mutations in the Chediak-Higashi syndrome gene (CHS1) indicate requirement for the complete 3801 amino acid CHS protein. Human Molecular Genetics. 1997; 6: 1087-89.

50. Wang JW, Howson J, Haller E et al. Identification of a novel lipopolysaccharide-inducable gene with key features of both A kinase anchor proteins and chs2/beige proteins. Journal of Immunology. 2001; 166:4586-95.

51. Mohlig H, Mathieu S, Thon L et al. The WD repeat protein FAN regulates lysosome size independent from abnormal downregulation/membrane recruitment of protein kinase C. Exp. Cell Research. 2007; 313: 2703-18.

52. Simonsen A, Birkeland HC, Gillooly DJ et al. Alfy, a novel FYVE-domain-containing protein associated with protein granules and autophagic membranes. Journal of Cell Science. 2004;117: 4239-51.

53. Wang X, Herberg FW, Laue MM et al. Neurobeachin: a protein kinase A anchoring beige/Chediak-higashi protein homolog implicated in neuronal membrane traffic. Journal of Neuroscience. 2000; 20: 8551-65 .

54. Su Y, Balice-Gordon RJ, Hess DM et al. Neurobeachin is essential for neuromuscular synaptic transmission. Journal of Neuroscience 2004; 24: 3627-36.

55. Jogl G, Shen Y, Gebauer D, et al. Crystal structure of the BEACH domain reveals an unusual fold and extensive association with a novel PH domain. EMBO. 2002; 21: 4785-95).

56. Liopoulos D, Guler G, Han SY et al. Roles of FHIT and WWOX fragile genes in cancer. Cancer Letters. 2006; 232:27-37.

57. Sutherland GR. Rare fragile sites. Cytpgenetics Genome Research. 2003; 100: 77-84.

58. Savelyeva L, Sagulenko E, Schmitt JG et al. The neurobeachin gene spans the common fragile site FRA13A. Human Genetics. 2006; 118: 551-8.

1.16 Tables

Table 1 Disease stages of Multiple Myeloma

	MGUS	SMM	Myeloma
% Bone Marrow PC	<10%	>10%	>10%
Monoclonal Protein	< 3g/dl	> 3g/dl	> 3g/dl
Osteolytic Bone Lesions	NO	NO	YES
Anemia	NO	NO	YES
Hypercalcemia	NO	NO	YES
Renal Failure	NO	NO	YES

MGUS: Monoclonal gammopathy of undetermined significance; SMM: Smouldering myeloma

Table 2 Primary Translocations in myeloma

Locus	Incidence	Gene(s) affected
11q13	15-20%	*CYCLIN D1*
4p16.3	15-20%	*FGFR3 MMSET*
16q23	2-10%	*c-MAF*
6p21	3-5%	*CYCLIN D3*
20q11	2%	*MAFB*
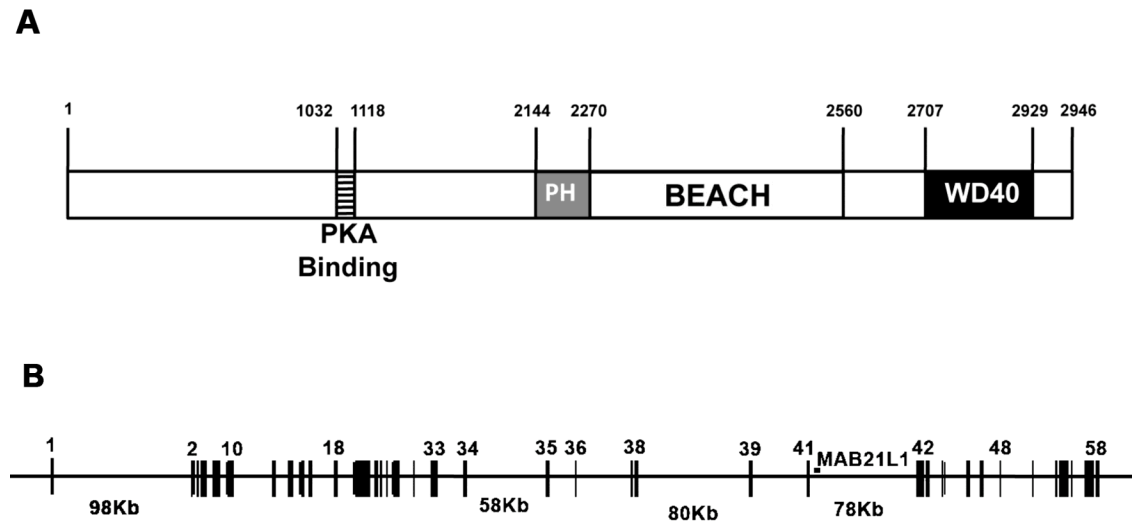
Figure 1

A

B

Figure 1. NBEA protein and exon structure
A. NBEA protein domains. Numbers correspond to amino acids. **B.** NBEA exon structure. Some exons are numbered (top) and sizes of the four largest introns are shown on bottom.

Chapter 2

Identification of chromosome 13 genes affected by DNA copy number decrease in MGUS and MM

2.1 Abstract

Chromosome 13 deletions, detected by metaphase cytogenetics, predict poor outcome in multiple myeloma (MM), but the gene(s) responsible have not been conclusively identified. We sought to identify tumor suppressor genes on chromosome 13 using a novel array comparative genomic hybridization (aCGH) strategy. We identified DNA copy number losses on chromosome 13 using genomic DNA isolated from CD138 enriched bone marrow cells (tumor) from twenty patients with MM, monoclonal gammopathy of undetermined significance (MGUS) or amyloidosis. We used matched skin biopsy (normal control) genomic DNA to internally control for copy number polymorphisms and a novel aCGH array dedicated to chromosome 13 to map somatic DNA gains and losses at unprecedented resolution (>385,000 probes; median probe spacing 60bp). Two distinct minimally deleted regions at 13q14.2 and 13q13 were defined that affected the *RB1* and *NBEA* genes, respectively. *RB1* is a canonical tumor suppressor previously implicated in MM. *NBEA* is implicated in membrane trafficking in neurons, PKA binding, and has no known role in cancer. Non-coding micro RNAs on chromosome 13 were not affected by interstitial deletions. Both the *RB1* and *NBEA* genes were deleted in 40% of cases (8/20; 5 patients with monosomy 13 detected by traditional methods and three patients with interstitial deletions detected by aCGH). Our data suggest further investigation of *RB1* and *NBEA* in MM is warranted.

2.2 Introduction

Chromosomal abnormalities in plasma cell (PC) dyscrasias

Multiple myeloma (MM) is a malignancy of terminally differentiated bone marrow plasma cells. It is the second most common hematological cancer in the United States, responsible for 2% of all cancer deaths. Overt MM can be preceded by Monoclonal Gammopathy of Undetermined Significance (MGUS), a premalignant tumor characterized by an accumulation of clonal plasma cells in the bone marrow. Primary Amyloidosis is a PC disorder characterized by overproduction of immunoglobulin light chains that form insoluble fibril deposits in a variety of organs. Amyloidosis PCs have many of the same chromosomal abnormalities detected in MGUS and MM patient samples [1.]

Numeric or structural chromosomal abnormalities are detected in nearly all MGUS and MM patients [2] and can be divided into two main groups (hyperdiploid and non-hyperdiploid) based on chromosome number. About half of MM is hyperdiploid (48-75 chromosomes), characterized by trisomies usually involving chromosomes 3, 5, 7, 9, 11, 15, 19 and 21. Non-hyperdiploid myeloma is comprised of hypodiploid, (<45 chromosomes), pseudodiploid (44-47 chromosomes), or near tetradiploid (75 or more). Near tetraploid appears to be 4N duplications of pseudodiploid or hypodiploid. Therefore, these latter three groups are usually grouped together as non-hyperdiploid (<45 chromosomes or >75 chromosomes) [3].

Non-hyperdiploid MM is distinguished by lack of trisomies, and presence of primary translocations that juxtapose the strong heavy chain enhancers (IgH) located on chromosome 14 with variant partner chromosomes. The three most common translocations detected are the t(11;14)(q13;q32), t(4;14)(p16.3;q32), and t(14;16)(q32;q23) affecting the *Cyclin D1*, *FGFR3/MMSET* and *c-MAF* genes, respectively. The t(11;14) correlates with good prognosis, [4,5] while the t(4;14) predicts poor prognosis [6]. In disease progression, other genetic events are detected including secondary IgH translocations, c-MYC translocations, and mutations affecting *Ras*, and/or *P53*. Monosomy 13 is found both hyperdiploid and non-hyperdiploid samples, but is found in a higher percentage of hypodiploid tumors [7]. It is detected in 30-50% of MGUS and MM its detection by cytogenetic or M-FISH is a potent predictor of reduced patient survival and decreased time to relapse [6-9].

13q14 and 13q34 are regions previously implicated as affected by copy number decrease in MM

Previous efforts have been made to identify the important tumor- promoting regions on chromosome 13. Mapping studies using comparative genomic hybridization (CGH) analysis with 10Mb resolution identified 13q14-q21 and 13q32-34 as regions on chromosome 13 commonly lost [10-12]. Fluorescent In Situ Hybridization (FISH), which probes for the presence or absence of known sequences, but with better resolution (1Mb) has highlighted similar regions [13-17]. Whole genome array CGH (0.73Mb resolution) combined with gene

expression analysis identified *CUL4A* (13q34) as a potentially relevant gene located within a 0.77Mb deletion on chromosome 13 [18]. Single nucleotide polymorphism (SNP) analysis (10Kb resolution) revealed a 1.9Mb minimally deleted region (MDR) in one patient spanning 13q13.3 to q21.3 [19].

We employed high-resolution array CGH to identify genes on chromosome 13 with DNA copy number loss. Our novel, chromosome 13 array enabled identification of recurring interstitial deletions involving 13q14.2 and 13q13. The high resolution of the array enabled mapping the MDR in 13q14 to exon 20 of *RB1* encoding part of the 'pocket domain' responsible for binding E2F transcription factors [20,21]. All patients with an interstitial deletion affecting *RB1* also harbored a deletion within a novel MM gene, *NBEA* (13q13). Our data suggest that copy number loss of multiple genes on chromosome 13 including *RB1* and *NBEA* could contribute to MM/MGUS biology.

2.3 Methods

2.3A Patients

Human bone marrow samples and skin punch biopsies were obtained during office visits after informed, written consent. Patient identification remained anonymous via use of Unique Patient Numbers (UPN). Cytogenetics and M-FISH were performed in clinic and those data were provided to us.

2.3B Isolation of plasma cells (PC)

Whole bone marrow was subjected to a ficoll gradient (Stem Cell Technologies, Vancouver, BC). Remaining mononuclear cells were stained with human CD138 microbeads and run over an AutoMACS magnetic column on an AutoMACS Cell Separator (Miltenyi Biotec, Aubern, CA). Fluorescence activated cell-sorting analysis using a PE-CD138 human antibody (Miltenyi Biotec, Aubern, CA) confirmed >97% purity (**Figure 1**). CD138+ and skin DNA was isolated using the Qiagen Miniprep Kit (Valencia, CA).

2.3C Array CGH Platform

The first 20 patient samples with ≥500,000 CD138+ cells were selected for aCGH, which required 1.5mg DNA. CD138+ (tumor) DNA was labeled with Cy3 and skin (normal control) DNA was labeled with Cy5. The custom array contained 385,272 oligonucleotide probes. Nimblegen built, and performed probe design and sample hybridization to the custom array (www.Nimblegen.com). Sequence source for the probe design was HG17/UCSC (http://genome.ucsc.edu/).

2.3D Circular Binary Segment (CBS) Analysis

Systematic CBS analysis [22] was performed using Signal Map Software (Nimblegen, Madison, WI). Data was analyzed using a non-overlapping window, which averaged the signal intensity from each probe over a 600bp region. Since probes were spaced approximately every 60bp apart, each window averaged 10 probes. This approach was used to condense the data and provided clean segment breaks. Systematic thresholds were set to eliminate false positives. Criteria for calling segments were: ≥3 data points involved (representing ~30 probes; 1800bp) and $\log_2$ ratio <-0.25. Magnified plots were generated with Graphpad/Prism 4, Version 4.02 (Graphpad Software Inc, San Diego, CA).

2.3E Process Control and whole chromosome plots

Process Control analysis was performed on unaveraged data set (no windows were used to condense data). Data was normalized using qspline [23]. To eliminate outliers, the raw data for the skin (reference, control) samples from each patient was analyzed. Probes with signal intensity >3X SD above the mean were discarded (range: 8,000-17,000, averaged 10,000 per patient (2-4.4% of total). Process control employs techniques using a Shewhart control chart, [24] a graphical and analytical tool used in industry for quality control purposes. It is applied to aCGH analysis to determine which probe intensities are different enough from mean variability to be considered meaningful. Probe intensity ratios were considered "significant" if they satisfied: eight probes *in a row* on one side of the overall mean. They also had to pass *either* A) two of three probes in a row

beyond two units of overall SD, *or* B) four of five points in a row beyond one unit

SD [25,26]. If an eight-probe region (representing   ~480bp) passed the criteria,

the first and last of the eight probes were mapped (~3.8Kb).   Genes were

mapped by aligning probes of interest to the Human Build 36.2 genome. Whole

chromosome plots using this same data set were generated using the program

[R] (**Figure 2A**).

2.3F PCR and sequence analysis of microdeletion

PCR was performed on original un-amplified patient genomic DNA. Control DNA

was kindly provided by Rhonda Ries, Dept. of Medicine, Washington University

School   of   Medicine,   Lab   of   Timothy   Ley   (WUSM)).   Primers:

RBValFWD3:CCATTGCCCACAGTCAGAAA

RBValREV3:GGTAGGGGAATAGGGGGTGA.   Products   were   cloned   into

TOPO2.1 vector (Invitrogen, Carlsbad, CA) and sequenced at the Protein and

Nucleic Acid Core Laboratories, Washington University.

2.3G Real Time PCR

Real time PCR assays were performed on the original, unamplified genomic DNA

isolated from CD138 cells from patient samples using the Taqman Universal

PCR Master Mix.   Primer concentration: 900nM; probe concentration: 2.5mM,

10ng template. Reactions were run on 7300 Real Time PCR System, and

analyzed using 7300 System Software (Applied Biosystems, Foster City, CA).

RBRTFwd1:5'GAATTAGAACATATCATCTGGACCCTTT3'

RBRTRev1:5'GGTCCAAATGCCTGTCTCTCA3'RBExon20Probe:5'56FAMCCA

GCACACCCTGCAGAATGAGTATGAA36-TAMSp3'

Glypican6Fwd:5'TTCTGGTTCGGGCAAACTTG3'

Glypican6Rev:5'GAAGGCGCCACTCAGACTGT3'

Glypican6Probe:5'56FAMCGACCGCAGTTTGCCCAGCG36-TAMSp3'

NBEARTF1:5'AATGGGTTACTACTGAAAACCTAGTGTAAA3'

NBEARTR1:5'TCGCCATCTAGTTTCATCAGTATACAG3'

NBEAProbe:5'56FAMCACAGAAAACTGAAATTGGGAGGCTTATGTGTAA36-

TAMSp3'. The DDCt method was used since control reactions confirmed equal

efficiency of primer/probes. Reactions were performed in triplicate and repeated

three (*RB1*) or two times (*NBEA*).

2.3H I-FISH

I-FISH was performed using standard techniques. Probes: LSI 13/*RB1*, and

CEP7 (Vysis Inc., Downers Grove, IL, USA). For each hybridization, a minimum

of 100 non-overlapping nuclei was analyzed.

2.4 Results

2.4A Patient characteristics

Deletions affecting chromosome 13 occur at similar frequencies in a variety of plasma cell dyscrasias, [3,11,16,27] so patients with the diagnosis of MM, MGUS, or amyloidosis, regardless of chromosome 13 status, were selected for array comparative genomic hybridization (aCGH). Twenty patients were selected solely on the basis bone marrow plasma cell yield after CD138 enrichment (**Table 1, Table 2, Figure 1**). We excluded low-yield samples to avoid the need for whole genome amplification (WGA), which can introduce bias or mutation (personal communication Matthew Walter, 2008). Genomic DNA was isolated from CD138-enriched bone marrow samples (tumor) as well as from patient-matched skin biopsy samples (normal) controls. Patient-matched skin biopsy samples were an important internal control for copy number polymorphisms known to occur in healthy populations [28,29].

To identify DNA copy number alterations across chromosome 13 with the greatest possible resolution, we performed comparative genomic hybridization using a custom CGH array (Nimblegen Inc, Madison, WI) dedicated to chromosome 13. The custom array had 385,272 probes spanning the entire length of chromosome 13 with median probe spacing of 60 base pairs.

2.4B DNA copy number losses identified by circular binary segment analysis

Array CGH data were plotted linearly along chromosome 13 using $\log_2$ tumor: germline signal intensity ratios. By eye, some regions of copy number change were obvious (**Figure 2**), but to systematically identify regions of DNA copy number loss across chromosome 13, we performed two independent, unsupervised analyses of the data. To identify minimally deleted regions (MDRs) across patient samples, we first used a CBS algorithm using stringent criteria to identify interstitial deletions [22].

By CBS analysis, eight of the 20 patient samples (40%) harbored at least one region of interstitial DNA copy number loss with a mean deletion size of 596Kb (range: 1.2Kb to 16Mb, **Table 3**). Among the eight patients with DNA copy number loss, the mean number of deletions was five (range: 1 to 13). The finding of a greater number of chromosome 13 deletions than previously reported using lower resolution techniques [12-14] suggested that our strategy could be useful for finding novel regions on chromosome 13 contributing to plasma cell diseases.

2.4C Array CGH identifies interstitial deletions not detected by FISH or cytogenetics

We compared chromosome 13 status determined by aCGH to analyses of chromosome 13 using standard techniques including metaphase cytogenetics,

metaphase fluorescent in situ hybridization (M-FISH) and interphase fluorescent in situ hybridization (I-FISH; Figure 2). Because the aCGH raw data were normalized to balance fluorochrome intensity, monosomy 13 (i.e. non-interstitial deletions) was undetectable via aCGH analysis. We therefore relied on clinical cytogenetic data for detection on monosomy 13 (Table 1, Figure 2). By cytogenetics, five of the 20 patient samples (25%) had monosomy 13 (Table 1, Figure 2). Additionally, two patients with monosomy 13 (22848 and 92896) also had aCGH-detected DNA copy number losses suggesting homozygous deletion at those loci (Table 3). A 1200bp deletion in patient sample 22848 did not map to known genes or microRNAs at 13q31, while patient sample 92896 harbored two deletions affecting *KATNAL1* and *DNAJC3* genes.

Notably, cytogenetic and FISH analysis failed to detect chromosome 13 DNA copy number loss in 25% of cases (5/20) that were positive by aCGH (Figure 2). This data demonstrates that high-resolution array CGH has the ability to detect chromosome 13 deletions undetected by standard FISH and cytogenetics. This result also highlights the utility of unbiased analysis of the entire chromosome to identify novel regions on chromosome 13 whose copy number changes could direct the study of genes relevant to MGUS and MM pathogenesis.

2.4D Mapping of chromosome 13 genes affected by DNA copy losses
To identify chromosome 13 genes whose loss could contribute to MM pathogenesis, we mapped all known genes that fell within the regions of copy

number loss identified by CBS analysis. We found 28 of 43 (65%) deleted segments mapped to at least one gene, rather than non-coding DNA (Table 3). None of the regions identified in our study mapped either of two micro RNA clusters on chromosome 13 known to undergo deletions or be downregulated in CLL [30]. (miR 15-16 at 13q14 and MiR 17-92 at 13q31.3) were not affected in our samples.

To independently identify genes with copy number loss on chromosome 13, we performed a separate, unsupervised analysis of the data by using an independent Process Control algorithm [24] shown to reliably call aCGH probe signals that deviate significantly from baseline (**Figure 3**). This second analysis identified 216 probes that mapped to 42 genes (**Table 4).** Twenty of the 42 genes (48%) identified by Process Control were also identified by the CBS analysis, underscoring the robustness of the aCGH data set (**Table 3**).

2.4E *RB1* and *NBEA* are recurrent targets of interstitial deletions in MGUS and MM

The region most affected in our patient group encompassed 13q12 to 13q14.3, (25 to 50Mb), **Figure 2**). CBS analysis of the $\log_2$ plots from three of five patient samples with interstitial deletions (58762, 64511, and 95295) revealed two distinct MDRs within 13q12-14.3 (**Figure 2** shaded bars**, Figure 4-5**). Patient sample 95295 harbored two DNA copy number losses that were extremely small (106Kb and 1200bp, respectively) and defined the MDRs at 13q14.2 and 13q13

(**Figure 2, 4-5, Table 3**). Within 13q14.2, only the *RB1* gene was affected in all three patient samples (**Figure 4**). Strikingly, the 13q14.2 MDR mapped to exon 20 of *RB1*, encoding the 'pocket domain' of RB1 critical to its tumor suppressor function [30].

Inspection of the $\log_2$ plots from the same three patient samples revealed each harbored a second and distinct interstitial deletion at 13q13, 13Mb centromeric to the *RB1* locus (**Figure 2, 5**). This second 13q13 MDR mapped to a single gene not previously implicated in myeloma biology: neurobeachin (*NBEA, BCL8B,* **Figure 5**). Every patient sample in our set that harbored a deletion affecting *RB1* (three with interstitial deletions and five with monosomy 13) simultaneously harbored copy number losses affecting the novel myeloma associated gene *NBEA* (**Table 3, Figure 2, 4-5**).

2.4F Confirmation of small interstitial deletion in patient sample 95295 leads to identification of novel *RB1* mutation

Since the segment of DNA copy number decrease within *RB1* in patient 95295 was small (3.49Kb) and contributed significantly to the mapping of the 13q14 MDR, we first performed PCR spanning the microdeletion on the same tumor and skin genomic DNA used in the aCGH analysis (**Figure 4**). Amplification of a truncated band and sequence analysis of the PCR product confirmed this deletion tumor-associated (**Figure 4**). This result confirms the novel micro-deletion affecting *RB1* in patient sample 95295.

To further characterize the small deletion in patient sample 95295, the PCR product was subcloned and sequenced. This revealed the deletion spanned 3486bp total, removing 2813bp of intron 19, all of exon 20, and 527bp of intron 20 (**Figure 5**). Additionally, in the middle of the deletion was an insertion of 435 base pairs identical to another sequence on chromosome 13, 35Kb downstream of the *RB1* locus and situated in the opposite orientation. This inserted sequence encoded a conserved splice acceptor and almost perfect branch sequence. To determine whether splicing into this region, or around this region occurred, we amplified cDNA from this patient sample and performed sequence analysis. We found that the transcript had been spliced from exon19 directly to exon 21, skipping the potential splice acceptor site within the insertion. This transcript revealed deletion of exon 20 that predicts a truncated protein, which we refer to as RB1^{del20}.

Analysis of the RB1^{del20} sequence revealed that splicing from exon 19 to 21 predicts a frame shift, such that there would be 17 unique amino acids followed by a stop codon. Therefore, this transcript is predicted to encode a truncated protein that would have 17 unique amino acids and a loss of 275 3'amino acids, with a predicted total size of about 70kD. Exon 20 encodes part of the 'pocket domain' comprised of the A and B regions, required for binding to E2F.

Some *RB1* mutations are predicted to encode unstable transcripts resulting in no or very little protein expression [31]. We therefore sought to determine whether RB1^{del20} would result in either robust or no protein expression. Both WT full length RB1 and RB1^{del20} were subcloned into the MSCV expression construct, and these DNA's were transfected into 293T cells. We found robust expression of both WT and RB1^{del20} protein (**Figure 5**). A point mutation within RB1, R661W is associated with low-penetrance retinoblastoma and lacks the ability to bind E2F [31]. Since our truncated RB1^{del20} lacks 113 AA of the B domain within the RB Pocket, it is highly unlikely it will retain the ability to actually bind E2F. Together, our aCGH analysis led to the identification of a novel *RB1* mutation, predicting inactive RB1 protein in patient sample 95295.

2.4G Confirmation of interstitial deletions affecting *RB1* and *NBEA* genes

To quantify and confirm the DNA copy loss across all three patient samples with interstitial *RB1* deletions (58762, 64511 and 95295), real time PCR was performed on CD138 purified tumor genomic DNA (**Figure 4**). Consistent with the qualitative PCR, patient sample 95295 had virtually no signal using a primer-probe set at this locus (fold copy number: 0.02). Patient samples 58762 and 64511 had a fold copy number of 0.86 and 0.62, respectively, consistent with loss of one copy of *RB1*. These results are concordant with the aCGH log_2 ratios for this region (average log_2 ratio of probes that span microdeletion: 95295: -0.977; 58762: -0.518; 64511: -0.754).

A similar analysis was used to quantify and confirm the interstitial *NBEA* deletions in patient samples 58762, 64511, and 95295. Consistent with the aCGH data, patient sample 95295 revealed homozygous deletion (fold copy number: 0.14). Patient samples 58762 and 64511 revealed heterozygous loss of *NBE*A (fold copy number: 1.22 and 0.9, respectively; **Figure 6**). These data confirm non-contiguous interstitial deletions on chromosome 13, affecting simultaneously the *NBEA* and *RB1* genes in three of 20 patient samples (15%).

2.4H Whole genome aCGH confirms large deletions detected within patient sample 95295

We were fortunate to have enough DNA from patient samples 95295, which marked both MDR's at 13q13 and 13q14.2. Whole genome aCGH (1.1Kb median probe spacing) analysis was performed on this sample (**Figure 7**) and revealed similar interstitial deletions to those found by the original analysis. The small deletion within *RB1* was undetectable by this analysis, due to the lower resolution, and further highlighting the extremely high resolution of the chromosome 13 novel array. Together, a separate analysis confirms the changes we detected within patient sample 95295.

2.5 Discussion

We used a novel ultra high-resolution aCGH strategy to map somatic chromosome 13 deletions with unprecedented resolution in 20 patients with MM, MGUS or amyloidosis. We used a custom CGH array dedicated solely to chromosome 13 (60bp median probe spacing) and genomic DNA from patient-matched skin biopsy samples as controls to eliminate signal noise due to DNA copy number polymorphisms [28,29].

We avoided noise introduced by whole genome amplification strategies by using non-amplified genomic DNA from cases with high yields of CD138+ bone marrow mononuclear cells. Patients with low bone marrow tumor burden may therefore have been underrepresented in this study. However, analysis by standard techniques of FISH and cytogenetics detected chromosome 13 deletions at expected frequencies [3,6] (**Table 1**) suggesting our patients were generally representative of other MM, MGUS and amyloidosis cohorts. Although our detection of del[13] by I-FISH was lower than other reports, our analysis was performed on non-enriched paraffin embedded bone marrow samples, which likely explains this discrepancy.

We found two regions of recurrent DNA copy number loss that were non-overlapping and mapped to two genes: *RB1*, the canonical tumor suppressor at 13q14.2, and *NBEA* at 13q13, a gene whose role in cancer is less clear. Two independent, unsupervised analyses (CBS and Process Control) generated gene

44

lists affected in our patient set that largely overlapped (**Table 3-4**) demonstrating the high quality of our aCGH data. Both lists included the *RB1* and *NBEA* genes. Visual inspection of $\log_2$ plots at these loci in high-resolution and PCR confirmed the identification of these as *bona fide* deletion events (**Figure 2**, **3-7**; data not shown). Extremely small (homozygous) deletions (3.49Kb and 106Kb) in a single patient (95295) significantly narrowed the MDRs we identified. In sample 95295, *NBEA* and *RB1* were the only two genes on chromosome 13 affected by DNA copy number loss. Re-sequencing analysis of the *RB1* gene within this patient sample revealed only homozygous SNPs (**Chapter 3**) demonstrating isodisomy/gene conversion across all or part of chromosome 13. These data strongly suggest that chromosome 13 DNA copy number decreases in this patient (i.e. *RB1* and/or *NBEA* loci) were selected for during disease development and likely contribute to MM biology.

Because homozygous deletions of *RB1* are rare in MM [15,32], we did consider the possibility that patient sample 95295 might be an outlier. This patient harbored the t(4;14) translocation, and had rapidly progressive disease characterized by treatment resistance (not shown). If the 95295 sample is removed from our analysis, however, our conclusions remain substantially unchanged. Two distinct MDRs are still defined by the remaining interstitial deletions and identify a small number of candidate genes. At 13q13, *NBEA* remains the sole gene affected. Without sample 95295, the MDR at the gene-rich 13q14.2 locus expands to include: *SUCLA2*, *NUDT15*, *MED4*, *ITM2B*, *RB1*,

P2RY5 and *RCBTB2*. In bladder cancer it was found genes nearby to *RB1* (including *ITM2B* and *P2RY5*) contribute to disease [33]. Until further experiments are performed, we cannot formally exclude the possibility that additional 13q14.2 genes contribute to myeloma biology.

Unsurprisingly, use of different window sizes within CBS analysis results in slight differences in chromosome breaks. We chose the 600bp window (avg. signal for ten probes in a row; probes spaced every ~60bp apart) since it provided clean segment breaks and mostly identified region consistent with visual analysis of the data. Both *RB1* and *NBEA* were called by all analyses independent of window size. A 428Kb region 384Kb telomeric to *RB1* within sample 95295 was not called by CBS with the 600bp window, but was called by the 1200 and 3000bp windows. This region affected the *FNDC3A*, *MLNR, RAD17P2* and *CDADC1* genes. Whole genome aCGH performed on sample 95295, also detected this 428Kb region (**Figure 7**) suggesting this is probably a true deletion. Even though these genes were affected by copy loss in patient sample 64511, *RB1* and *NBEA* remain the only genes affected in three patient samples. None of those four genes were found in our microarray analysis of a large, independent patient set to be decreased in samples with monosomy 13 (**Chapter 3**).

The region of copy number decrease detected in patient sample 64511 at 13q14.2 (appears complex as the $\log_2$ ratios vary (**Figure 4**). I-FISH analysis of this patient revealed potentially multiple clones as the copy number of *RB1* was

complex (**Table 2**). Almost 30 percent of the cells were null for both copies of *RB1*, 10.5% had three copies and 9.5% had four copies. Due to this finding, it is not surprising the aCGH results at this locus were varied and suggests this sample is comprised of multiple clones.

Our aCGH identified the novel myeloma associated gene, *NBEA* that was affected by copy number decrease. *NBEA* spans 730Kb and encompasses the FRA13A fragile site [34]. Although common fragile sites are detected in normal cells, some fragile sites are prone to translocations or deletion and are thought to contribute to malignancy via alteration of expression of affected genes. For example, FRA3B (3p14.2) is involved in a translocation detected in renal cancer and affects the Fragile Histidine Triad (*FHIT, FRA3B, AP3Aase)* gene that likely functions as a tumor suppressor [35]. The breakpoints we observed were centromeric to the most fragile FRA13A breakpoint region in *NBEA*, suggesting that the *NBEA* deletion events we observed were not "bystander mutations" and suggest breaks within *NBEA* could have pro- tumor affects (**Chapter 4**).

In addition to *RB1* and *NBEA*, our data reveal a number of genes worth noting. Located on 13q34, *CUL4A* was a gene of interest in the context of our analysis, given previous reports [18] that identified it as a target in MM. *CUL4A* was not identified within the minimally deleted regions we describe here. This does not exclude a potential role for *CUL4A* in MM biology, as MM is a disease with diverse clinical presentations and complex genetics. Our analysis did identify

47

TFDP1 (DP1), also located at 13q34. DP1 is known to heterodimerize with E2F1 [36] and therefore the RB1 pathway may be altered in those patient samples with *TFDP1* deletions. The deletions affecting *RB1* and *TFDP1* were mutually exclusive; patient samples never harbored both, suggesting affecting two different genes in the same pathway could be leading to the same downstream effects. *TFDP1* was not identified in our microarray analysis of genes downregulated in del 13 samples (**Chapter 3**). Further experiments are required to independently confirm the copy loss detected within *TFDP1* and to address its potential functional contribution to myeloma biology.

Finally, there has been a great deal of interest in the microRNAs known to exist on chromosome 13. There are two miRNA clusters on chromosome 13. First, miR-15a and miR-16-1, located at 13q14.3 are deleted or downregulated in lymphocytic leukemia (CLL) patient samples [30]. These miRNA's result in downregulation of the antiapoptotic molecule BCL2; therefore in patient samples with loss of miRNA-15a and miR-16-1 BCL2 is stabilized, leading to tumor cell survival [37]. The other miRNA cluster (miRNA-H1 miRNA-17, miRNA-18, miRNA-19a, miRNA-20, miRNA-19b-1 and miRNA-92-1) is located at 13q31.3 and a recent report indicates this cluster is upregulated MM [36]. None of the deletions we identified overlapped either of these miRNA loci. Our data suggest in our patient samples miRNA's were not targeted by copy number decrease, although since identification of new miRNA's and determining how they are

regulated is still ongoing, it remains a formal possibility they contribute to myeloma biology.

Our data demonstrate for the first time recurring non-contiguous coordinate interstitial deletions affecting the *RB1* and *NBEA* genes on chromosome 13 in myeloma. Examination of larger patient groups will be required to validate the associations we observed, but our data support a multi-gene model to explain the biological effects of chromosome 13 deletions in myeloma. Loss of an entire chromosome might be the simplest mechanism for a myeloma cell to inactivate multiple genes at distinct loci, and provides an attractive explanation for the prevalence of whole chromosome 13 deletions in MM. Our data suggest compound heterozygosity of *RB1* and *NBEA* may contribute to MM/MGUS biology.

2.6 Acknowledgements

2.7 References

1. Harrison, CJ., Mazzullo H., Ross, FM., et al. Translocations of 14q32 and deletions of 13q14 are common chromosomal abnormalities in systemic amyloidosis. British Journal of Haematology. 2002; 117: 427-435.

2. Zandecki M. Multiple Myeloma: Almost all patients are cytogenetically abnormal. British Journal of Hematology. 1996; 94: 217-227.

3. Fonseca R, Barlogie B, Bataille R. et al. Genetics and Cytogenetics of Multiple Myeloma: A Workshop Report. Cancer Research. 2004; 64: 1546-1558.

4. Fonseca R, Blood EA, Oken MM, et al. Myeloma and the t(11;140(q13;q32); evidence for a biologically defined unique subset of patients. Blood 2002, 99:3735-41.

5. Moreau P, Facon T, Leleu X, et al. Recurrent 14q32 translocations determine the prognosis of multiple myeloma, especially in patients receiving intensive chemotherapy. Blood. 2002, 100: 1579-83.

6. Chiecchio L, Protheror RKM, Ibrahim AH. et al. Deletion of chromosome 13 detected by conventional cytogenetics is a critical prognostic factor in myeloma. Leukemia. 2006; 1-8.

7. Shaughnessy J, Jr, Tian E, Sawyer J, et al. Prognostic impact of cytogenetic and interphase fluorescence in situ hybridization-defined chromosome 13 deletion in multiple myeloma: early results of total therapy II. British Journal of Haematology. 2003;120: 44-52.

8. Zojer N, Konisburg R, Ackerman J, et al. Deletion of 13q14 remains an independent adverse prognostic variable in multiple myeloma despite its frequent detection by interphase fluorescence in situ hybridization. Blood. 2000; 95: 1925-30.

9. Shaughnessy J, Jacobson J, and McCoy J. Continuous absence of metaphase-defined cytogenetic abnormalities, especially of chromosome 13 and hypodiploidy, ensures long-term survival in multiple myeloma treated with Total Therapy I: interpretation in the context of global gene expression. Blood. 2003; 101: 3849-56.

10. Nomdedeu, JF, Lasa A, Ueeda J, et al. Interstitial deletions at the long arm of chromosome 13 may be as common as monosomies in multiple myeloma. Haematologica 2002; 87: 828-835.

11. Aalto Y, Nordling S, Kivioja AH, Karaharju E, Elomaa I, Knuutila S. Among numerous DNA copy number changes, losses of chromosome 13 are highly recurrent in plasmacytoma. GenesChromosomes Cancer. 1999; 25:104-107.

12. Avet-Loiseau H, Andree-Ashley LE, Moore D, 2nd, et al. Molecular cytogenetic abnormalities in multiple myeloma and plasma cell leukemia measured using comparative genomic hybridization. Genes Chromosomes Cancer. 1997;19:124-133.

13. Shaughnessey J, Tian E, Sawyer J, et al. High incidence of chromosome 13 deletion in multiple myeloma detected by multiprobe interphase FISH. Blood. 2000; 196: 1505-11.

14. Elenaei MO, Hamoudi RA, Swansbury J, et al. Delineation of the Minimal Region of Loss at 13q14 in Multiple Myeloma. Genes, Chromosomes and Cancer. 2003; 36: 99-106.

15. Fonseca R, Oken, MM., Harrington D, et al. Deletions of chromosome 13 in multiple myeloma usually denote large deletions of the q arm or monosomy. Leukemia. 2001; 15:981-86.

16. Konigsberg R, Ackermann J, Kaufmann H, et al. Deletions of chromosome 13q in monoclonal gammopathy of undetermined significance. Leukemia. 2000;14:1975-1979.

17. Agnelli L, Bicciato, S, Fabris S, et al. Integrative genomic analysis reveals distinct transcriptional and genetic features associated with chromosome 13 deletion in multiple myeloma. Haematologica. 2007; 92: 56-65.

18. Carrasco DR, Tonon G, Huang Y, et al. High-resolution genomic profiles define distinct clinico-pathogenetic subgroups of multiple myeloma patients. Cancer Cell. 2006; 9: 313-325.

19. Walker BA, Leone PE, Jenner MW, et al. Integration of global SNP-based mapping and expression arrays reveals key regions, mechanisms, and genes important in the pathogenesis of multiple myeloma Blood. 2006; 108: 1733-43.

20.Flemington EK, Speck SH, and Kaelin WJ. E2F-1-mediated transactivation is inhibited by complex formation with the retinoblastoma susceptibility gene product. PNAS. 1993; 90: 6914-18.
21. Helin K, Wu C, Fattaey AR, et al. Heterodimerization of the transcription factors E2F-1 and DP-1 leads to cooperative *trans*-activation. MCB. 1993; 7: 1850-61.

22. Venkatraman ES, Olshen AB. A faster circular binary segmentation algorithm for the analysis of array CGH data. Bioinformatics. 2007; 23: 657-663.

23. Workman C, Jensen LJ, Jarmer H, et al. A new non-linear normalization method for reducing variability in DNA microarray experiments. Genome Biol. 2002; 3: 1-16.

24. Li Xia AA, Zhang Z, Walter M et al. Analysis of Comparative Genomic Hybridization Array Data Using Statistical Process Control. 2007;Invited Paper, Submitted.

25. Company WE. Statistical Quality Control Handbook; 1956.

26. Inc SI. SAS Language (version 8); 1999.

27. Harrison CJ, Mazzullo H, Ross FM, et al. Translocations of 14q32 and deletions of 13q14 are common chromosomal abnormalities in systemic amyloidosis. British Journal of Hematology. 2002;117: 427-35.

28. Sebat J, Lakshmi B, Troge J, et al. Large-scale copy number polymorphism in the human genome. Science. 2004; 305: 525-528.

29. Redon R, Ishikawa S, Fitch KR, et al. Global variation in copy number in the human genome. Nature. 2006; 444: 444-54.

30. Cimmino A, Calin GA, Fabbri, et al. MiR-15 and miR-16 induce apoptosis by targeting BCL2. PNAS. 2005; 102: 13944-49.

31. Whitaker LL, Su H, Baskaran R, et al. Growth suppression by an E2F-binding-defective retinoblastoma protein (RB): contribution from the RB pocket. MCB. 1998; 18: 4032-42.

32. Avet-Loiseau H, Daviet A, Saunier S, et al. Chromosome 13 abnormalities in multiple myeloma are mostly monosomy 13. British Journal of Haematology, 2000; 111:1116-17.

33. Lee S. Jeong, J. Majewski T. et al. Forerunner genes contiguous to RB1 contribute to the development of in situ neoplasia. PNAS. 2007; 104: 13732-37.

34. Iyeva L, Sagulenko E, Schmitt JG, et al. The neurobeachin gene spans the common fragile site FRA13A. Hum Genet. 2006; 118: 551-8.

35. Iliopoulos D, Guler G, Han SY, et al. Roles of FHIT and WWOX fragile genes in cancer. Cancer Lett. 2006; 232: 27-36.

36. Helin K, Wu CL, Fattaey AR, et al. Heterodimerization of the transcription factors E2F-1 and DP-1 leads to cooperative trans-activation. Genes and Development. 1993; 7: 1850-61.

37. Pichiorri F, Suh, S, Ladetto, M., et al. MicroRNAs regulate critical genes associated with multiple myeloma pathogenesis. PNAS 2008; 105: 12885-90.

2.9 Figures and Tables

Table 1. Patient Characteristics and chromosome 13 status

UPN	Age	Sex	Disease	M-Ab	Deletion of Chromosome 13		
					Cyto	M- FISH	I- FISH
95295	65	M	MM (IIIa)	IgA κ light	-	-	-
92896	51	F	MM (IIIa)	IgA κ	+	ND	+
68319	75	F	MM (IIIa)	IgA κ	-	ND	-
64511	55	F	MM (IIIa)	IgA κ	-	+	-
66704	50	M	MM (IIa)	IgA κ	ND	ND	-
33172	63	M	MM (IIIa)	IgA κ	+	ND	+
54092	71	M	MM (IIIa)	Free κ Light	-	-	-
492710	58	M	MM	ND	-	-	-
802718	63	F	MM	IgA	-	-	ND
58762	74	M	MGUS	ND	-	-	-
22848	66	F	MM (Ia)	IgG κ	+	+	-
73586	67	F	MM (IIIb)	IgA κ	+	ND	-
86267	48	F	MM (IIa)	IgG κ	-	-	ND
90866	53	M	MM (Ia)	ND	-	ND	-
247748	58	M	MM	IgG κ	-	-	-
45980	56	M	MM (IIa)	IgA κ	-	ND	-
18467	70	M	MM (IIIa)	IgG κ	-	-	-
98461	61	M	MM (IIa)	IgG κ	+	-	-
10901	46	M	Amyloidosis	IgG λ	-	-	-
19367	61	F	MGUS	IgG κ	-	ND	-

UPN refers to Unique Patient Number; M-Ab: Monoclonal Antibody; Cyto: Cytogenetics;
M-FISH: Metaphase FISH; I-FISH: Interphase FISH; κ: kappa; λ: Lambda;
-: no abnormality found; +: abnormality found; ND: No Data

Table 2. Patient Information

UPN	Prior Rx	I-FISH	Metaphase FISH	Cytogenetics
95295	yes	t(4;14) (45%)	normal	46,XY
92896	yes	t(4;14) (60%)	ND	42X,-X,der(1)t(1;14)(p13;q11.2),+8,der(10)t(10;15)(p11.2;q11.1), der(12)t(1;12)(p32;p13),-13,-14,-15,-22,+mar[17]/46,XX[3]
68319	yes[a]	none	17p del(p53 gene), IgH abnormal	47~49,X,-X,der(3)(3;?)(q22;?),+t(3;5)(p14;p13),-4,+7,-8,+der(9)t(8;9)(p22;q21),-10,+11,del(12)(p11.2),?t(14;20)(q32,q11),del(17)(p11.2),+19,+21[cp3]/46,XX[17]
64511	no	none	trisomy 7 (65.5%), tetrasomy 7(9.5%), loss *RB1* both alleles (29.8%), 3 copies *RB1* (10.5%), 4 copies *RB1* (9.5%)	57~61, XX,-X, add(2)(q35),+3,+5,+5,+6,add(6)(q11),+7,-8,+9,+9, add(9)(p24)x2, add(10)(q26),+11,+11,+11, add(13)(p11.2),+15,der(15)t(8;15)(q12;q11.2)x2,-16,+17,+18,+19,+21,der(22)t(1;22)(q12;p11.2),+3-5mar[cp15]/46,XX[5]
66704	ND	ND	ND	ND
33172	yes	none	ND	54,XY,del(1)(p13p36.1),+del(1)(p13p36.1)x2, add(2)(p?21),+6,+7,del(7)(q22q32),add(8)(p23),+12,-13,+15,add(15)(p11.2),-16,add(16)(q23),+19,+21,+2mar]cp5]/46,XY[15]
54092	yes	none	trisomy7 (31%)	52-53,XY,del(1)(p13p32),add(2)(q35),+3,-4,+5,del(5)(q15q22),+7,t(8;19)(p11.1;q13.1),+9,+11,der(14)t(4;14)(q25;q32),+15,+21,+1-2mar[cp8]/52,idem,der(7;10)(q10;q10)[2],46,XY[10]
492710	no	none	normal	46,XY
802718	no	none	normal	46,XX
58762	no	none	normal	45,X,-Y[18]/46,XY[5]
22848	no	t(4;14) (13%)	RB1 del (25.8%), t(4;14) (14.4% cells)	3/22 cells: 48,XX,+9,+12,-13,+15,-18,-20,+2-3 (mar[cp3]/19/22 cells: 46,XX[19]
73586	yes	none	ND	36~42,der(X)t(X;?)(p22.1;q31),-X,der(1)t(1;19)(p13;p13.1),der(2)t(1;2)(q12;q31),t(3;8)(p11;q11),-4,der(6)t(6;15)(q12;q11.2),del(7)(q11.2q22),del(8)(p21),-8,del(11)(q21q23),-12,-13,der(14)t(4;14)(p11;p11),-16,add(17)(p13),-17,-18,der(19)t(7;19)(q21;p13.1),-20,-22,add(22)(q13)[cp8]/46,XX[16]
86267	yes	none	normal	46,XX
90866	yes[b]	none	ND	46,XY
247748	no	none	normal	46,XY[18]/46XY,t(1;12)(p13;q24)[1]/51X,-Y,+1,del(1)(p21),+9,+9,-10,+11,+15,-16,+19,+marr[1]
45980	yes	none	ND	46,XY
18467	no	none	trisomy 7 (19.4% cells)	46,XY
98461	yes[c]	none	trisomy7 (6% cells)	47,-48,X,-Y,+7, del(8)(q21q22), +9, add(12)(p10),-13, +15, -22]cp2]/46,XY[17]/46,X, -Y, add(12)p11 with additional nonclonal abnormalities
10901	ND	none	ND	46,XY
19367	no	none	ND	46,XX

a   Started Dexamethasone
b   *radiation only on R Femur
c   *VAD 8 cycles
I-FISH: t(11;14) and t(4;14) analyzed

Figure 1
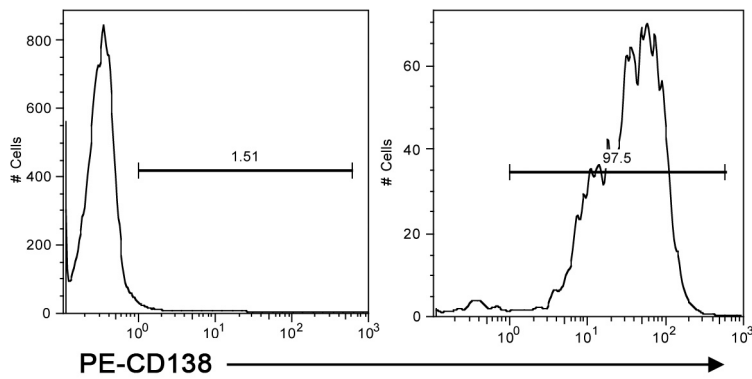
Figure 1. Purity of CD138 Selection from human bone marrow

Shown is FACS analysis of whole bone marrow sample prior to CD138 selection (left) and after selection (right). Samples were stained with human PE-CD138 antibody.

Figure 2
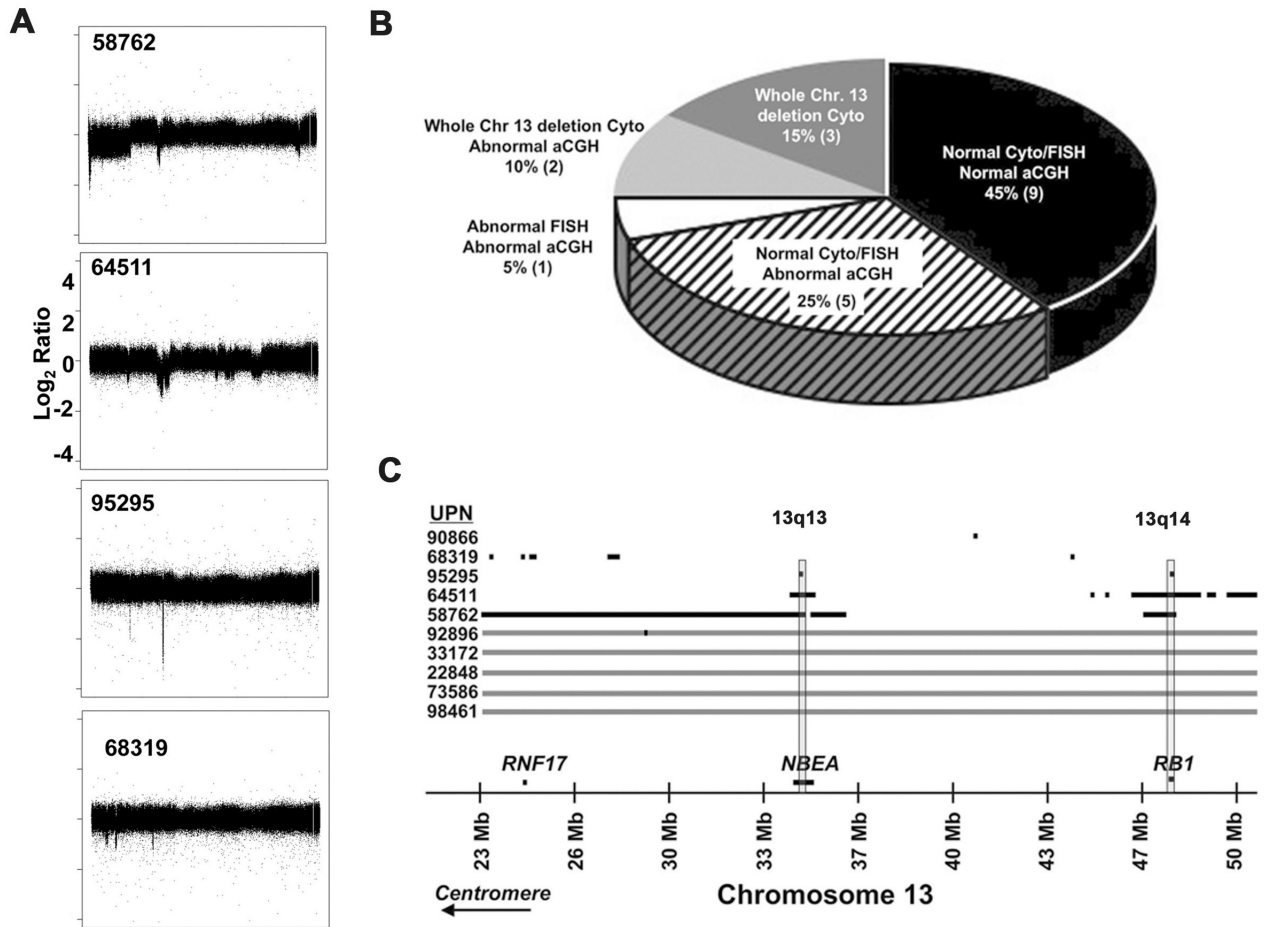
Figure 2. Array CGH identifies DNA copy number loss on chromosome 13 not detected by FISH or cytogenetics

A. Whole chromosome 13 log$_2$ plots of four patients with visually detectable chromosome 13 copy number loss (58762, 64511, 95295 and 68319).   **B**. Pie chart summary of chromosome 13 abnormalities detected by cytogenetics, M-FISH, I FISH and/or aCGH.   Eight patient samples harbored a chromosome 13 abnormality detected by aCGH. Five of these appeared normal by cytogenetic

and FISH analysis. The number of patient samples is indicated in parentheses. **C.** Visual analysis of patients with interstitial deletions revealed by CBS analysis (black lines) within 23 to 50Mb (13q12-13q14.3) on chromosome 13. Figure is to scale except for deletions smaller than 150Kb, which required scaling up to be visualized. Exact sizes of all segments shown are in **Table 2**. Cytogenetic data was used for whole chromosome 13-deletion information (gray lines). Eight patient samples had coordinate copy number loss involving *RB1* and *NBEA* (five patient samples with whole chromosome 13 deletion and three with interstitial deletions) highlighted by vertical rectangles. Patient sample 95295 harbored interstitial deletions affecting only *RB1* and *NBEA* and defined the minimally deleted region across these eight samples. Patient sample 92896 had monosomy chromosome 13 by cytogenetics, but also a region of copy number loss indicated by black spot, suggesting homozygous deletion at that site.

Table 3 Chromosome 13 regions with DNA copy number decrease

UPN	Start	End	Data points	Log$_2$ ratio	Location	Genes
95295	34514100	34620300	77	-0.6743	13q13	*NBEA*
	47930100	47931300	3	-1.4512	13q14.2	*RB1*
64511	33657900	34546500	947	-0.2766	13q13	*NBEA*
	44793300	44824500	39	-0.3671	13q12-14	*TPT1*
	46244100	46247700	5	-0.4766	13q14.1-14.2	*ESD*
	46454100	47760300	1218	-0.4553	13q14.2	*SUCLA2, NUDT15, MED4, ITM2B*
	47760900	48469500	698	-0.7028	13q14.2	*RB1, P2RY5, RCBTB2, CYSLTR2,* ***FNDC3A***
	48470700	48719100	204	-0.3458	13q14.2	***FNDC3A****, RAD17P2, MLNR*
	48719700	48892500	186	-0.6435	13q14.2	*CDADC1,* ***CAB39L***
	49647300	49967100	369	-0.4726	13q14.3	
	49968900	51534300	1800	-0.439	13q14.2-14.3	*DLEU7, INTS6,* ***WDFY2****, ATP7B, UTP14C*
58762	18242100	18255300	7	-0.5696	13q11	
	18401700	18412500	15	-1.017	13q11-12.11	
	18413100	18437700	34	-0.4102	13q12.11	
	18438300	18495900	62		13q12.11	
	18497700	34566900	17376	-0.3127	13q12.11-13	*TUBA3C, TPTE2, MPHOSPHO8, PSPC1, ZMYM5, ZMYM2, GJA3, GJB2, GJB6, CRYL1, FFT88, IL17D,* ***XPO4****, LATS2, SAP18, C13ORF3, MRP63, FGF9, SGCG,* ***SACS****, TNFRSF19,* ***MIPEP****, SPATA13, PARP4, ATP12A,* ***RNF17****,* ***CENPJ****, PABPC3, MTMR6, NUPL1, ATP8A2, RNF6, CDK8, WASF3,GPR12,* ***USP12****, RPL21, RASL11A, GTF3A, MTIF3, LNX2, DOLR1D, GSX1, PDX1, CDX2, FLT3, PAN3, FLT1, POMP, SLC7A1,* ***UBL3****, KATNAL1, HMGB1, VSPL1, ALOX5AP, HSPH1,* ***B3GALTL****,* ***RXFP2****, BRCA2, PFAAP5, PDS5B,* ***KL****, STARD13,RFC3,* ***NBEA***
	34605900	35860500	1378	-0.2939	13q13-13.3	***NBEA****, MAB21L1,* ***DCLK1****, SPG20*
	46973700	48119100	1051	-0.4193	13q14.2-14.3	***SUCLA2****, NUDT15, MED4 ,* ***ITM2B****,* ***RB1****, P2RY5,* ***RCBTB2***
	106593300	107048700	554	-0.3385	13q33.3	
	107112900	107145300	43	-0.283	13q33.3	
68319	23969100	24009300	43	-0.4901	13q12.12	
	24009900	24039900	30	-0.3091	13q12.12	*PARP4*
	24250500	24406500	130	-0.4715	13q12.12	*RNF17, CENPJ*
	24492900	24767100	316	0.4239	13q12-.13	*PABPC3, MTMR6*
	28064100	28500900	444	-0.5472	13q12.3	*POMP*
	43793100	43950900	198	-0.5347	13q14.11	*C13ORF21*
22848	89660700	89662500	3	-1.07	13q31.3	
92896	29706900	29710500	4	-0.7369	13q12.3	*KATNAL1*
	95130900	95152500	17	-0.4041	13q32	*DNAJC3*
90866	18138300	18139500	3	-0.8112	13q11	
	18210300	18218100	14	-0.3984	13q11	
	19862700	19874700	17	-0.4905	13q12.11	
	40136700	40138500	4	-0.4942	13q14.11	*FOXO1*
	111978300	112020900	31	-0.6372	13q34	
	112194900	112196700	4	-0.8487	13q34	*TUBGCP3*
	112727100	112728300	3	-1.2328	13q34	
	112728900	112808100	117	-0.2555	13q34	*MCF2L*
	112808700	112811700	5	-1.0978	13q34	*F7*
	113048700	113050500	4	-0.9167	13q34	*GRTP1*
	113136900	113139300	5	-1.4808	13q34	***ADPRHL1***
	113295300	113296500	3	-1.3918	13q34	*TFDP1*
	113496300	113497500	3	-1.3736	13q34	
86267	113327100	113328300	3	-0.7278	13q34	*TFDP1*

Patients listed displayed significant regions of copy number decrease using Circular Binary Segment Analysis (methods).
Genomic locations are based on Build 35. Genes in bold type were also identified by Process Control Analysis (Table S2)
UPN: unique patient number

Figure 3
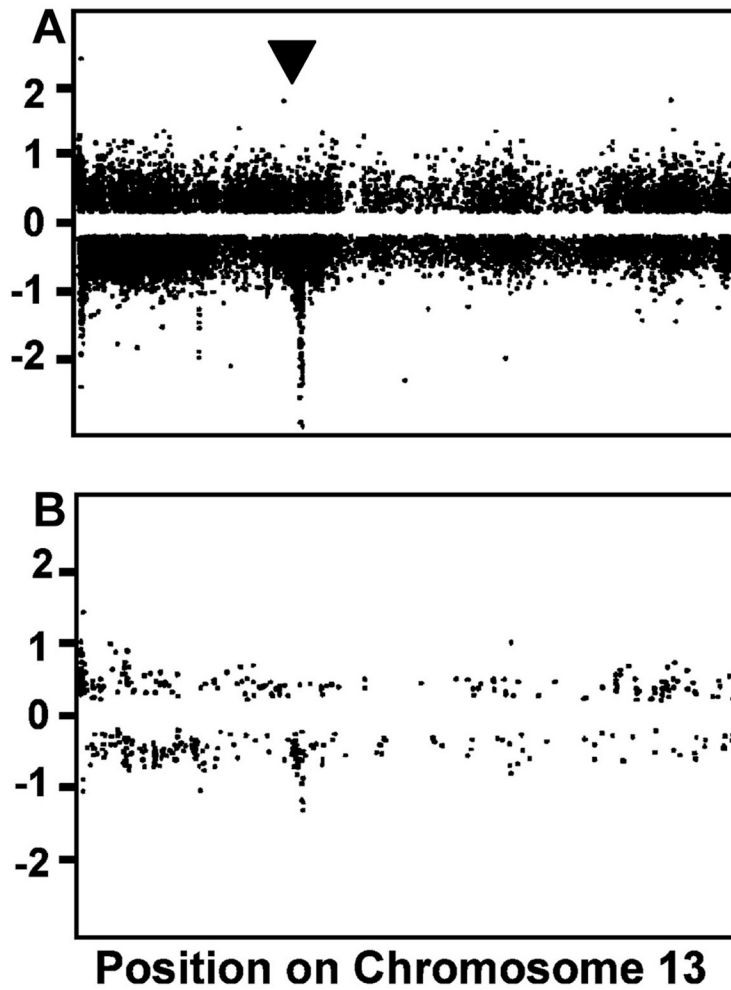
Figure 3. Significant chromosome 13 probes representing DNA copy number changes identified by Process Control.

A. Probes representing deleted and amplified regions in any of the 20 patient samples identified by Process Control Analysis. Data are plotted in a linear fashion across chromosome 13 beginning with the p arm to the left and extending throughout the long q arm to the right. 8844 probes marked regions of DNA copy number decrease and 6706 probes marked regions of DNA copy number increase. Arrowhead indicates region of copy number loss in 13q14. **B**. Process Control probes as in **A** detected in two or more patients. In two or more patient samples, 216 probes indicated DNA copy loss and 274 probes indicated DNA copy number gains. We found 69 of the 216 probes with DNA copy number decrease mapped to 42 genes (**Table S2, Table 2**).

Table 4. Genes with DNA copy number loss identified by Process Control Analysis

Location	Gene	Gene Name
13q11	XPO4	Exportin
13q12	SACS	Spastic ataxia of Charlevoix-Saguenay
13q12	MIPEP	Mitochondrial intermediate peptidase
13q12.12	RNF17	Ring finger protein 17
13q12.13	CENPJ	Centromere protein J
13q12-13	ATP8A2	ATPase, aminophospholipid transporter-like, Class I, type 8A, member 2
13q12.13	USP12	Ubiquitin specific peptidase 12
3q12-13	UBL3	Ubiquitin-like 3
13q12.3	B3GALTL	β 1,3-galactosyltransferase-like
13q13.1	RXFP2	Relaxin/insulin-like family peptide receptor 2
13q12	KL	Klotho
13q13	NBEA	Neurobeachin
13q13	DCLK1	Doublecortin like kinase 1
13q13.3	ALG5	Asparagine-linked glycosylation 5 homolog
13q13.1-2	TRPC4	Transient receptor potential cation channel, subfamily C, member 4
13q13.3	COG6	Component of oligomeric golgi complex 6
13q14.11	NARG1L	NMDA receptor regulated 1-like
13q14	TNFSF11	Tumor necrosis factor (ligand) superfamily, member 11/osteoprotegerin
13q14	TSC22D1	TSC22 domain family, member 1
13q14.13-q14.2	LRCH1	Leucine-rich repeats and calponin homology (CH) domain containing 1
13q14.2	SUCLA2	Succinate-CoA ligase, ADP-forming, b subunit
13q14.2	ITM2B	Integral membrane protein 2B
13q14.2	RB1	Retinoblastoma 1 (including osteosarcoma)
13q14.2	RCBTB2	Regulator of chromosome condensation (RCC1) 2
13q14.2	FNDC3A	Fibronectin type III containing 3a
13q14.2	CAB39L	Calcium binding protein 39-like
13q14.3	RCBTB1	Regulator of chromosome condensation (RCC1) 1
13q14.3	RNASE H2B	Ribonuclease H2, subunit B
13q14.3	WDFY2	WD repeat and FYVE domain containing 2
13q21.2	DIAPH3	Diaphanous homolog 3
13q14.3-q21.1	PCDH9	Protocadherin 9
13q22	DACH1	Dachshund homolog 1
13q22.2	LMO7	LIM domain 7
13q21.1-q22	POU4F1	POU domain, class 4, transcription factor 1
13q32	GPC5	Glypican 5
13q34	RAP2A	RAP2A, member of RAS oncogene family
13q32	ZIC2	Zic family member 2
13q33.3	MYO16	Myosin XVI
13q34	COL4A1	Collagen type IV, α1
13q34	ADPRHL1	ADP ribosylhydrolase like 1
13q34	TMCO3	Transmembrane and coiled-coil domains 3
13q34	RASA3	RAS p21 protein activator 3

Genes that corresponded to significant probe regions identified in two or more patient samples
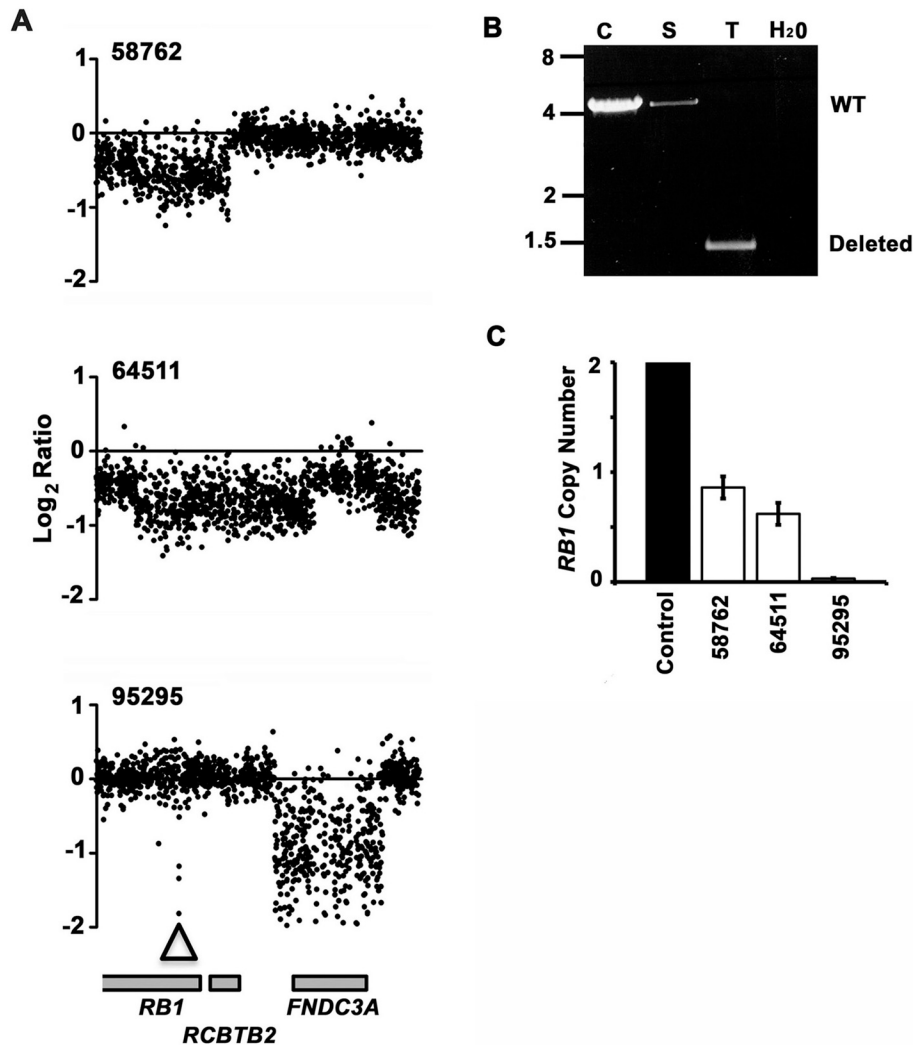
Figure 4

Figure 4. High-resolution aCGH and PCR analysis confirms *RB1* is a target of recurrent interstitial deletions at 13q14.2

A. Magnified view of DNA copy number losses located at 13q14.2. The smallest region of overlap across all three patients was defined by patient 95295, and mapped to exon 20 of *RB1* (arrowhead). Locations of two genes in the region are shown for reference at the bottom. Each dot represents the average signal of ten consecutive probes.   Figure includes 1244 data points spanning 1.29Mb. The

64

region telomeric to *RB1* within sample 95295 was not called by the 600bp CBS analysis, and therefore genes within that region are not listed in (**Table 2**; methods). That region was called by the analysis using different window sizes (1200bp or 300bp). Genes affected were *FNDC3A*, *MLNR* and *CDAC1*. Both *RB1* and *NBEA* were called by all analyses independent of window size. **B**. PCR analysis confirms *RB1* deletion within tumor sample of patient 95295. Germline skin DNA from patient sample 95295 (Skin: S), and an independent control sample (pooled DNA isolated from blood of four normal donors, Control: C), produced the expected full-length (4.4Kb) PCR product. In contrast, CD138 purified tumor plasma cells from patient sample 95295 (Tumor: T) revealed a smaller PCR product (1.5Kb). Sequence analysis revealed the micro-deletion spanned 3486bp, which removed 2813bp of the 3' end of intron 19, all of exon 20 (146bp), and 527bp of the beginning of intron 20. In the middle of the sequencing product was a 435bp insertion with sequence identity to a region located 35Kb downstream of *RB1* on chromosome 13 that did not map to any known gene, and was situated in the opposite orientation. The full-length 4.4Kb band was not detected in the tumor sample, suggesting a homozygous deletion. Water control is shown. Size in Kb is shown on left of gel image. **C.** Real Time PCR analysis confirms *RB1* copy number changes identified by aCGH. Control is patient 54092, with no DNA copy number changes detected by aCGH, FISH, or cytogenetics (**Table 1 and S1**, data not shown). Error bars are SD of three experiments each performed in triplicate.

Figure 5
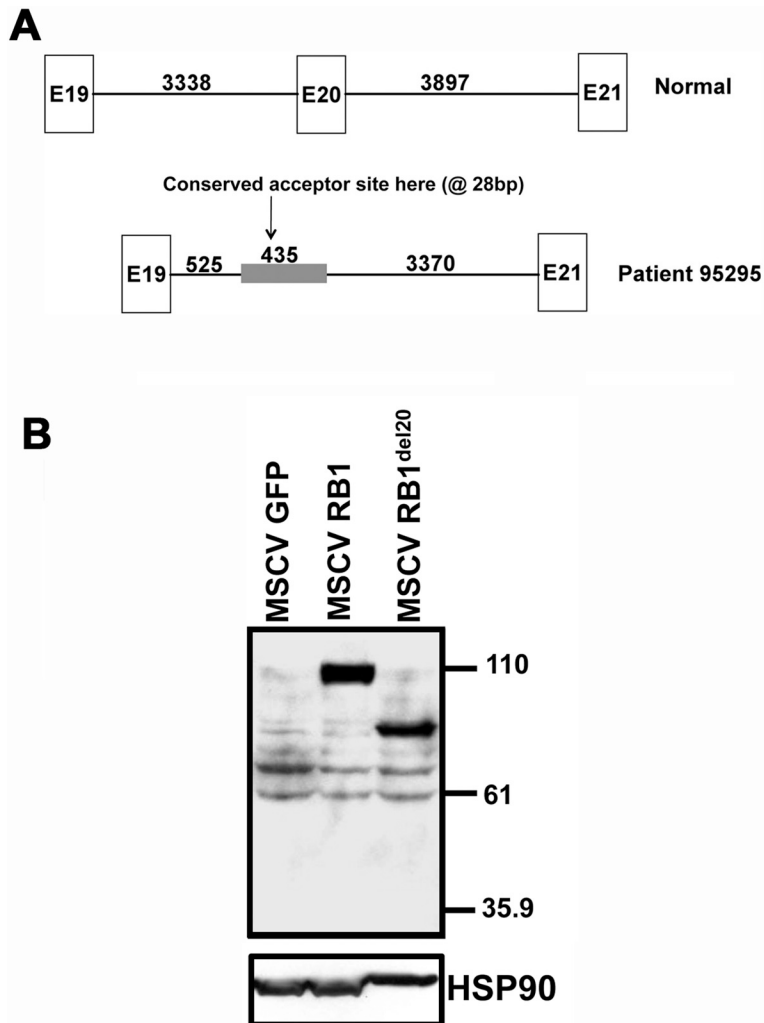
Figure 5. The novel RB1 mutation, RB1[del20] encodes a transcript resulting in expressed truncated protein

A. Schematic of novel *RB1* deletion in patient sample 95295 revealing deletions within intron 19, all of exon 20, and within intron 20. Numbers above lines represent length (bp) of retained sequences (and full length sequence in Normal, above). Gray box depicts insertion within deletion. **B**. Western Blot analysis of subcloned normal and mutated forms of RB1 in MSCV vector transiently

transfected into 293T cells. Truncated proteins run at predicted sizes (RB1 at 110kDa and RB1^{del20} ~85kDa).

Figure 6
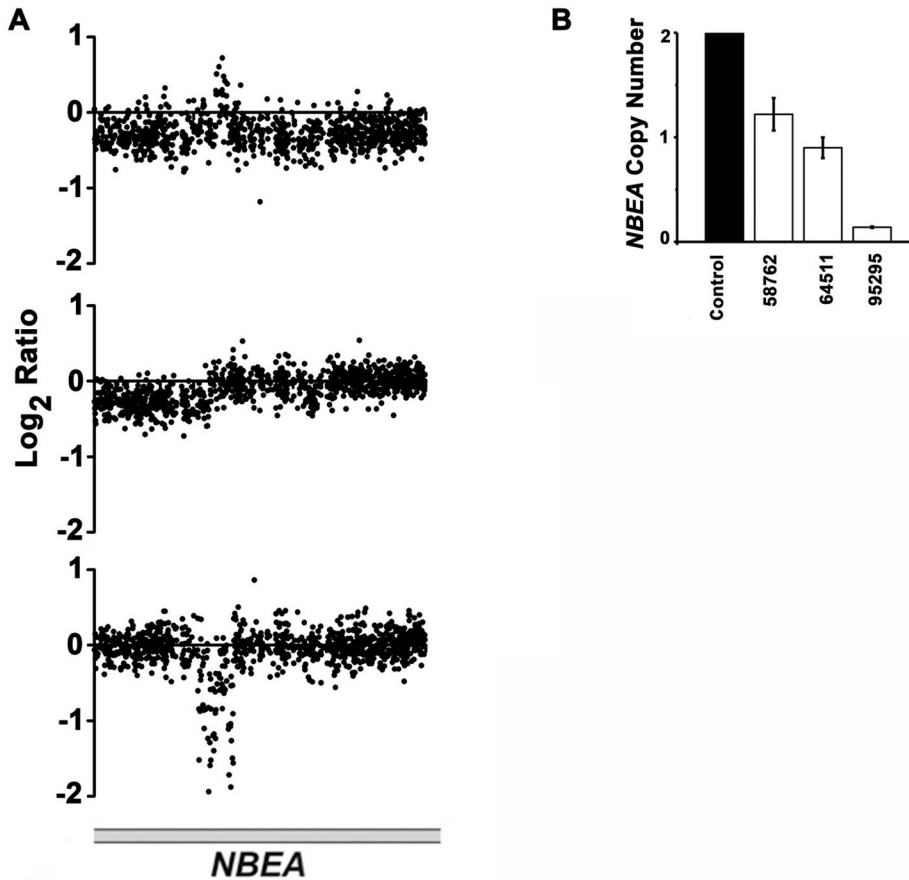
Figure 6. *NBEA* is a target of recurrent interstitial deletions at 13q13

A. Magnified view of overlapping region of DNA copy number loss across patient samples 58762, 64511 and 95295. The only gene identified within this region is *NBEA*. The region of DNA copy number decrease within patient 64511 spanned 885Kb mapping to exon 1-9 of *NBEA*. Within patient 95295, the region spanned 107Kb mapping to *NBEA* exons 3-19. Each dot represents the average signal of 10 consecutive probes as in **Figure 2**. Plots include 950 data points spanning a region of 0.998Mb. In patient samples 58762 and 64511 there appears to be a

small region with DNA copy increase. Examination of the raw data within this region from the reference sample (skin) from all 20 patients revealed the average of these probes was below 10,000, suggesting this is not an array artifact and was also flagged by CBS algorithm. **B**. Real time PCR confirms DNA copy number loss within *NBEA*. Control is patient 54092, with no DNA copy number changes detected by aCGH, FISH, or cytogenetics (**Table 1 and S1,** data not shown). Error bars are SD of two experiments performed in triplicate.

Figure 7
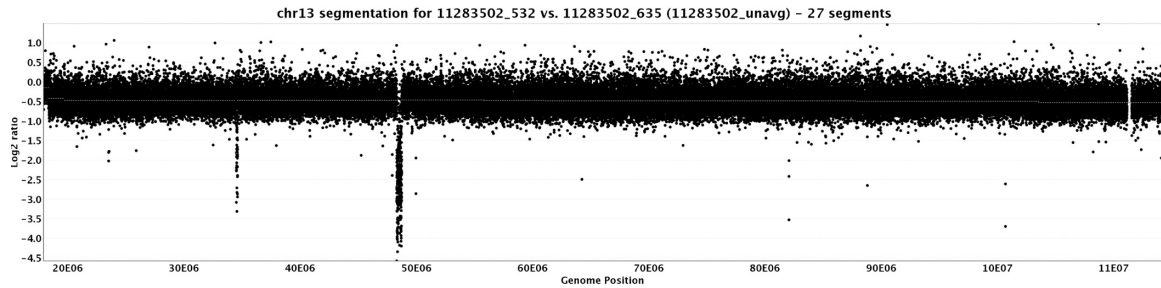
Figure 7. Whole genome aCGH analysis of patient sample 95295 reveals similar regions of copy number loss found in chromosome 13- focused array

Whole genome aCGH (Nimblegen, median probe spacing 1.1Kb) was performed on DNA isolated from patient sample 95295. The data from chromosome 13 is shown.

Chapter 3

Characterization of Retinoblastoma (*RB1)* in Multiple Myeloma

3.1 Abstract

We identified *RB1* as part of a minimally deleted region on chromosome 13 affected by copy loss in myeloma, and therefore set out to characterize *RB1* mutation status and expression in myeloma primary samples and cell lines. Re-sequencing analysis of all 27 *RB1* exons on DNA purified from CD138 selected cells from 41 primary patient samples revealed no exonic mutations, suggesting retained *RB1* alleles in myeloma are wild type. We examined whether patient samples and myeloma cell lines with monosomy 13 expressed reduced levels of RB1 transcripts or protein, respectively, and found lower RB1 transcripts and protein in cells with monosomy chromosome 13. Since RB1 can be inactivated by phosphorylation, we sought to determine whether RB1 protein was phosphorylated in MM. We found RB1 was phosphorylated in MM cell lines, but RB1 phosphorylation was rare in primary patient samples. Together, our data suggest a model whereby wild type RB1 protein is expressed at lower dose in samples with monosomy 13, and becomes phosphorylated late in myelomagenesis.

3.2 Introduction

3.2A *RB1* is a tumor suppressor gene regulated by phosphorylation

RB1 was the first identified tumor suppressor gene, and is highly studied, as disabling the "RB1 pathway" is believed to be essential for virtually all tumor formation [1]. Mutations in, or deletions of, both copies of RB1 in the retina are causative for development of retinoblastoma tumors in humans. Studies of DNA isolated from retinoblastoma patients led to Knudson's famous "two hit" model of tumor suppressor genes. Knudson observed patients with inherited predisposition to retinoblastoma and correctly predicted that one defective *RB1* allele was inherited, and the other was somatically mutated, ultimately leading to inactivation of both copies of the gene [2].

RB1 is a nuclear phosphoprotein that functions in multiple cellular processes including cell cycle, apoptosis, differentiation, and senescence. It's most well studied function is to inhibit the cell cycle, which is regulated by phosphorylation. Hypo-phosphorylated is the "active" form of RB1 that represses transcription of cell cycle-promoting genes in two ways. First, RB1 can directly to bind to the transactivation domain of the E2F transcription factor [3,4] Second, while RB1/E2F complexes bind DNA, RB1 can recruit chromatin remodeling enzymes that downregulate gene expression [5-8]. Both events prevent transcription of E2F targets including genes required for replication, DNA metabolism and synthesis, cyclin E, and cyclin A [9,10].

RB1 has 16 serine/threonine phosphorylation sites whose phosphorylation status changes throughout cell cycle. RB1 gets partially phosphorylated during the cell cycle by cyclin dependent kinase (CDK, CDK4/CDK6) - Cyclin D (and then E) complexes. CDK's require cyclins for active kinase activity. There are two protein families that act to inhibit cyclin/CDK complexes from phosphorylating RB1. First, the INK family (P16^{INK4a}, P15^{INK4b}, P18^{Ink4C}, P19^{Ink4D}) can specifically block the kinase activity of CDKs. Second, the "Cip/Kip" family (p27^{KIP1}, P21^{CIP1} and p57^{Kip2}) can bind to and sequester cyclins from CDKs. Both of these negative regulators, when intact, prevent phosphorylation (and therefore inactivation) of RB1. Together, these proteins comprise the "RB1 pathway".

Inactivation of RB1 pathway occurs via mutation, deletion, methylation, or phosphorylation

Inactivation of the RB1 pathway occurs in different ways in a different tumor types. Deletion or mutation of *RB1* is found in retinoblastoma, breast, bone, brain, bladder, and some lung cancers. However, genetic inactivation of *RB1* is not universal to all cancers, including those with heterozygous *RB1* mutations [10]. In many tumors, the remaining RB1 is inactivated post-translationally by phosphorylation. This occurs via deletion, mutation or methylation of the INK4a locus (*CDKN2A*) affecting p16. Alternatively, over-expression of Cyclin D, (which can activate CDK4/6) also results in hyper-phosphorylated RB1. Together, multiple mechanisms inactivate RB1.

74

We identified *RB1* as being part of a minimally deleted region in plasma cell dyscrasias, and therefore sought to further characterize RB1 in myeloma. Our aCGH, cytogenetic, and FISH analysis of chromosome 13 in primary patient samples revealed that samples with deletions affecting one copy of *RB1*, retained the remaining allele (except for sample 95295, that harbored a homozygous mutation), in MGUS and MM (**Chapter 2)**. We examined whether patient samples and myeloma cell lines with monosomy 13 expressed reduced levels of RB1 transcripts or protein, respectively, and found lower RB1 transcripts in primary patient samples and protein in cell lines with monosomy chromosome 13. To determine if *RB1* is inactivated in MM via mutation, we performed comprehensive re-sequencing of *RB1* in 41 primary patient samples and found inactivating mutations of *RB1* to be a very rare event in myeloma. Immunohistochemistry and Western blot analysis on primary patient samples and MM cell lines, respectively, revealed RB1 was phosphorylated in MM cell lines, but not primary patient samples, suggesting phosphorylation of RB1 is a late event in myeloma.

3.3 Methods

Large-scale sequencing of *RB1* in primary human samples

High-throughput sequence analysis of *RB1* was performed by the Genome Sequencing Center at Washington University (WUSTL) as described [11] Detailed protocols are available on WUSM GSC website (http://genome.wustl.edu/platforms.cgi?id=7). PCR validation of *RB1* SNPs was performed on genomic DNA isolated from CD138+ selected bone marrow (tumor) and skin biopsy (normal) patient samples. The independent control DNA was kindly provided by Rhonda Reis, Division of Oncology, WUSTL. Products were cloned into and sequenced from TOPO2.1 vector (Invitrogen, Carlsbad, CA).

Microarray Expression Analysis

Two independent microarray datasets were analyzed. First, a Mayo Clinic dataset [12] included 162 samples (101 MM, 24 SMM, 22 MGUS, and 15 normal PC's; GEO GSE6477; chromosome 13 status was determined by FISH). Second, we used a multiple myeloma research consortium (http://www.themmrc.org; MMRC) dataset that included 100 MM samples (Chromosome 13 status was determined by aCGH).

Expression values were derived against a PM/MM difference background using Robust Multichip Average (RMA) [13]. Present/Absent probes were called using Affymetrix Microarray Suite version 5. Only probes detected in at least one

76

sample were used in subsequent comparisons. In pooled Chromosome 13 Deletion *versus* no Deletion comparisons, Significance Analysis of Microarrays (SAM), [14] was used to detect differentially expressed genes based on a q-value of less than 5%. SAM was run with 100 permutations for correction of False Discovery Rate. These genes were clustered and visualized in DChip [15] (http://www.dchip.org). aCGH data was first smoothed with region=2, outlier scale =4, smoothing SD=2 and trimming proportion of 0.025. CBS was then run with default parameters (alpha=0.01, window.size= NULL, with 10000 permutations).

Western blot and cell lines

LP-1, KMS-11, OPM-2 and UTMC2 lines were provided by W. Michael Kuehl, (Genetics Branch, NIH) and maintained in RPMI with 1% Penicillin/Streptomycin (both Cambrex Bioscience, Walkersville, MD), 10% fetal bovine serum (HyClone, Logan, Utah). RPMI-8226, U266, and H929 cells were obtained from and grown per ATCC recommendations. Lysates were prepared as described [16] Antibodies: total RB1: IF8 (Santa Cruz Biotechnologies, Santa Cruz, CA); anti-phospho-RB1(Serine Ser807/811; Cell Signaling, Beverly, MA); Actin (Sigma, St. Louis, MO).

FACS analysis

One million cells/sample were permeabilized and fixed using the protocol in the BRDU kit (BD Pharmingen, San Diego, CA), since this method was found to be

amenable to adaptation for our intracellular RB1 staining. Prior to antibody staining, a block step was added to prevent non-specific antibody binding (20 minute incubation of cells in PBS with 2.5g/500mL Bovine Serum Albumin; Sigma-Aldrich, St. Louis, MO). Cells were stained with same phospho- Ser 807/811 antibody used in Western Analysis.

Immunohistochemical staining of RB1 in primary samples

This analysis was performed per standard techniques in clinical pathology lab at Washington University. Antibodies: total RB1 antibody (4H1, Cell Signaling, Boston, MA); phospho-Serine 807/811 antibody used in Western and FACS analysis was used for this analysis. Samples were scored blind for generation of semi-quantitative analysis.

Analysis of murine hematopoeisis

Rb1 WT (n=4) and HET (n=6) mice were provided by Katherine Wikenheiser (Dept. of Pathology, University of Cincinnati) initially generated by Tyler Jacks [17]. These were provided to us as fifth generation C57BLACK/6 X129 mix. We performed backcrossing to C57BLACK/6 generation ten. Two and a half month old mice were analyzed. Mice were injected i.p. with 200ml 10%w/v SRBC or PBS (generation five mice- all other experiments-generation ten) and analyzed mice seven days post treatment. FACS analysis and blood counts were performed as described previously [18].

3.4 Results

3.4A Retained *RB1* alleles in MGUS/MM patient samples are mostly wild type

Our data suggested one copy of *RB1* is a target of deletions in MM, yet in most patient samples (7/8 in our set) the other copy is retained. Limited sequence analysis in myeloma has failed to show mutations in *RB1* exons 20-24 [19] (mutation hotspots in retinoblastoma) [20, 21] but other domains of *RB1* have not been re-sequenced in MM. We therefore performed comprehensive sequencing of all 27 *RB1* exons and surrounding intronic sequences in 41 MM/MGUS patient samples (including 16 of our 20 patient set; **Table 1**). We found no non-synonymous sequence changes affecting the coding or promoter sequences (bp -474 to -182) of *RB1*, suggesting that, in contrast to retinoblastoma tumors, most myeloma tumors retain at least one wild-type *RB1* allele.

We detected eleven intronic SNPs (**Table 1**). Since myeloma is twice as prevalent in African American populations compared to Caucasians (www.seer.cancer.gov), race matched minor allele frequencies (MAFs) from our patient samples were compared to published MAFs in the Hap Map database for the nine of eleven SNPs with available data (**Table 2**). Two *RB1* SNPs (rs198580 and rs198617) were significantly more common in our Caucasian patients (*P* < 0.001 and *P* < 0.018, respectively), suggesting a possible role in MM

pathogenesis. No significant differences were found between subgroups for the other seven SNPs.

We identified six novel SNPs, not reported in the NCBI or HapMap databases (**Table 3**). To confirm this result, DNA from tumor samples with novel SNPs were used for PCR and subsequent sequence analysis. To determine whether these were tumor-associated changes, the matched skin samples were subjected to the same analysis. The novel SNPs were confirmed, and all were found to be present in both tumor and matched skin genomic DNA, demonstrating these to not be tumor associated and instead normal sequence variants. Since both the known and novel SNPs were located near exon boundaries (range: 10-171bp from the start or end of an exon), we considered the possibility that *RB1* SNPs might play a role in MM pathogenesis by affecting RNA splicing. Examination of *RB1* cDNA isolated from seven patients with reported or novel SNPs revealed only *RB1* transcripts of expected size (not shown). Together, our re-sequencing analysis demonstrated no somatic mutations affecting *RB1* in the retained allele.

3.4B RB1 protein is decreased in MM cell lines with monosomy 13

Even in the setting of chromosome 13 deletions, *RB1* transcripts are abundant in MM cells, consistent with the finding that epigenetic silencing of the *RB1* promoter does not occur in MM [22]. To determine whether RB1 protein levels were related to chromosome 13 copy number, we performed Western Blot

analysis on a panel of MM cell lines with known genetic copy number of the *RB1* locus. RB1 protein was detected in all cell lines that retained at least one *RB1* allele (**Figure 1**). U266, shown to have undergone rare biallelic loss of *RB1* [23] involving deletion of exon 13 and 14 [24] expressed no RB1 protein as expected, as did UTMC2 cells (**Figure 1**). LP-1 and KMS-11 cells, which retain only one copy of chromosome 13, [23] expressed lower levels of RB1 protein than OPM-2 and RPMI-8226 cells, which retain two copies of the *RB1* locus [23]. These data suggest RB1 protein levels were related to *RB1* genomic copy number in myeloma cell lines.

To further confirm this result, we performed FACS analysis to examine RB1 protein levels on a per-cell basis. Consistent with the Western Blot analysis, we found cell lines with two copies of *RB1* (OPM2) had higher protein than those cells with one genomic copy of *RB1* (LP-1; **Figure 1**).

3.4C *RB1* transcripts are decreased in primary patient samples with monosomy 13

Our cell line data implied RB1 protein levels were related to genomic copy number. We hypothesized *RB1* transcript levels would be decreased in primary patient samples with monosomy chromosome 13. Since our data set was relatively small, examined a large patient data set that included patient samples with and without monosomy 13. We analyzed two published data sets comprising 162 (101 MM, 24SMM, 22 MGUS, and 15 normal PC's; Mayo GSE 6477; [11] and 100 (MMRC) patient samples (methods) and compared *RB1*

transcript levels between patient samples with our without monoallelic deletion of chromosome 13. In both datasets, *RB1* transcript levels were decreased in patient samples with monosomy 13 (**Table 4**; Mayo: -0.69 Fold Change; MMRC -0.67 Fold Change). These data suggested in the majority of patient samples, *RB1* transcript levels were decreased in samples harboring copy number loss of chromosome 13, consistent with prior reports [25-27].

3.4D *Rb1* heterozygous mice have normal hematopoeisis

Although at odds with RB1's canonical tumor suppressor role, our RB1 expression data above prompted us to consider a model of *RB1* haploinsufficiency, whereby half RB1 protein dose alters the B cell compartment to contribute to MM pathogenesis. To this end, we examined hematopoietic compartments of *Rb1* heterozygous mice (*Rb1*$^{+/-}$; [17] compared to wild type (*Rb1*$^{+/+}$) littermates. We found similar absolute spleen weights (*Rb1*$^{+/+}$: average 0.067g, SD: 0.005, *n*=4; *Rb1*$^{+/-}$: average 0.064g, SD 0.008, n=6) and peripheral blood counts (*Rb1*$^{+/+}$: 5.80k/μl, SD 2.02, *n*=4; *Rb1*$^{+/-}$: 8.74k/μl, SD 4.40, *n*=6) in both groups of mice. We found similar distributions of B cells (B220), myeloid cells (GR-1/MAC1), and T cells (CD4, CD8) isolated from bone marrow and spleen mononuclear cells at baseline **(Figure 2)**.

To determine whether haploinsufficiency of *Rb1* affects the B cell compartment in stress conditions, wild type and heterozygous mice were inoculated with sheep red blood cells, known to induce germinal center (GC) reactions [28]. Spleen

weights and plasma cell percentages increased in all mice independent of genotype to similar levels cells (**Figure 2**, not shown), suggesting GC reactions formed independent of *Rb1* genotype. Together, these data fail to support a role of *RB1* haploinsufficiency as the single genetic abnormality in MM pathogenesis, and suggests additional events cooperate with *RB1* deletions in myeloma pathogenesis.

3.4E RB1 protein is phosphorylated in MM cell lines, but is rarely phosphoryated in primary patient samples

Since we did not find *RB1* mutations in this study, we hypothesized RB1 would be inactivated by phosphorylation in MM. Western Blot analysis was performed on the same MM cell line panel as above using an antibody that recognizes only phosphorylated RB1 protein (Ser807/811). All MM lines that retained at least one copy of *RB1*, expressed phosphorylated RB1 protein (**Figure 1**) consistent with a previous analysis [29]. Levels of phosphorylated RB1 protein, as with total RB1 protein above, were more abundant in cells with two *RB1* alleles compared to those with one. These data show RB1 protein is phosphorylated MM cell lines.

Since MM cell lines are isolated from plasmacytomas, (extramedullary, late stage myeloma), we wanted to determine whether RB1 protein was phosphorylated in primary patient samples. To address this, we performed immunohistochemical staining of a set of 25 primary patient samples (1 MGUS, 1SMM, 22MM, and 1 PCL) using two RB1 antibodies (**Figure 3, Table 5**). First, we used an antibody

(4H1) that recognizes RB1 protein independent of phosphorylation status. The second antibody recognizes only phosphorylated RB1 protein (Serine 807/811). As expected, total RB1 protein was found in most patient samples using the antibody that binds to RB1 independent of phosphorylation status. To our surprise, we found very little to no phosphorylated RB1 in most patient samples, independent of disease stage. These data suggest a model whereby RB1 protein is phosphorylated only very late in myeloma development.

3.5 Discussion

Mutation of *RB1* is rare in Myeloma

The *RB1* tumor suppressor has a long and famous history, as it was the first identified tumor suppressor gene and the basis for Knudsen's model of tumor suppressor genes originally worked out by examining *RB1* in retinoblastoma patients [2]. In myeloma, *RB1* has gained much attention since it is a recurrent site of deletion and in fact, the *RB1* locus is commonly used as the probe in clinical FISH analysis to examine chromosome 13 deletions. Our aCGH analysis revealed *RB1* was the sole gene affected in a minimally deleted region at 13q14.2 (**Chapter 2**).

We hypothesized retained *RB1* alleles would be mutated in myeloma. We performed large- scale exonic sequencing of *RB1* on 41 primary CD138 purified patient sample DNAs, but did not detect mutations affecting *RB1* exons. The only tumor-associated *RB1* exonic mutation we identified was found by aCGH, and not this sequence analysis (**Chapter 2**). The deletion was not identified by large-scale sequencing approach because of the small amplicon size, which was entirely deleted in patient sample 95295. The wild type *RB1* sequence in sample 95295 was likely amplified from the WT *RB1* allele present in residual normal plasma cells. Overall, our sequence analysis revealed retained *RB1* alleles are essentially unaffected by exonic mutation in myeloma. This suggests that if

inactivation of RB1 is relevant to MM pathogenesis, it occurs via a different mechanism than mutation of the *RB1* coding sequence.

Inactivation of "RB1 pathway" in myeloma remains controversial and largely unconvincing

There are multiple ways tumor cells can inactivate the "RB1 pathway" ultimately leading to phosphorylated and inactive RB1 protein unable to regulated cell cycle. Methylation of the *CDKN2A* locus (encoding P16^{INK4A} and P19^{ARF}) results in reduced to no expression of P16, leading to downstream activation of cyclin/CDK complexes and subsequent RB1 phoshorylation. Methylation of *CDKN2A* is detected in 23-53% of myeloma patient samples. [22,30-32]. However, most studies report lack of P16 downregulation in samples with *CDKN2A* [32,33]. P16 methylation is not related to plasma cell labeling index [32], patient or progression- free survival [30, 32]. *P15* methylation is detected in 17-35% of MM samples, but *RB1*, P18 and *P14* were not [22,30]. Methylation of genes within the "CIP/KIP" family is rare [33]. Although methylation of some genes within the RB1 pathway is detected in MM, levels may be insufficient to sufficiently downregulate gene expression. Together, there is lack of convincing evidence that methylation of *INK4* and *CIP/KIP* loci contribute to MM.

Up-regulation of Cyclin 1, 2, or 3 is reported to be universal in myeloma [34] via the (11;14)(q13;32) translocation, trisomy 11, translocations affecting genes that positively regulate cyclin D2 (c-MAF via the t(14;16)(q32;q23), or by as yet

undetermined mechanisms. These predict Cyclin D accumulation, formation of Cyclin D-CDK4/6 complexes, phosphorylation (and inactivation) of RB1, and increased cell cycle due to inactivation of RB1 via phosphorylation. However, multiple lines of evidence lead to the conclusion that the expression of cyclin D does not lead to myeloma cell growth via increased proliferation. Paradoxically, the presence of the t(11;14)(q13;32) translocation confers good prognosis [35] as does detection of cyclin D1 expression [36]. Proliferation rates (BRDU) in t(11;14)+ myeloma cells revealed lower proliferative index than other myeloma samples [37,38]. Finally, in primary MM samples, expression of cyclin D1 or D3 was insufficient to promote RB1 phosphorylation, and levels of cyclin D1 were unrelated to MM cell proliferation [29]. Levels of CDK4/6 in cells expressing Cyclin D may be too low to fully inactivate RB1 [29, 39]. Our own analysis revealed phosphorylation of RB1 was rare in primary patient samples. Together, these data suggest the contribution of RB1 protein to MM is not via the "canonical RB1 inactivation" pathway.

RB1 haploinsufficiency may contribute to MM via non-traditional mechanisms

Our analysis of RB1 protein in MM cell lines, and *RB1* transcripts in primary patient samples, revealed levels of RB1 were related to *RB1* genetic copy number. In other words, we observed RB1 levels were lower in cells with single *RB1* deletion compared to cells that retained two alleles, consistent with prior reports [25-26] and verified with Q- RT-PCR analysis [27]. Protein analysis via

Western Blot analysis has largely been limited by insufficient sample quantity. We were unsuccessful in our efforts to examine a panel of primary patient samples, however it is a future goal of the lab to extend our FACS assay on primary samples.

Because we, and others [25-27] found *RB1* levels correlated with genomic *RB1* copy number, we seriously considered the possibility *RB1* haploinsufficiency alone might contribute to myeloma. The *Drosophila* homologue of the *RB1/Rb1*gene family, *Rbf*, has a haploinsufficient phenotype in a genetic model of eye tumors [40]. Many tumor suppressors including, for example, the CIP/KIP family member p27^{kip1} display haploinsufficient phenotypes in mice, whereby heterozygous mice expressing wild type protein at reduced dose display cancer prone phenotypes [41].

However, much data supports the conclusion that *RB1* haploinsufficiency alone does not appear to contribute to malignancy in humans and mice. No myeloma related phenotype has been reported in long-term follow up of surviving retinoblastoma patients with germline inactivating *RB1* mutations [42]. Loss of one copy of *RB1* as a sole abnormality is not prognostic for reduced patient survival in myeloma [43]. *Rb1*$^{+/-}$ mice develop tumors only after loss of the remaining *Rb1* allele [17] and when Eμ-Myc mice (known to develop B cell neoplasms), are mated to *Rb1*$^{+/+}$ or *Rb1*$^{+/-}$ mice, no survival differences are observed [44].

Our analysis of 8-9 week old $Rb1^{+/+}$ versus $Rb1^{+/-}$ mice (backcrossed to generation 10 C57BL/6) revealed no differences in basal hematopoeisis or plasma cells development upon antigen stimulation, consistent with another report [45]. However, in $Rb1$ null retina cells, the $Rb1$ family member, p107 compensates for Rb1 [46,47]. In hematopoeisis, p107 sometimes, [45] but not always, [48] compensates for loss of $Rb1$. To avoid the issue of p107 compensation completely, generation of mice with conditional deletion of $Rb1$ in plasma cells in the context of p107$^{-/-}$ is necessary. We are currently mating $Rb1^{flox/flox}$ [49] mice to mice expressing Cre recombinase under the control of the Cγ1 heavy chain isotype whose transcription is induced in germinal centers upon stimulation with T cell dependent antigens [50] to generate mice with $Rb1$ deletions in germinal center B cells. These mice will be mated to $p107^{-/-}$ mice to generate Cγ1Cre$Rb1^{+/+}p107^{-/-}$ and Cγ1CreRb1$^{Flox/+}p107^{-/-}$ mice. If haploinsufficiency of $Rb1$ is sufficient to contribute to myelomagenesis, then we predict to see tumor or MGUS phenotypes in the *Cγ1CreRb1$^{Flox/+}p107^{-/-}$* mice but not in the Cγ1CreRb1$^{+/+}p107^{-/-}$ mice.

Myeloma cells follow an observation made in solid tumors: RB1+ tumors tend to be slow-growing, chemotherapy resistant, and have little spontaneous apoptosis, whereas RB1- tumors proliferate fast, are chemotherapy sensitive, and have high rates of spontaneous apoptosis [51]. Heterozygous loss of $RB1$ is detected in MGUS and MM, suggesting it is an "early" event in PC dyscrasias. Retention of

expressed, half dose RB1 protein could be selected for in MGUS or MM cells due to its ability to inhibit apoptosis. Although paradoxical, that RB1 can prevent apoptosis, (a pro-tumor event opposite its well-described tumor suppressor function), this actually makes sense since during much of myeloma, cell cycle occurs at a low rate and these cells are able to evade apoptosis. Myeloma cells heterozygous for *RB1* may express sufficient protein to sequester enough E2F to prevent complete dysregulation of cell cycle, and also inhibit activation/transcription of the E2F mediated apoptotic pathway including P73 (a P53 family member). Analysis of P73 expression could address this possibility, and would be predicted to be low. RB1 mediated inhibition of apoptosis could occur via an E2F independent mechanism via its association with Abl or Jnk kinases, known to inhibit apoptosis [52]. Immunoprecipitation experiments could experimentally address this possibility. Alternatively, RB1 can regulate senescence and differentiation [53]. Haploinsufficiecy of RB1 in myeloma cells may result in a reduced ability to drive these cells to senescence. Together, it remains a testable hypothesis, that via alternative mechanisms than in other tumor types, haploinsufficiency of RB1 contributes to MGUS and MM.

Although RB1 is the subject of over 1400 research articles, there is still much to learn. The "binary switch" model whereby hyper-phosphorylated RB1 is inactive and unable to prevent cell cycle, and hypo-phosphorylated RB1 is active is too simple [54]. It is likely differential phosphorylation of the 16 serine/threonine sites in RB1 affects it ability to regulate its other functions including differentiation,

prevention of apoptosis, and senescence. For example, Serine 567 does not get phosphorylated during regular cell cycle; however when phosphorylated, RB1 protein becomes destabilized and cell death occurs [55]. Cell type specific phospho peptide mapping may elucidate which sites are phosphorylated in early B cells, MGUS and MM cells and provide insight to which phosphorylated residues regulate different the RB1 effector functions discussed above.

3.6 Acknowledgements

The data from this chapter would not have been possible without a lot of help.

First, the Washington University Genome Sequencing Center is responsible for

helping us obtain the sequence analysis. Yumi Kasi was instrumental in this

effort. Anjum Hassan and the Clinical Pathology lab generated the IHC data,

which has also been a lot of work, but provided insights we would not have

otherwise had. Punit Vachharajani and Yuron (Mack) Su were both outstanding

STARS students I was fortunate to work with. They both put in a lot of effort to

get the phospho-flow analysis up, running, and to the point that it may actually be

feasible to look at primary patient samples with this labor-intense technique.

Rachel Delston in Bill Harbour's lab has been a wonderful "RB1 friend" and she

has really given me a lot of advice and tools to enable studies of RB1.

3.7 References

1. Sherr CJ and McCormick F The RB and P53 pathways in cancer. Cancer Cell. 2002; 2:103-112.

2. Knudson AG. Mutation and cancer: Statistical study of retinoblastoma. PNAS. 1971; 68: 820–23.

3. Flemington EK, Speck SH, and Kaelin WJ. E2F-1-mediated transactivation is inhibited by complex formation with the retinoblastoma susceptibility gene product. PNAS. 1993; 90: 6914-18.

4. Helin K, Wu C, Fattaey AR, et al. Heterodimerization of the transcription factors E2F-1 and DP-1 leads to cooperative *trans*-activation. MCB. 1993; 7: 1850-61.

5. Weintraub SJ, Chow KNB, Luo RX et al. Mechanisn of active transcriptional repression by the retinoblastoma protein. Nature. 1995; 375: 812-15.

6. Sellers WR, Rodgers JW and Kaelin WG. A potent transrepression domain in the retinoblastoma protein induces a cell cycle arrest when bound to E2F sites. PNAS.1995; 92: 11544-48.

7. Bremner R, Cohen BL, Sopta M et al. Direct Transcriptional repression by pRB and its reversal by specific cyclins. MCB. 1995; 15: 3256-65.

8. Adnane J, Shao Z, and Robbins PD. The retinoblastoma susceptibility gene product represses transcription when directly bound to the promoter. JBC. 1995; 270: 8837-43.

9. Johnson DG. Schwartz JK, Cress WD. et al. Expression of transcription factor E2F1 induces quiescent cells to enter S phase. Nature. 1993; 365: 349-52.

10. Horowitz JM, Park SH, Bogenmann E, et al. Frequent inactivation of the retinoblastoma anti-oncogene is restricted to a subset of human tumor cells. PNAS. 1990; 87: 2775-79.).

11. Link DC, Kunter G, Kasai Y, et al. Distinct patterns of mutations occurring in de novo AML versus AML arising in the setting of severe congenital neutropenia. Blood. 2007;110:1648-1655.

12. Chng WJ, Kumar, S, Van Wier S et al. Molecular dissection of hyperdiploid multiple myeloma by gene expression profiling. Cancer Research. 2007; 67: 2982-89.

13. Bolstad, BM, Irizarry RA, Astrand, M, et al. A Comparison of Normalization Methods for High Density Oligonucleotide Array Data Based on Bias and Variance. Bioinformatics. 2003 19(2):185-193.

14. Tusher, VG, Tibshirani, R & Chu, G. Significance analysis of microarrays applied to the ionizing radiation response .PNAS USA 2001; 98: 5116–5121

15. Li C, and Wong, WH. Model-based analysis of oligonucleotide arrays: Expression index computation and outlier detection. PNAS USA. 2001; 98: 31-36.

16. Xiang Z, Kreisel F, Cain J, Colson A, Tomasson MH. Neoplasia driven by mutant c-KIT is mediated by intracellular, not plasma membrane, receptor signaling. Mol Cell Biol. 2007;27:267-282.

17. Jacks T, Fazeli A, Schmitt EM, Bronson RT, Goodell MA, Weinberg RA. Effects of an Rb mutation in the mouse. Nature. 1992;359:295-300.

18. Cain JA, Xiang Z, O'Neal J, et al. Myeloproliferative disease induced by TEL-PDGFRβ displays dynamic range sensitivity to Stat5 gene dosage. Blood. 2007;109:3906-3914.

19. Zandecki M, Facon T, Preudhomme C, et al. The retinoblastoma gene (RB-1) status in multiple myeloma: a report on 35 cases. Leukemia and Lymphoma. 1995; 18: 497-503.

20. Valverde JR, Alonso J, Palacios I, Pestana A. RB1 gene mutation up-date, a meta-analysis based on 932 reported mutations available in a searchable database. BMC Genet. 2005;6:53.

21. Nichols KE, Houseknecht MD, Godmilow L, et al. Sensitive multistep clinical molecular screening of 180 unrelated individuals with retinoblastoma detects 36 novel mutations in the RB1 gene. Hum Mutat. 2005;25:566-574.

22. Chim CS, Fung TK and Liang, R. Disruption of INK4/CDK/RB cell cycle pathway by gene hypermethylation in multiple myeloma and MGUS. Leukemia. 2003; 17: 2533-35.

23. Juge-Morineau N, Mellerin MP, Francois S, et al. High incidence of deletions but infrequent inactivation of the retinoblastoma gene in human myeloma cells. Br J Haematol. 1995;91:664-667.

24. Corradini P, Inghirami G, Astolfi, M et al. Inactivation of Tumor suppressor genes, p53 and RB1 in Plasma Cell Dyscrasias. Leukemia; 8: 758-67.

25. Carrasco DR, Tonon G, Huang Y, et al. High-resolution genomic profiles define distinct clinico-pathogenetic subgroups of multiple myeloma patients. Cancer Cell. 2006; 9: 313-325.

26. Shaughnessy J, Jacoboson J, Sawyer J, et al. Continuous absence of metaphase defined cytogenetic abnormalitiies, especially of chromosome 13 and hypodiploidy, ensures long-term survival in multiple myeloma treated with Total Therapy I: Interpretation in the context of global gene expression. Blood. 2003; 101: 3849-56.

27. Agnelli L, Bicciato, S, Fabris S, et al. Integrative genomic analysis reveals distinct transcriptional and genetic features associated with chromosome 13 deletion in multiple myeloma. Haematologica. 2007; 92: 56-65.

28. Shinall SM, Gonzalez-Fernandez M, Noelle RJ, Waldschmidt TJ. Identification of murine germinal center B cell subsets defined by the expression of surface isotypes and differentiation antigens. J Immunol. 2000;164:5729-5738.

29. Ely S, Di Liberto M, Niesvizky R, et al. Mutually exclusive cyclin-dependent kinase 4/cyclin D1 and cyclin-dependent kinase 6/cyclin D2 pairing inactivates retinoblastoma protein and promotes cell cycle dysregulation in multiple myeloma. Cancer Res. 2005; 65:11345-11353.

30. Martin P, Garcia-Cosio M, Santon A et al. Aberrant gene promoter methylation in plasma cell dyscrasias. Experimental and Molecular Pathology. 84; 2008: 256-61.

31. Dib A, Barlogie B, Shaughnessy J et al. Methylation and expression of the p16INK4A tumor suppressor gene in multiple myeloma. Blood. 109; 2007: 1337-38.

32. Gonzalez-paz, chng WJ, McClure RF et al. Tumor suppressor p16 methylation in multiple myeloma:biological and clinical implications. Blood. 2006; 109: 1228-32.

33. Chim CS, Liang R, Fung TK et al. Infrequent epigenetic dysregulation of CIP/KIP family of cyclin-dependent kinase inhibitors in multiple myeloma. Leukemia. 2005; 19: 2352–55.

34. Bergsagel PL, and Juehl WM. Critical roles for immunoglobulin translocations and cyclin D regulation in multiple myeloma. Immunological Reviews. 2003; 194: 96-104.

35. Fonseca R., Barlogie B., Bataille R. et al Genetics and Cytogenetics of Multiple Myeloma: A Workshop Report. Cancer Research. 2004; 64: 1546-1558.

36. Soverini S, Cavo M, Cellini L et al. Cyclin D overexpression is a favorable prognostic variable for newly diagnosed multiple myeloma patients treated with high dose chemotherapy and single or double autologous transplantation. Blood. 2003; 102: 1588-94.

37. Fonseca R, Blood EA, Oken MM et al. Mytloma and the t(11;14)(q13;q32); evidence for a biologically defined unique subset of patients. Blood. 2002; 99: 3735-41.

38. Wilson CS, Butch AW, Lai R. et al. Cyclin D1 and E2F-1 immunoreactivity in bone marrow biopsy specimens of multiple myeloma: relationship to proliferative activity, cytogenetic abnormalities and DNA ploidy. British Journal of Hematology. 2001; 112: 776-82.

39. Lessage DL, Troussard X, and Sola B. The enigmatic role of cyclin D1 in multiple myeloma. International Journal of Cancer. 2005; 115: 171-76.

40. Ferres-Marco D, Gutierrez-Garcia I, Vallejo DM, Bolivar J, Gutierrez-Avino FJ, Dominguez M. Epigenetic silencers and Notch collaborate to promote malignant tumours by Rb silencing. Nature. 2006;439:430-436.

41. Santarosa M, and Ashworth, A. Haploinsufficiency for tumor suppressor genes: when you don't need to go all the way. Biochimica et Biophysica Acta. 2004; 105-22. 278; 19358-66.

42. Mohney BG, Robertson DM, Schomberg PJ, Hodge DO. Second nonocular tumors in survivors of heritable retinoblastoma and prior radiation therapy. Am J Ophthalmol. 1998;126:269-277.

43. Gutierrez NC, Castellanos MV, Martin ML, et al. Prognostic and biological implications of genetic abnormalities in multiple myeloma undergoing autologous stem cell transplantation: t(4;14) is the most relevant adverse prognostic factor, whereas RB deletion as a unique abnormality is not associated with adverse prognosis. Leukemia. 2007; 21:143-150.

44. Schmitt CA, McCurrach ME, de Stanchina E, Wallace-Brodeur RR, Lowe SW. INK4a/ARF mutations accelerate lymphomagenesis and promote chemoresistance by disabling p53. Genes Dev. 1999;13:2670-2677.

45. Walkley CR, Shea JM, Sims NA et al. Rb Regulates Interactions between Hematopoeitic Stem Cells and their Bone Marrow Microenvironment. Cell. 2007; 129: 1081-95.

46. MacPherson D, Sage J, Kim T, et al. Cell type specific effects of Rb deletion in the murine retina. Genes and Development. 2004; 18: 1681-1694.

47. Donovan SL, Schweers B, Martins R, et al. Compensation by tumor suppressor genes during retinal development in mice and humans. BMC Biology. 2006; 4: 14.

48. Viatour, P, Somervaille TC, Venkatasubrahmanyan S et al. Hematopoeitic stem cell quiescence is maintained by compound contributions of the retinoblastoma gene family. Cell Stem Cell. 2008; 3: 416-428.

49. Sage, J., A. L. Miller, P. A. Pérez-Mancera, J. M. Wysocki, and T. Jacks. 2003. Acute mutation of retinoblastoma gene function is sufficient for cell cycle re-entry. Nature 424:223-228.

50. Casola S, Cattoretti G, Uytterspro N, et al. Tracking germinal center B cells expressing germ-line immunoglobulin -1 transcripts by conditional gene targeting. PNAS. 2006; 103: 7396-7401.

51. Shackney, SE and Shankey TV. Cell cycle models for molecular biology and molecular oncology: exploring new dimensions. Cytometry. 1999; 35: 97-116.

52. Chau BN, and Wang JY. Coordinated regulation of life and death by RB. Nature Reviews Cancer. 2003; 3: 130-38.

53. Sharpless, NE and Depinho RA. Telomeres, stem cells, senescence and cancer. Journal of Clinical Investigation. 2004;113: 160-68.

54. Delston RB, and Harbour JW. Rb at the interface between cell cycle and apoptotic decisions. Current Molecular Medicine. 2006; 6: 713-18.

55. Ma D, Zhou, P, Harbour JW. Distinct mechanisms for regulating the tumor suppressor and antiapoptotic functions of RB. The Journal of Biological Chemistry. 2003

Table 1

Table 1. *RB1* sequencing summary

SNP ID	NOVEL	rs3092865	NOVEL	rs520342	rs198617	NOVEL	rs198616	NOVEL	NOVEL	rs3092883	rs185587	NOVEL	rs198580	rs4151610	rs4151624	rs3020646	rs3092904
RB1 Location	E2-171	E2+75	E3+37	E3+46	E4+23	E4+121	E5-77	E9-159	E9-183	E10+58	E12-72	E18	E20-77	E24-45	E25-11	E25+33	E26-10
Ref location	47779246	47779618	47814888	47814896	47817359	47817457	47819885	47836872	47836848	47839798	47845470	47925204	47931748	47945452	47948827	47949013	47949482
95295	AA	TT	AA	CC	GG	CC	GG	CC	TT	GG	TT	TT	AA	AA	GG	TT	TT
92896	AA	TT	AA	CC	GG	CC	GG	CC	TT	GG	TT	TT	AA	AA	GG	TT	TT
68319	AA	CT	AA	CC	GG	CC	GG	CC	TT	GG	TT	TT	AG	AG	GG	CT	TT
64511	NN	TT	AA	CC	GG	CC	GG	CC	TT	GG	TT	TT	AA	AA	GG	TT	TT
33172	AA	TT	AA	CT	GG	CC	GG	CC	TT	GG	TT	TT	AA	AA	GG	TT	TT
54092	AA	TT	AA	CC	GG	CC	GG	CC	TT	GG	TT	TT	AA	AA	GG	TT	AT
802718	CC	TT	GG	CC	GG	CC	GG	TT	CC	CC	TT	TT	GG	GG	AA	TT	TT
58762	NN	TT	AA	CC	GT	CC	AG	CC	TT	GG	GG	TT	AG	AA	GG	CC	TT
22848	AA	TT	AA	CC	GG	CC	GG	CC	TT	GG	TT	TT	AA	AA	GG	TT	TT
73586	AA	TT	AA	CC	GG	CC	GG	CC	TT	GG	TT	TT	AA	AA	GG	TT	TT
86267	AA	TT	AA	CT	GG	CC	GG	CC	TT	GG	TT	TT	AA	AA	GG	TT	AT
90866	AA	TT	AA	CC	GG	CC	GG	CC	TT	GG	TT	TT	AA	AA	GG	TT	TT
45980	AA	TT	AA	CC	GG	CC	GG	CC	TT	GG	TT	TT	AA	AA	GG	TT	TT
18467	AA	TT	AA	CT	GG	CC	GG	CC	TT	GG	TT	TT	AA	AA	GG	TT	AT
98461	CC	TT	GG	CC	GG	CC	GG	TT	CC	CC	AA	CC	GG	GG	AA	TT	TT
10901	AA	TT	AA	CC	GG	CC	GG	CC	TT	GG	TT	TT	AA	AA	GG	TT	TT
526983	AA	TT	AA	CT	TT	CC	GG	CC	TT	GG	TT	TT	AA	AA	GG	TT	AA
135980	AA	TT	AA	CC	GG	CC	GG	CC	TT	GG	TT	TT	AA	AA	GG	TT	TT
14851	AA	TT	NN	CC	GG	CC	GG	CC	TT	GG	TT	TT	AA	AA	GG	TT	TT
91369	AA	TT	AA	CC	GG	CC	GG	CC	TT	GG	TT	TT	AA	AA	GG	TT	TT
14823	AA	TT	AA	CT	NN	CC	GG	CC	TT	GG	TT	TT	AA	AA	GG	TT	AT
53628	AA	TT	AA	TT	GG	CC	GG	CC	TT	GG	TT	TT	AA	AA	GG	TT	AA
78826	AA	TT	AA	CT	GG	CC	AG	CC	TT	GG	TT	TT	AG	AA	GG	CT	TT
47250	AA	TT	AA	CT	GG	CC	GG	CC	TT	GG	TT	TT	AA	AA	GG	TT	AT
99070	AA	TT	AA	CC	GG	CC	GG	CC	TT	GG	TT	TT	AA	AA	GG	TT	TT
69606	AA	TT	AA	CT	GG	CC	GG	CC	TT	GG	TT	TT	AA	AA	GG	TT	AT
229077	AA	TT	AA	CC	GG	CC	GG	CC	TT	GG	TT	TT	AA	AA	GG	TT	TT
898125	AA	TT	AA	TT	GG	CC	GG	CC	TT	GG	TT	TT	AA	AA	GG	TT	AA
38633	AA	TT	AA	CT	GG	CC	GG	CC	TT	GG	TT	TT	AA	AA	GG	TT	AT
48128	AA	TT	AA	CC	GG	CC	GG	CC	TT	GG	TT	TT	AA	AA	GG	TT	TT
60196	NN	TT	AA	TT	GG	CC	GG	CC	TT	GG	TT	TT	AA	AA	GG	NN	AA
41153	AA	TT	AA	CC	GG	CC	GG	CC	TT	GG	TT	TT	AA	NN	NN	TT	TT
57457	AA	TT	AA	CC	GG	CC	GG	CC	TT	GG	TT	TT	AA	AA	GG	TT	TT
37804	AA	TT	AA	CC	GG	CT	GG	CC	TT	GG	TT	TT	AG	AA	GG	TT	TT
94368	AA	TT	AA	CC	GG	CC	GG	CC	TT	GG	TT	TT	AA	AA	GG	TT	TT
83958	AA	TT	AA	CC	GG	CC	GG	CC	TT	GG	TT	TT	AA	AA	GG	TT	TT
60430	AA	TT	AA	CC	GG	CC	GG	CC	TT	GG	TT	TT	AA	AA	GG	TT	TT
47313	AA	TT	AA	CC	GG	CC	GG	CC	TT	GG	TT	TT	AA	AA	GG	TT	TT
34667	AA	TT	AA	CT	GG	CC	GG	CC	TT	GG	TT	TT	AA	AA	GG	TT	AT
51925	AA	TT	AA	CT	GG	CC	GG	CC	TT	GG	TT	TT	AA	AA	GG	TT	AT
34124	NN	TT	AA	CT	GG	CC	GG	CC	TT	GG	TT	TT	AA	AA	GG	TT	AT

Novel: SNP's were considered novel if not in pubmed database of *RB1* SNP's
Known SNP reference numbers are listed
RB1 location: SNP location is number of base pairs either before (-) or after an exon (E)
Ref location: Reference location, genomic reference location from NCBI Build 35 genome

Table 2

Table 2. MAF in MGUS/MM compared to HapMap controls

SNP ID	MM CAUC	HAP MAP CAUC	FISHERS Exact Test	MM AA	HAP MAP AA	Fishers Exact Test
	MAF		*P* Value	MAF		*P* Value
rs3092865	0	0	1	0.17	0.203	1
rs520342	0.26	0.25	1	0	0.142	0.585
rs198617	0.046	0	0.018	0.17	0.178	0.593
rs198616	0.015	0	0.281	0.17	nd	N/A
rs198580	0.077	0.008	0.001	0.5	0.433	0.692
rs4151610	0.06	0.008	1	0.17	0	0.032
rs4151624	0.17	nd	N/A	0	0	1
rs3020646	0.03	0	0.07	0.33	0.358	1
rs3092904	0.277	0.258	1	0	0.092	1

MAF indicates minor allele frequency, CAUC: caucasian; AA: African

Table 3

Table 3. Novel Base changes identified in *RB1*

UPN	Gene Location	Chromosome Location	Change
802718	E2-171	47779246	A>C
98461			
802718	E3+37	47814888	A>G
98461			
37804	E4+121	47817457	C>T
98461	E9-183	47836848	T>C
98461	E9-159	47836872	C>T
98461	E18	47925204	T>C

UPN indicates unique patient number; E, exon, Chromosome location based on NCBI Build 35

Table 4

Table 4. Genes with decreased expression in deletion 13 samples

Gene	Gene ID	Score(d)	Fold Change	q-value(%)
TUBGCP3	203690_at	-4.83	0.57	0
RNF6	203403_s_at	-5.68	0.60	0
GTF3A	215091_s_at	-5.77	0.62	0
UBL3	201534_s_at	-4.49	0.63	0
NBEA	221207_s_at	-3.44	0.67	0
ITM2B	217731_s_at	-4.24	0.70	0
RB1	211540_s_at	-2.92	0.74	1.3
HMGB1	216508_x_at	-4.52	0.74	0
MRP63	204387_x_at	-4.48	0.77	0
PSPC1	222612_at	-3.89	0.79	0
CRYL1	220753_s_at	-2.50	0.80	4.06
TPT1	214327_x_at	-3.84	0.85	0
ESD	228162_at	-2.83	0.89	1.72
MTMR6	228789_at	-2.63	0.90	2.73

Genes in bold were identified by Process Control and CBS analysis

Figure 1

Figure 1. RB1 protein levels relate to genomic copy number in MM cell lines

A. Western blot analysis of MM cell lines OPM2, RPMI 8226 (8226), KMS11, LP-1, H929, UTMC2 and U266, using an antibody that detects RB1 independent of phosphorylation status (top, IF-8 antibody). HCT is colon cancer line used for a positive control. Top band is RB1. Non-specific bands are marked by an asterisk. Duplicate blots were probed with a phospho specific RB1 (Serine 807/811: P807/811) antibody (bottom). Actin was used as a loading control. **B.** Representitative FACS analysis of three MM cell lines analyzed for RB1 protein (Phospho RB Serine 807/811). U266 cells have no RB1 protein, LP1 cells have one copy and OPM2 has two.

Figure 2
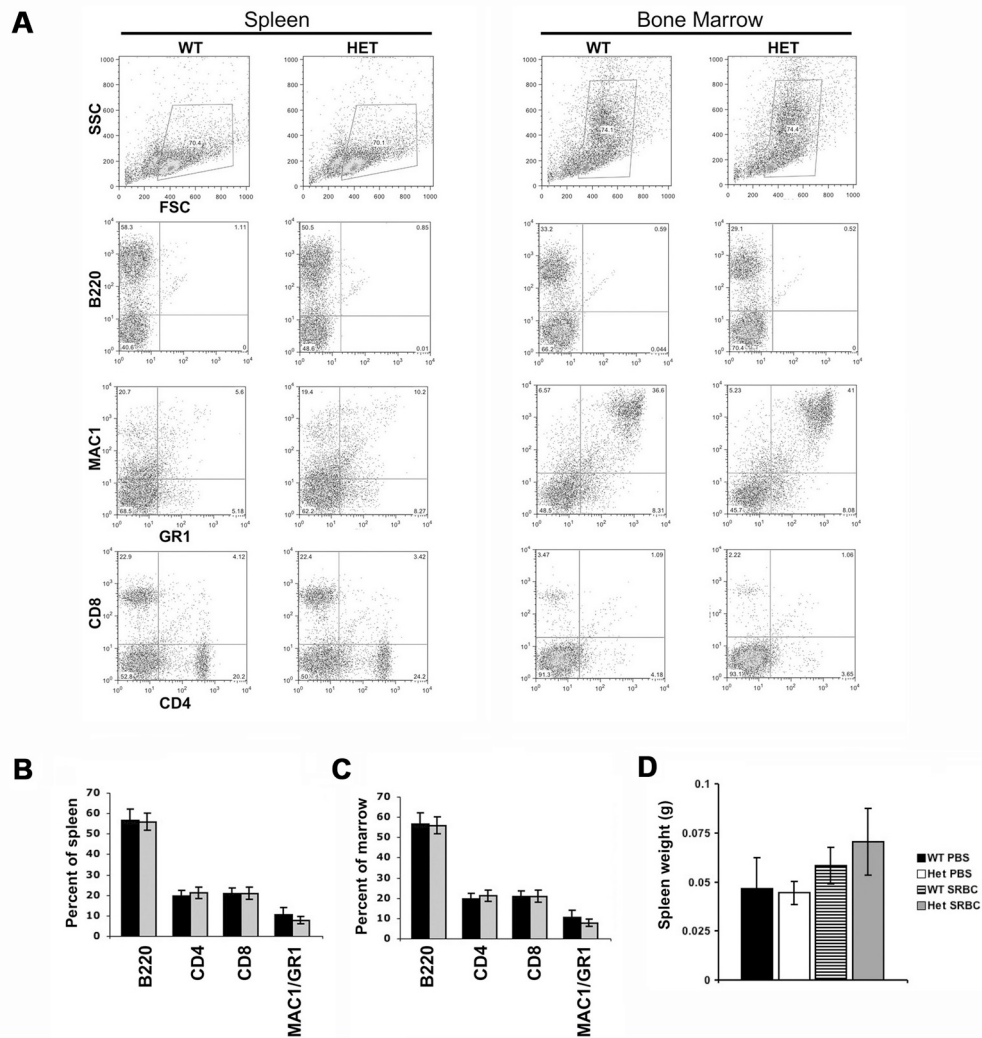
Figure 2. Hematopoeitic cell subsets in *Rb1* WT and HET mice are similar

A. Representative FACS analysis of spleen and bone marrow isolated from *Rb1* WT or HET mice using B cell (B220), T cell (CD4/CD8), and myeloid (MAC1/GR1) markers. Representative plots shown. Compiled FACS analysis of spleen (**B**.) and bone marrow (**C**). Black bars represent WT mice, and gray bars represent HET mice. Error bars are standard deviation. *n*=4, WT; *n*=6, HET

D. Spleen weights of WT or HET *Rb1* mice seven days post treatment with PBS as a control or sheep red blood cells to induce germinal centers

Figure 3

Figure 3. RB1 is expressed in myeloma, but rarely phosphorylated

Shown is a representative patient sample (UPN 35945) that was stained with CD138 (left), total RB1 independent of phosphorylation status (4H1; middle) or phoshorylated RB1 (phospho Serine 807/811).

Table 5

Table 5. Summary of RB1 IHC Analysis in primary patient myeloma samples

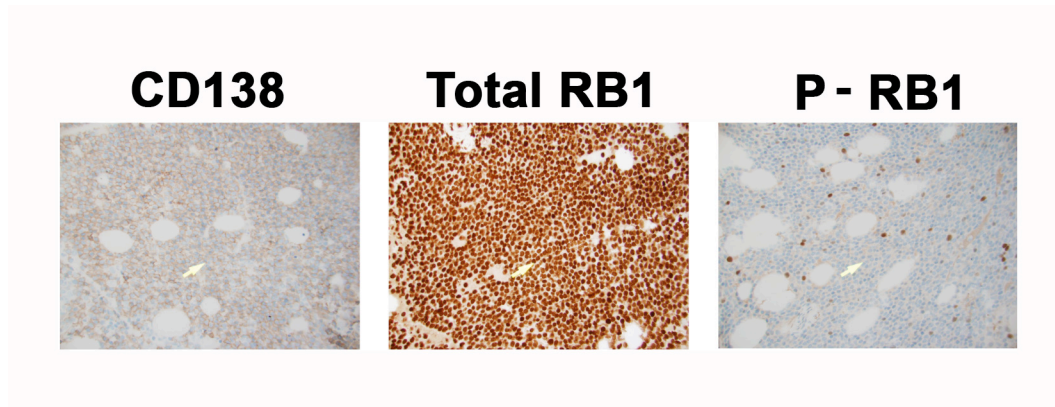| Case #	%CD138	%Total Rb (4H)	Total Rb intens	Overall TRb	%Phosph Rb (PH)	P- Rb intense	Overall PRb	Comment
S06-35945	95	100	3	3+	10	2	1+	PRb+ cells likely not CD138+
S06-1371	90	100	3	3+	10	1	1+	
S06-47375	90	100	3	3+	10	2	1+	
S06-20609	90	100	3	3+	10	2	1+	
S06-4052	90	100	3	3+	20	2	2+	
S06-211	80	100	3	3+	20	2	2+	
S06-25893	80	100	3	3+	10	2	1+	PRb+ cells likely not CD138+
S06-46900	70	100	3	3+	20	2	2+	
S06-39548	70	100	3	3+	40	2	2+	?Cytoplasmic PRb stain - likely high background
S06-16057	70	0	0	0	30	2	2+	TRb IHC may not have worked
S06-39912	60	100	3	3+	20	2	2+	CD138 focally 90% - these areas PRb neg
S06-15028	60	90	3	3+	20	2	2+	
S06-30911	60	100	3	3+	30	2	2+	
S06-20415	50	0	0	0	30	2	2+	TRb IHC may not have worked
S06-33974	40	100	3	3+	50	2	2+	
S06-41569	40	0	0	0	30	2	2+	TRb IHC may not have worked
S06-32384	30	100	3	3+	30	2	2+	
S06-43365	20	100	3	3+	30	2	2+	
S06-45334	20	100	3	3+	40	2	2+	
S06-40297	20	100	3	3+	40	2	2+	?Cytoplasmic PRb stain - likely high background
S06-25529	20	100	2	3+	30	2	2+	
S06-29254	10	100	3	3+	30	2	2+	
S06-37173	10	100	3	3+	50	2	2+	
S06-46199	10	100	3	3+	30	2	2+	
S06-13807	10	100	3	3+	30	2	2+	

Total Rb stains all nucleated cells, including megas and osteocytes. Phosph Rb stains mainly erythroid lineage and does not stain CD138+ cells.

Chapter 4

Characterization of Neurobeachin (*NBEA, BCL8B)* in myeloma and hematopoeisis

4.1 Abstract

A role potential role for NBEA in myeloma was revealed by its identification at sites of interstitial deletions in DNA isolated from primary patient MGUS and MM samples (**Chapter 2**). We found NBEA was decreased in patient samples with monosomy 13 *vs*. those that retained both copies, but in some MM cell lines and patient samples, NBEA expression was high. RNAi mediated knockdown of NBEA in OPM2 cells that express high endogenous NBEA grew poorly compared to controls, suggesting these cells required NBEA for growth. Our expression analysis of Nbea in the hematopoietic system revealed it was expressed in spleen in thymus. Colony assays performed on $Nbea^{-/-}$ and $Nbea^{+/+}$ fetal liver cells revealed no differences between genotypes, suggesting hematopoietic progenitor cells in $Nbea^{-/-}$ mice are functional. To determine if *Nbea* was required for adult hematopoeisis, we performed fetal liver transplants using $Nbea^{+/+}$ and $Nbea^{-/-}$ donor cells and found *Nbea* was dispensable for engraftment and basal adult hematopoietic development.

4.2 Introduction

4.2A Neurobeachin *(NBEA, BCL8B)* is a BEACH domain containing protein implicated in vesicle trafficking

We identified interstitial deletions affecting *NBEA*, and found it to be the sole gene affected in a minimally deleted region at 13q13 in DNA isolated from patients with PC dyscrasias (**Chapter 2**). *NBEA* is large; it's genomic sequence spans 0.73Mb and produces a 9.5Kb transcript encoding a 327KDa protein. *NBEA* has homologs in mice (*Nbea*), *C elegans* (*Sel-2*), which is shared with *LRBA* [1], and *drosophilia* (*rugose*, DAKAP550). NBEA protein is comprised of a BEACH, Pleckstrin Homology (PH), WD40 and a Protein Kinase A (PKA) binding domains (**Figure 1**).

The BEACH domain was first discovered in the protein encoded by the Lysosomal Trafficking Regulator gene (*LYST, CHS1*). Homozygous deletions within the CHS coding sequences resulting in expression of truncated proteins missing the BEACH domain are found in patients with Chediak-Higashi Syndrome (CHS) [2-4]. This is a rare, autosomal recessive disorder characterized by variable albinism, bleeding tendency, progressive neurologic abnormalities and severe immunodeficiency with lack of natural killer cell activity. The cellular hallmark of CHS is enlarged lysosomal and lysosomal related organelles in almost all granulated cells [5-7], suggesting the BEACH domain regulates vesicle size, structure or function [5,7].

Other mammalian BEACH encoding proteins are implicated in aspects of vesicle function [5]. LPS-Responsive Vesicle Trafficking, Beach and Anchor containing (*LRBA, BGL, CDC4L*), which like *NBEA*, encodes a Protein kinase A (PKA) binding domain (discussed in section 4.2), is implicated in vesicle release in polarized cells [8]. Neutral Spingomyelinase Activation Associated Factor (*NSMAF, FAN*) encoding the protein FAN is implicated in TNF signaling and activation of neutral sphingomyelinase. *Nsmaf* deficient mice have slightly enlarged lysosomes [9]. The protein encoded by the WD Repeat and FVYE Domain-containing 3 (*WDFY3, ALFY*) gene binds Phosphoinositol 3 phosphate that regulates endocytic and autophagic trafficking [5]. Finally, *NBEA* is implicated in induced vesicular release at the neuromuscular junction [10, 11].

Crystal structure analysis of the BEACH domain and the 130 amino acids N-terminal to it revealed it is situated C-terminal to a structurally conserved PH domain [12]. These two domains physically interact, suggesting they function as a single unit [12]. Although PH domains can bind either to fatty acids or proteins, the interaction of the PH domain with the BEACH domain physically blocks the alpha helix known to mediate fatty acid binding, suggesting the PH domain of NBEA mediates protein-protein interactions [12].

4.2B NBEA is a Protein Kinase A (PKA) Anchoring Protein (AKAP)

The *NBEA* gene encodes a transcript generating a protein that includes a PKA binding site. The term PKA comprises its enzyme complex composed of four

regulatory subunits (RIα, RIβ, RIIα and RIIβ) and two catalytic subunits (Cα and Cβ) with serine/threonine kinase activity that is activated in response to increases in cAMP. Murine Nbea binds to PKA regulatory subunits RIIα (Kd: 10nM) and RIIβ (Kd: 30nM) [10] and since murine and human PKA regions are highly conserved, human NBEA is predicted to bind PKA. Neurobeachin is therefore characterized as an AKAP that localizes PKA to correct cellular locations such that upon cAMP increases, PKA signaling only occurs at correct locations, facilitating appropriate phosphorylation of downstream targets.

4.2C NBEA expression is highest in brain

NBEA transcripts and protein are detected at very high levels in both mouse and human brain [10-13; our own data). Lower, but relatively robust transcripts are found in the uterus, adrenal gland, ovary, testes, lung, and kidney with even lower expression in heart, spleen, stomach, and small intestine [11,13]. Mice that lack *Nbea* die immediately after birth due to a block in synaptic transmission at the neuromuscular junction, supporting a functional role in the nervous system [11].

A potential role for NBEA in myeloma was revealed by its identification at sites of interstitial deletions in DNA isolated from primary patient MGUS and MM samples (**Chapter 2**). A prior study showed increased NBEA expression with advancing disease stage in primary plasma cell dyscrasias [14], and in another study was one of a small set of genes whose expression was *increased* in patient

samples harboring single chromosome 13 deletions [15]. We found NBEA was decreased in patient samples with monosomy 13 *vs*. those that retained both copies, but in some MM cell lines and patient samples, NBEA expression was high. RNAi mediated knockdown of NBEA in OPM2 cells (that express high endogenous NBEA) grew poorly compared to controls, suggesting these cells require NBEA for growth. Our characterization of Nbea expression in the hematopoietic system revealed it was expressed in spleen in thymus. Colony assays performed on Nbea$^{-/-}$ and Nbea$^{+/+}$ fetal liver cells revealed no differences between genotypes, suggesting hematopoietic progenitor cells in Nbea$^{-/-}$ mice are functional. To determine if *Nbea* was required for adult hematopoeisis, we performed fetal liver transplants using *Nbea*$^{+/+}$ and *Nbea*$^{-/-}$ donor cells that revealed *Nbea* was dispensable for engraftment and basal adult hematopoietic development.

4.3 Methods

4.3A Microarray Expression Analysis

Two independent microarray datasets were analyzed. First, a Mayo Clinic dataset [16] included 162 samples (101 MM, 24 SMM, 22 MGUS, and 15 normal PC's; GEO GSE6477; chromosome 13 status was determined by FISH). Second, we used a multiple myeloma research consortium (http://www.themmrc.org; MMRC) dataset that included 100 MM samples (Chromosome 13 status was determined by aCGH).

Expression values were derived against a PM/MM difference background using Robust Multichip Average (RMA) [17]. Present/Absent probes were called using Affymetrix Microarray Suite version 5. Only probes detected in at least one sample were used in subsequent comparisons. In pooled Chromosome 13 Deletion *versus* no Deletion comparisons, Significance Analysis of Microarrays (SAM), [18] was used to detect differentially expressed genes based on a q-value of less than 5%. SAM was run with 100 permutations for correction of False Discovery Rate. These genes were clustered and visualized in DChip [19] (http://www.dchip.org). aCGH data was first smoothed with region=2, outlier scale =4, smoothing SD=2 and trimming proportion of 0.025. CBS was then run with default parameters (alpha=0.01, window.size= NULL, with 10000 permutations).

4.3B Q-RT-PCR

RNA was isolated from whole tissues harvested from 4 week-old C57BL/6 mice using Trizol Reagent (Roche Molecular Biochemicals, Indianapolis, IN) per manufacturer's instructions. First strand cDNA was generated using SuperScript First Strand Synthesis Kit (Invitrogen, Carlsbad, CA) per manufacturer's directions. Prior to lysis in trizol reagent, red blood cells were removed from bone marrow by brief incubation in hypotonic lysis buffer (150 mM NH_4Cl, 10 mM $KHCO_3$, 0.1 mM EDTA, pH 7.4). Standard curves were made using cDNA generated from brain RNA (input range: 25ng to 0.3ng). Standard curve graphs were generated by plotting the cycle threshold (Ct) versus the log of DNA input concentration and reactions analysed using the standard curve method (www.appliedbiosystems.com). Assays were performed with Taqman Universal PCR Master Mix with the total volume of each reaction 25μl. Primer concentration: 900nM; probe concentration: 2.5mM, 12.5ng template. Experimental reactions were run in triplicate and presented as the average of two separate experiments. Error bars are standard deviation of duplicate runs. Reactions were run on 7300 Real Time PCR System, and analyzed using 7300 System Software (Applied Biosystems, Foster City, CA). Primers: Nbea Exon6F: A5'GG TTT CCA GCA CTG TGT GAA GT3' Nbea Exon7R: 5'TGT GGA CGA TGC TGA TCA TGT3' Nbea Probe 5'6-FAMTGA TTT CCA GCC TCG CAA GTG36TAM3' GapdhF 5'TGC ACC ACC AAC TGC TTA G3' GapdhR 5'GGA TGC AGG GAT GAT GTT3' Gapdh Probe5'6FAMCAG AAG ACT GTG GAT GGC CCC TC36TAM3'.

113

4.3C Western Blot Analysis

Tissues for generation of cell lysates were harvested from 5-6 week old C57BL/6 mice. Lysates were isolated from mouse whole tissues by cutting tissues with scissors in tissue lysis buffer (0.32M sucrose, 1mM EDTA, 10mM Tris pH 7.6, with inhibitors as described [20] and cells homogenized for 20 seconds. Samples were placed on ice for ten minutes, and spun to pellet unlysed cellular debris. Lysates were run on gels with three layers: 4% stack, 5%resolving and 9% resolving gels. The NBEA polyclonal antibody was generously provided by Manfred Kilimann (Department of Cell and Molecular Biology, Uppsala University, Sweden).

4.3D Lentiviral infection and knockdown of NBEA

Lentiviral vectors encoding siRNA targets to NBEA and controls were purchased from Sigma (St. Louis, MO). Si1: CGGGATGAAATTCGCAGTGTT Exon 2; Si2: CCGACTCTTTGCAGTGAATA Exon 51; Si3: GGACTACAATGTTTCGTCGTATT Exon 24. Lentivirus was generated using calcium phosphate mediated transfection of 293T cells using the purchased expression vectors and packaging sequences. Viral supernatents were used to infect OPM2 or LP1 cells for 1.5hours and 2500rpm. One day after infection, cells were plated in (0.5μg/ml) puromycin and after 1 week (when all mock infected cells treated with puromycin were dead), 100,000 cells were plated in triplicate and counted using trypan blue exclusion daily (samples were blinded to person counting).

4.3F Fetal liver transplants and colony assays

Nbea$^{+/+}$ (WT), Nbea$^{+/-}$ (HET) and *Nbea*$^{-/-}$ (KO) or fetal livers were obtained from day 13.5-15.5 d.p.c. fetuses. These were generated by timed matings of *Nbea* heterozygous mice (breeder pairs were allowed to breed for three nights, and then male was removed). Fetuses were placed in PBS, and fetal livers isolated by dissection. Fetal livers were placed in 1ml Fetal Liver Transplant Media (FLTM; RPMI containing 1% pen/strep, 20% fetal bovine serum, 10 ng/mL IL6, 100 ng/mL SCF, 50 ng/mL FLT3, and 10 ng/mL Tpo), passed through a 27.5 gauge needle attached to a 1 ml syringe to break up cell clumps and red blood cells lysed using hypotonic lysis buffer (150 mM NH$_4$Cl, 10 mM KHCO$_3$, 0.1 mM EDTA, pH 7.4). Cells were incubated for 48 hours at 37°C at 5% CO$_2$ in FLTM and 1.5-2 X 10^6 cells were injected by lateral tail-vein into lethally irradiated (1100 or 1200 rads) Ly5.1 mice (to facilitate evaluation donor chimerism). On the day of transplant, 5X10^5 (M3630) or 2X10^4 (M3434) were plated in triplicate into methocellulose (Stem Cell Technologies, Vancouver, Canada) and counted on day seven.

4.3E Flow Cytometric analysis

Spleen, bone marrow and blood were harvested from recipient mice 8-10.5 weeks post transplant. Single cell suspensions of spleen cells were made by passing cut-up spleens through 100μm cell strainer (BD Falcon, Bedford, MA) and spun at 1500 rpm. RBC's were lysed as above. Single cell suspensions were stained with B220, CD43, DX1, TER119, MAC1, GR1, CD23, IgM, CD4, and CD8 (ebiosciences, San Diego, CA) for 30 minutes on ice. Data were

collected using Cytomics FC 500 (Beckman Coulter, Fullerton, CA). Figures were

prepared using FloJo software (Tree Star, San Carlos, CA).

4.4 Results

4.4A *NBEA* expression in MM samples with monosomy 13

We identified interstitial deletions affecting *NBEA*, and found it to be the sole gene affected in a minimally deleted region at 13q13 in DNA isolated from patients with PC dyscrasias (**Chapter 2**). *NBEA* has no known role in myeloma, although transcripts assessed by expression microarrays were associated with disease progression in myeloma [14]. We sought to validate NBEA as a deletion target by characterizing its expression in MM cells. We anticipated that patient samples harboring monosomy 13 would have lower *NBEA* expression than patient samples without chromosome 13 deletions. We analyzed two large microarray data sets (methods; total n=262) for expression changes based on chromosome 13 status. In both datasets, *NBEA* transcript levels were significantly decreased in patient samples with monosomy 13 *versus* those without, revealing *NBEA* expression levels were related to genomic copy number (**Table 1**).

We developed a quantitative real-time reverse transcriptase PCR (Q-RT-PCR) assay to quantitate *NBEA* transcript expression, and first assayed a panel of MM cell lines. Some myeloma cell lines expressed low levels of *NBEA* transcript, as anticipated, but surprisingly, several expressed *NBEA* at high levels (**Figure 2).** We found UTMC2 cells expressed *NBEA* at levels three times higher than in a human brain sample, where *NBEA* is normally most highly expressed [10-13, our own data]. OPM2 cells had levels 30% of brain while U266 had levels 18% of

brain. RPMI-8226 and LP1 had low/undetectable *NBEA* transcripts (**Figure 2).** We next examined NBEA protein levels in these cell lines by Western Blotting of whole cell lysates. Consistent with the Q-RT-PCR data, we found NBEA protein expression varied significantly between cell lines (**Figure 2**). The UTMC2, OPM2, and H929 cell lines had the highest NBEA protein levels, while RPMI 8226, U266 and LP1 had low to undetectable NBEA protein.

Finally, we measured *NBEA* transcripts and protein levels in a set of CD138-enriched primary MM bone marrow samples (n=14) using Q-RT-PCR and Western blotting. We found *NBEA* transcript expression varied significantly across samples and, consistent with our MM cell line data, some MM patient samples, even with monosomy 13, harbored high *NBEA* transcript levels (**Figure 2**). Because of the large number of CD138 cells needed for Western analysis we were forced to analyze a separate set of MM patient samples by Western blot (only sample 14216 had both RNA and protein data; expression was low by both analyses). Consistent with the RNA data, Western blotting using an NBEA-specific antibody demonstrated that NBEA protein was strikingly dysregulated in patient MM cells (**Figure 2**).

4.4B Decreased NBEA expression caused a reduction in OPM2 cell growth

Our initial NBEA expression data revealed it was robustly expressed in a subset of MM cell lines including OPM2, UTMC2, and H929. We hypothesized high levels of NBEA would be required for MM cell growth. To address this hypothesis, we used SiRNA-mediated knockdown of NBEA in OPM2 cells.

OPM2 cells were infected with a lentivirus expressing a double- stranded small interfering RNA (siRNA) directed to *NBEA,* or vector alone. Efficient knockdown of NBEA protein with three separate NBEA silencing target sequences (siRNA1, siRNA2, and siRNA3) was demonstrated (range: 11-72% of vector; **Figure 3**). After infection and selection in puromycin, 100,000 cells from each construct were plated in triplicate and live cells were counted by trypan blue exclusion for five days. Compared to empty vector control (**Figure 3),** and a vector expressing a non-targeting siRNA (not shown), OPM2 cells infected with lentivirus expressing siRNA targeted to NBEA revealed a dramatic decrease in growth rate that was most pronounced with siRNA2, which caused the most efficient reduction in NBEA protein (**Figure 3**).

To confirm this result was specific to cells expressing high levels of NBEA, the experiment was repeated in LP1 cells that express low levels of NBEA protein (**Figure 2**). We found that although the cells infected with NBEA siRNA displayed reduced growth compared to vector control (67% or 63% of control cells for Si1 and Si2, respectively on day 5 of culture), these cells grew much better than the OPM2 cells (51% or 20% for Si1 and Si2, respectively on day 5 of culture, **Figure 3**). The slightly reduced growth indicates either a low level of siRNA toxicicity in LP1 cells, or that reduction of even the low levels of NBEA was enough to generate a slight growth disadvantage. Infection of LP1 cell lines with siRNAs targeting *RB1* (not shown) did not result in a growth disadvantage, suggesting the reduced growth is not the result of siRNA toxicity. Although the mechanism

of altered growth in OPM2 cells is not currently fully understood, these data suggest expression of NBEA is required for normal growth of OPM2 cells and that expression of NBEA may play a role in tumor maintenance, or that NBEA provides a required survival signal.

4.4C Nbea is expressed in spleen and thymus

Because *NBEA* is dysregulated in plasma cell dyscrasias, we sought to determine its expression levels in hematopoietic tissues. Qualitative analysis has been performed on a tissue panel including spleen [11,13], but other hematopoietic cell types including bone marrow and thymus have not been examined. To quantitatively assess *Nbea* transcript levels, we performed Quantitative Real-Time PCR (Q-RT-PCR) on cDNA isolated from a panel of murine tissues including heart, lung, kidney, liver, and the hematopoietic tissues bone marrow, spleen and thymus (**Figure 4**). Consistent with prior reports [11,13], *Nbea* transcript levels were higher in lung, kidney and heart tissues than liver, validating our Q-RT-PCR system. We found spleen and thymus had higher *Nbea* transcript levels (*Nbea:Gapdh* ratio: 0.1 and 0.055, respectively) compared to liver (*Nbea:Gapdh* ratio: 0.03) and *Nbea* was almost undetectable in bone marrow (*Nbea:Gapdh* ratio: 0.0009).

To determine if Nbea protein levels in murine tissues were related to transcript levels, Western Blot analysis was performed on whole tissue lysates isolated from kidney, liver, thymus and spleen. We found Nbea protein in kidney, thymus,

and spleen but very low protein in liver, consistent with the Q-RT-PCR analysis (**Figure 4**). No Nbea protein was detected in *Nbea*$^{-/-}$ fetal brain tissue but robust detection of Nbea was found in adult and fetal brain lysates isolated from control mice, as expected.

4.4D *Nbea* is not required for myeloid or pre-B cell colony formation

Because we identified NBEA as a target in the B cell cancer myeloma and also showed it was expressed in hematopoietic tissues, we hypothesized its expression would be required for hematopoietic development. Since *Nbea*$^{-/-}$ mice die at birth [11], we performed timed breedings to isolate day 14.5-15.5 d.p.c. fetal liver cells since that is time of maximal hematopoietic stem cell activity in developing embryos [21,22]. *Nbea*$^{+/+}$, *Nbea*$^{+/-}$ and *Nbea*$^{-/-}$ fetal liver cells were plated in directly into methocellulose cultures containing either myeloid or pre-B cell cytokines (**Figure 5,** methods). We found *Nbea*$^{-/-}$ and Nbea$^{+/-}$ fetal liver cells were as proficient as Nbea$^{+/+}$ fetal liver cells in their ability to form colonies of both myeloid and pre B cell type, suggesting hematopoietic progenitor cells in Nbea$^{-/-}$ mice are functional.

4.4E *Nbea* is dispensable for engraftment and basal adult hematopoeitic development

To determine the requirement of *Nbea* to *in vivo* baseline hematopoietic engraftment and development, we performed fetal liver transplantation assays. Fetal liver cells isolated from Nbea$^{+/+}$ or *Nbea*$^{-/-}$ cells (Ly5.2/CD45.2) were

injected into lethally irradiated (Ly5.1/CD45.1) recipients and mice were analyzed 8.5-10.5 weeks post transplant. PCR performed on DNA isolated from fetal liver cells and embryonic tissue, and Western blot analysis performed on fetal brain tissue confirmed appropriate genotypes (**Figure 5**). The Ly5.2/Ly5.1 (common leukocyte antigens) were used to quantitate donor chimerism. We found on average (92%, 86%, 90%) percent donor (Ly5.2) cells in blood, spleen and bone marrow, respectively, demonstrating successful engraftment (**Figure 6,** data not shown).

Peripheral white blood counts were similar in recipient mice injected with either $Nbea^{+/+}$ or $Nbea^{-/-}$ donor cells (WT mean: 8.25k/μl, range 5.38-10.58; KO mean: 5.9k/μl, range 3.86-7.24, n=4 both groups), as were spleen weights (WT mean: 0.029g, range 0.027-0.03; KO mean: 0.033g, range 0.028-0.043, n=4 both groups). To examine whether there were differences in cell type distribution, FACS analysis was performed in bone marrow and spleen. In bone marrow, we found similar numbers of myeloid (GR1/Mac1), T cells (CD4, CD8), B cells (B220), NK cells (DX5) and erythroid (Ter119) cells in both WT and KO chimeras (**Figure 6**).   In spleen, we also found similar numbers of all cellular subtypes listed above, although in one outlier mouse, we saw increased Ter119 in an $Nbea^{-/-}$ reconstituted chimera (not shown).

We examined further the B cell compartment since NBEA expression is dysregulated in PC dyscrasias. To this end, spleen cells were stained with IgM,

CD23 and CD43. IgM marks splenic B cells, which can be further divided into Follicilar (IgM+CD23+), Marginal Zone and Immature B cells (IgM+CD23-CD43-), and B-1 cells (IgM+CD23-CD43+). We found similar numbers of these B cell subsets in recipient mice of both genotypes, suggesting *Nbea* was dispensable for basal B cell development (**Figure 6**). Together, although *NBEA* is dysregulated in MM, and expressed in hematopoietic tissues, *Nbea* was dispensable for engraftment and basal adult hematopoietic development including formation of mature B, T, NK, and myeloid cells when assayed in steady-state conditions. Future experiments are required to assess the functional capabilities of these cells in stress conditions.

4.5 Discussion

The reduced expression of NBEA in samples harboring monosomy 13 suggests *NBEA* is a novel tumor suppressor gene.

A functional role for *NBEA* in MM was suggested by the dysregulation of its expression in MM patient samples. DNA microarray data from a large number of patient samples (n=262) demonstrated that compared to patients with normal chromosome 13, there was a decrease in *NBEA* expression in patient samples harboring single copy loss of *NBEA*. These data suggest that *NBEA* may be a novel tumor suppressor gene in MM.

To our surprise, our Q-RT-PCR and Western blot analysis performed on a separate cohort of MM samples revealed that some patients, even with monosomy 13, harbored very high NBEA expression, suggesting instead a pro-tumor role for NBEA in MM (**Figure 3)**. However, inactivating mutations in the p53 tumor suppressor gene are often associated with high p53 expression [23], so these data may still be consistent with a role for *NBEA* as a tumor suppressor. Sequencing of *NBEA* genes in MM patient samples will be required to prove that *NBEA* mutations occur in myeloma that potentially result in expression of functionally null NBEA protein.

Mice heterozygous for tumor suppressor genes are often tumor prone. For example, *Rb1* heterozygous mice develop pituitary tumors that have undergone

mutation at the remaining allele [24]. We are currently aging a cohort of $Nbea^{+/-}$ and $Nbea^{+/+}$ mice (*n=15* for each genotype) to determine if the $Nbea^{+/-}$ mice succumb to tumors. The oldest mice are 587 days old and appear healthy, arguing against a tumor- suppressor function for *Nbea*. Mating *Nbea* heterozygous mice to tumor prone strains can be used to determine if decreased *Nbea* reduces time to disease onset or increases disease severity compared to wild type controls. Eμ-XBP-1 mice develop MGUS and progress to MM with lytic bone lesions [25]. If Nbea functions as a tumor suppressor, Eμ-XBP1 mice mated to $Nbea^{+/-}$ mice are predicted to succumb to disease with decreased latency or increased severity.

Since *Nbea* null mice die at birth [11], generation of mice with conditional deletion of *Nbea* in plasma cells is required to determine the effects of plasma cell specific deletions of *Nbea*. This can be accomplished by generating $Nbea^{Flox/Flox}$ mice, and then breeding them to the Cγ1-CRE mice, which express CRE in post germinal center plasma cells upon antigen stimulation [26]. Analysis of Cγ1-CRE $Nbea^{Flox/Flox}$ and Cγ1-CRE $Nbea^{+/+}$ plasma cells will determine whether deletion of *Nbea* specifically in plasma cells alters that compartment.

Robust detection of NBEA in MM suggests an oncogenic function

On the other hand, the high-level NBEA expression detected in a subset of MM primary samples and cell lines supports the hypothesis that NBEA, when

expressed, plays a pro-tumor role in PC dyscrasias. A prior study showed increased *NBEA* expression with advanced disease stage in primary plasma cell dyscrasias [14]. Furthermore, *NBEA* was one of a small set of genes whose expression was *increased* in monosomy 13 patient samples in another study [15]. *Nbea* was upregulated almost seven fold in mature versus less mature B cell tumors in two separate mouse models [27]. In our microarray study, although most patient samples with deletion 13 revealed decreased *NBEA* levels, there were identifiable outliers with robust expression of *NBEA* (**Figure 2**, not shown). Additionally, Q-RT-PCR and Western Blot analysis on a subset of patient samples expressed high levels of NBEA, and a number of those patient samples had poor prognosis, suggesting a potential association. Large-scale analysis of NBEA (via Q-RT-PCR or Western blotting) is needed in uniform patient groups (i.e. with similar treatment regimens) to address the hypothesis that elevated expression of NBEA relates to poor patient outcome.

Examining functional properties of genes related to *NBEA* can shed insight to the hypothesis that NBEA functions as an oncogene. *NBEA* shares 62% sequence identity at the amino acid level to *LRBA*, a homolog encoding both a BEACH and PKA domain, and is implicated in cancer cell growth [28]. Knock-down of *LRBA* in cancer cell lines decreased the growth of cells in culture, and was found to be upregulated by E2F and downregulated by P53. These authors proposed that *LRBA* functions as an oncogene by facilitating EGFR [28]. Knockdown of NBEA in OPM2 cells led to reduced growth (**Figure 3**). We have undertaken the task of

subcloning the entire *NBEA* cDNA for use in overexpression studies. We initially planned on using a retroviral mediated high level expression and bone marrow transplantation system to express NBEA in mouse hematopoietic cells, but have been unable to accomplish this, since the large size of *NBEA* has prevented generation of high-titer retrovirus. We are currently generating a DNA construct to direct expression of NBEA to B cells using the Eμ regulatory sequences in a transgenic mouse model.

The requirement of NBEA for OPM2 growth suggests a survival function.

Our data that OPM2 cells grew poorly when NBEA levels were decreased, suggests NBEA provides a survival signal. The interpretation of this data is confounded by the fact that until sequenced, we do not know if wild type or mutated NBEA protein is expressed in OPM2 cells (and in samples isolated from patient with PC dyscrasias). However, the conclusion remains the same: cells that express NBEA required its expression for growth. It is an unanswered question as to what cellular function NBEA is providing to these cells (discussed further in **Chapter 5**).

***Nbea* is dispensable for adult hematopoietic engraftment and development in fetal liver transplant system**

We showed Nbea was expressed in spleen and thymus tissues in steady state conditions. IHC staining for Nbea in spleen sections will determine the spleen localization of Nbea. Also, experiments are underway to sort spleen cell subsets

127

based on cell surface expression of cell type specific markers (GR-1, B220, CD4, CD8, DX5) followed by Q-RT-PCR. Because Nbea is dysregulated in myeloma, we hypothesize Nbea is expressed in plasma cells. To determine if Nbea is expressed in plasma cells, mice will be challenged with sheep red blood cells and plasma cells will be sorted using cell surface markers PNA/B220 one week post injection when formation of spleen GCs are maximal [29]. Q-RT-PCR will be used to quantitively assess Nbea expression in these cells.

We showed *Nbea* was dispensable for engraftment and basal adult hematopoietic development including formation of mature B, T, NK, and myeloid cells when assayed in steady-state conditions (**Figure 5,6**). This was somewhat surprising based on the finding Nbea was expressed in spleen (**Figure 4**). However, we did not examine plasma cell development or function in our fetal liver transplantation assay. Therefore, it remains a possibility Nbea has a function in plasma cells (perhaps by promoting plasma cell differentiation or production of class switched antibodies).

To test the hypothesis *Nbea*$^{-/-}$ plasma cells have defects in germinal center formation, Nbea KO and Nbea WT chimera reconstituted mice will be challenged with SRBC, and flow cytometry for detection of germinal center plasma cells (PNA+/B220+) will be performed [29]. If NBEA functions in vesicle traffic or PKA mediated regulation of AID in class switch recombination (CSR) or secretion, *Nbea* null plasma cells may have deficiencies in antibody formation and/or

secretion. To assess this, we will use our fetal liver transplantation system to generate mice with null or wild type *Nbea* hematopoietic systems**.** *In vivo* analysis of basal CSR will be assessed by performing ELISA assays on serum and levels of IgM, IgG1, IgG2a, IgG2B, IgG3 and IgA will be determined [30]. If Nbea null chimeras are deficient in CSR, it predicts detection of IgM (which does not undergo CSR), but not the other isotypes. If there are secretion defects, detection of all antibody isotypes is predicted to be low/undetectable.

To assess CSR in an antigen stimulated system, mice will be injected with SRBC and serum will be subject to ELISA for IgM and IgG1 over a three-week time course. *In vitro* assessment of class switch recombination will be performed by isolating splenocytes from engrafted mice (*Nbea*$^{+/+}$ and *Nbea*$^{-/-)}$ by stimulating purified B cell splenocytes with LPS, LPS and Il-4, pr LPS and TGFβ and then quantitating antibody isotypes in culture supernatents by ELISA as described above [27, 30, 31].

4.6 Acknowledgements

4.7 References

1. DeSouza N, Vallier LG, Fares H, et al. SEL-2 SEL-2, the *C. elegans* neurobeachin/LRBA homolog, is a negative regulator of *lin-12/Notch* activity and affects endosomal traffic in polarized epithelial cells. Development. 2007; 134: 691-702.

2. Perou CM, Moore KJ, Nagle DL et al. Identification of the murine *beige* gene by YAC complementation and positional cloning. Nature Genetics. 1996; 13: 303-08.

3. Nagle DL, Karim MA, Woolf EA et al. Identification and mutation analysis of the complete gene for Chediak-Higashi syndrome. Nature Genetics. 1996; 14: 307-11.

4. Certain S, Barrat, F, Pastural E et al. Protein truncation test of LYST reveals heterogeneous mutations in patients with Chediak-Higashi syndrome. Blood. 2000; 95: 979-83.

5. Kaplan J, De Domenico I and Ward DM. Chediak-Higashi syndrome. Current Opinion in Hematology. 2008; 15: 22-29.

6. Westbroek W, Adams D, Huizing M, et al. Cellular defects in Chediak-Higashi Syndrome correlate with the molecular genotype and clinical phenotype. Journal of Investigative Dermatology. 2007; 127: 2674-77.

7. Karim M, Nagle DL, Kandil HH et al. Mutations in the Chediak-Higashi syndrome gene (CHS1) indicate requirement for the complete 3801 amino acid CHS protein. Human Molecular Genetics. 1997; 6: 1087-89.

8. Wang JW, Howson J, Haller E et al. Identification of a novel lipopolysaccharide-inducable gene with key features of both A kinase anchor proteins and chs2/beige proteins. Journal of Immunology. 2001; 166:4586-95.

9. Mohlig H, Mathieu S, Thon L et al. The WD repeat protein FAN regulates lysosome size independent from abnormal downregulation/membrane recruitment of protein kinase C. Exp. Cell Research. 2007; 313: 2703-18.

10. Wang X, Herberg FW, Laue MM et al. Neurobeachin: a protein kinase A anchoring beige/Chediak-higashi protein homolog implicated in neuronal membrane traffic. Journal of Neuroscience. 2000; 20: 8551-65.

11. Su Y, Balice-Gordon RJ, Hess DM et al. Neurobeachin is essential for neuromuscular synaptic transmission. Journal of Neuroscience 2004; 24: 3627-36.

12. Jogl G, Shen Y, Gebauer D, et al. Crystal structure of the BEACH domain reveals an unusual fold and extensive association with a novel PH domain. EMBO. 2002; 21: 4785-95.

13. Dyomin V, Chaganti SR, Dyomina K, et al. *BCL8* Is a novel, evolutionarily conserved human gene family encoding proteins with presumptive protein Kinase A anchoring function. Genomics. 2002; 80: 158-65.

14. Zhan F, Barlogie B, Arzoumanian V, et al. A gene expression signature of benign monoclonal gammopathy evident in multiple myeloma is linked to good prognosis. Blood. 2006; 109: 1692-1700.

15. Walker BA, Leone PE, Jenner MW, et al. Integration of global SNP-based mapping and expression arrays reveals key regions, mechanisms, and genes important in the pathogenesis of multiple myeloma. Blood. 2006;108:1733-1743.

16. Chng WJ, Kumar, S, Van Wier S et al. Molecular dissection of hyperdiploid multiple myeloma by gene expression profiling. Cancer Research. 2007; 67: 2982-89.

17. Bolstad, BM, Irizarry RA, Astrand, M, et al. A comparison of normalization methods for high density oligonucleotide array data based on bias and variance. Bioinformatics. 2003; 19:185-193.

18. Tusher, VG, Tibshirani, R & Chu, G. Significance analysis of microarrays applied to the ionizing radiation response. PNAS USA. 2001; 98: 5116–5121.

19. Li C, and Wong, WH. Model-based analysis of oligonucleotide arrays: Expression index computation and outlier detection. PNAS USA. 2001; 98: 31-36.

20. Xiang Z, Kreisel F, Cain J, Colson A, Tomasson MH. Neoplasia driven by mutant c-KIT is mediated by intracellular, not plasma membrane, receptor signaling. Mol Cell Biol. 2007; 27: 267-282.

21. Ikuta K, Weissman IL (1992) Evidence that hematopoietic stem cells express mouse c-kit but do not depend on Steel factor for their generation. PNAS USA 89:1502–1506.

22. Morrison SJ, Hemmati HD, Wandycz AM, Weissman IL (1995) The purification and characterization of fetal liver hematopoietic stem cells. PNAS USA 92:10302–06.

23. Levine AJ, Momand J, and Finlay CA. The P53 tumour suppressor gene. Nature.1991; 351: 453-56.

24. Jacks T, Fazeli A, Schmitt EM, Bronson RT, Goodell MA, Weinberg RA. Effects of an Rb mutation in the mouse. Nature. 1992; 359:295-300.

25. Carrasco DR, Sukhdeo K, Protopopova M, et al. The differentiation and stress response factor XBP-1 drives multiple myeloma pathogenesis. Cancer Cell. 2007; 11: 349-60.

26. Casola S, Cattoretti G, Uytterspro N, et al. Tracking germinal center B cells expressing germ-line immunoglobulin -1 transcripts by conditional gene targeting. PNAS. 2006; 103: 7396-7401.

27. Laura Pasqualucci, Govind Bhagat, Mila Jankovic, et al. AID is required for germinal center–derived lymphomagenesis. Nature Genetics. 2008; 40, 108-112.

28. Wang JW, Gamsby JJ, Highfill SL, et al. Deregulated expression of LRBA facilitates cancer cell growth. Oncogene. 2004; 4089-97.

29. Shinall SM, Gonzalez-Fernandez M, Noelle RJ, Waldschmidt TJ. Identification of murine germinal center B cell subsets defined by the expression of surface isotypes and differentiation antigens. J Immunol. 2000;164:5729-5738

30. Muramatsu M, Kinoshita K, Fagarasan S, et al. Class switch recombination and hypermutation require activation-induced cytidine deaminase (AID), a potential RNA editing enzyme. Cell. 2000; 102: 553-63.

31. Vuong BQ, Lee M, Kabir, S et al. Specific recruitment of protein kinase A to the immunoglobulin locus regulates class-switch recombination. Nature Immunology. 2009; 10: 420-26.

Figure 1

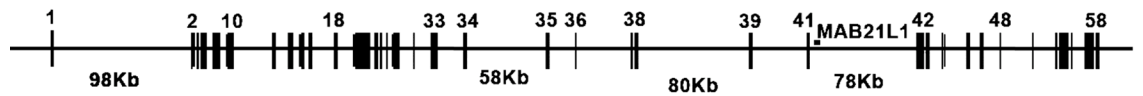**A**
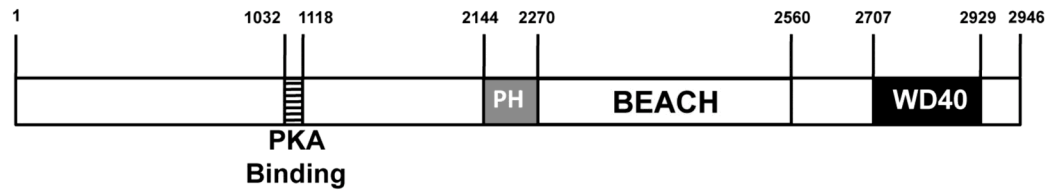
B

Figure 1. NBEA protein and exon structure
A. NBEA protein domains. Numbers correspond to amino acids. **B.** NBEA exon structure. Some exons are numbered (top) and sizes of the four largest introns are shown on bottom.

Table 1

Table 1. Genes with decreased expression in deletion 13 samples

Gene	Gene ID	Score(d)	Fold Change	q-value(%)
TUBGCP3	203690_at	-4.83	0.57	0
RNF6	203403_s_at	-5.68	0.60	0
GTF3A	215091_s_at	-5.77	0.62	0
UBL3	201534_s_at	-4.49	0.63	0
NBEA	221207_s_at	-3.44	0.67	0
ITM2B	217731_s_at	-4.24	0.70	0
RB1	211540_s_at	-2.92	0.74	1.3
HMGB1	216508_x_at	-4.52	0.74	0
MRP63	204387_x_at	-4.48	0.77	0
PSPC1	222612_at	-3.89	0.79	0
CRYL1	220753_s_at	-2.50	0.80	4.06
TPT1	214327_x_at	-3.84	0.85	0
ESD	228162_at	-2.83	0.89	1.72
MTMR6	228789_at	-2.63	0.90	2.73

Genes in bold were identified by Process Control and CBS analysis

Figure 2

A

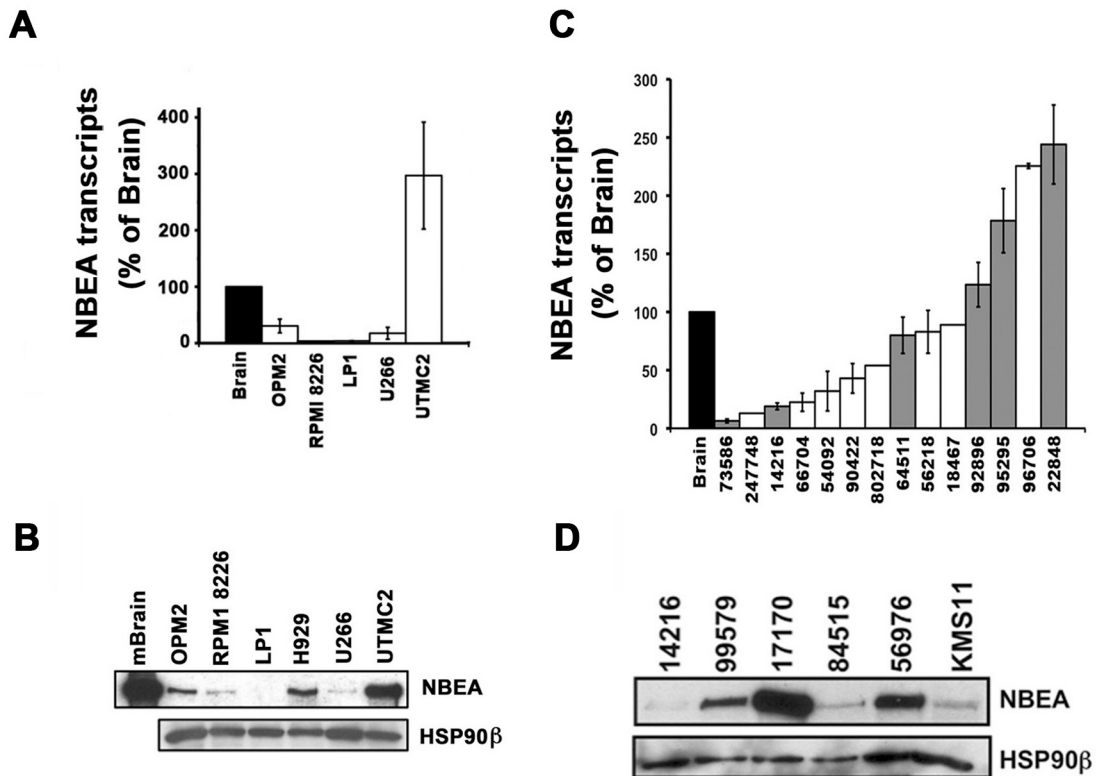**C**

B

D

Figure 2. NBEA is variably expressed in myeloma

A. Quantitative Q-RT-PCR analysis of *NBEA* on a panel of MM cell lines. *NBEA* levels were normalized to *GAPDH* and plotted as a percentage of human brain where *NBEA* expression is known to be high. **B.** Western Blot analysis of NBEA on a panel of human MM cell lines. Murine brain (mBrain) was used as positive control and HSP90b is shown as loading control. **C**. Quantitative RT-PCR analysis of *NBEA* on a panel CD138 purified primary patient samples including nine of the 20 patient samples included in aCGH analysis plus an additional five. White bars indicate patient samples with normal chromosome 13 status. Gray bars indicate patient samples with full or partial chromosome 13 deletions

(determined by cytogenetics, FISH or aCGH analysis). *NBEA* levels were normalized to *GAPDH* and plotted as a percentage of human brain as in A. **D.** Western Blot analysis on CD138 purified lysates from five primary patient samples. Due to limited sample quantity, these patients are different from the twenty included in aCGH analysis. HSP90b was used as loading control. KMS11 is MM cell line shown since repeat analysis showed NBEA protein levels were low.
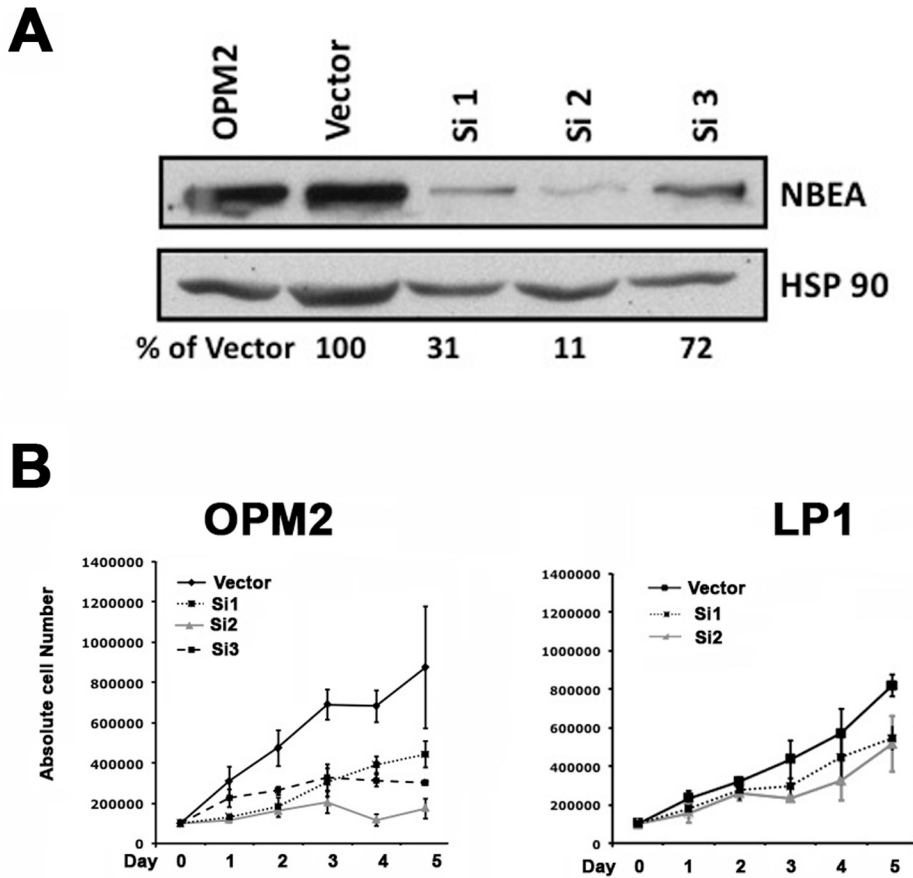
Figure 3

Figure 3. NBEA is required for growth of OPM2 cells

A. Western Blot analysis of OPM2 cells infected with lentivirus expressing nothing, or one of three siRNAs that target NBEA. Uninfected OPM2 cells are shown as a control. HSP 90 was used as loading control and for controls in densitometry results, shown below blot. B. Growth curves of OPM2 or LP1 cells infected with vector alone or siRNA targeting NBEA. Cells were selected in puromycin for one week and then 100,000 cells from each group were plated in triplicate and live cells counted using trypan cell exclusion. Error bars are standard deviation of a representative triplicate experiment.

Figure 4

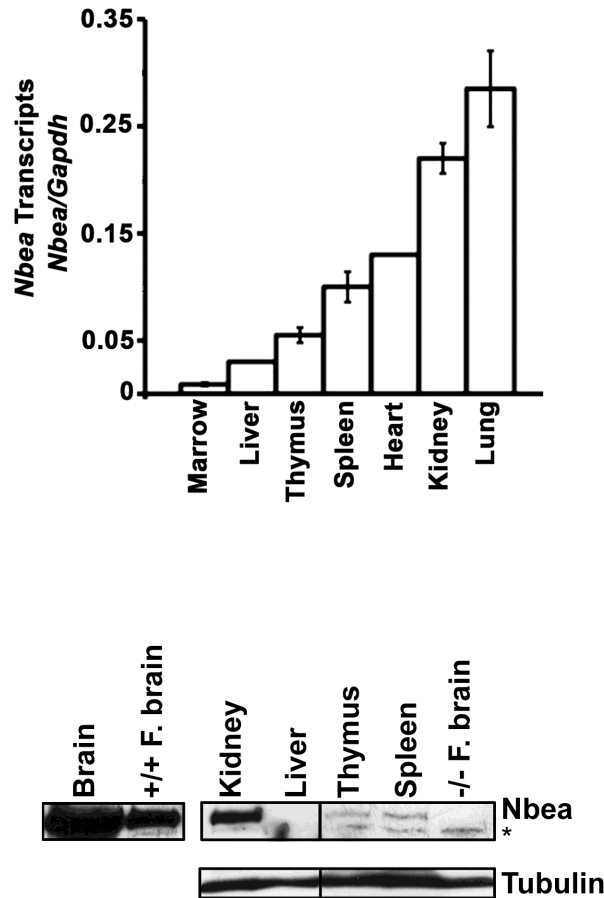**Figure 4. Nbea is expressed in thymus and spleen**

A. Q-RT-PCR analysis of Nbea was performed on a panel of murine tissues. Data are plotted as the ratio of *Nbea/Gapdh* signal. Reactions were performed in triplicate and experiment was performed in duplicate. Error bars are standard

deviation of two separate experiments. **B**. Western blot analysis of Nbea in panel of whole tissue lysates.

Figure 5
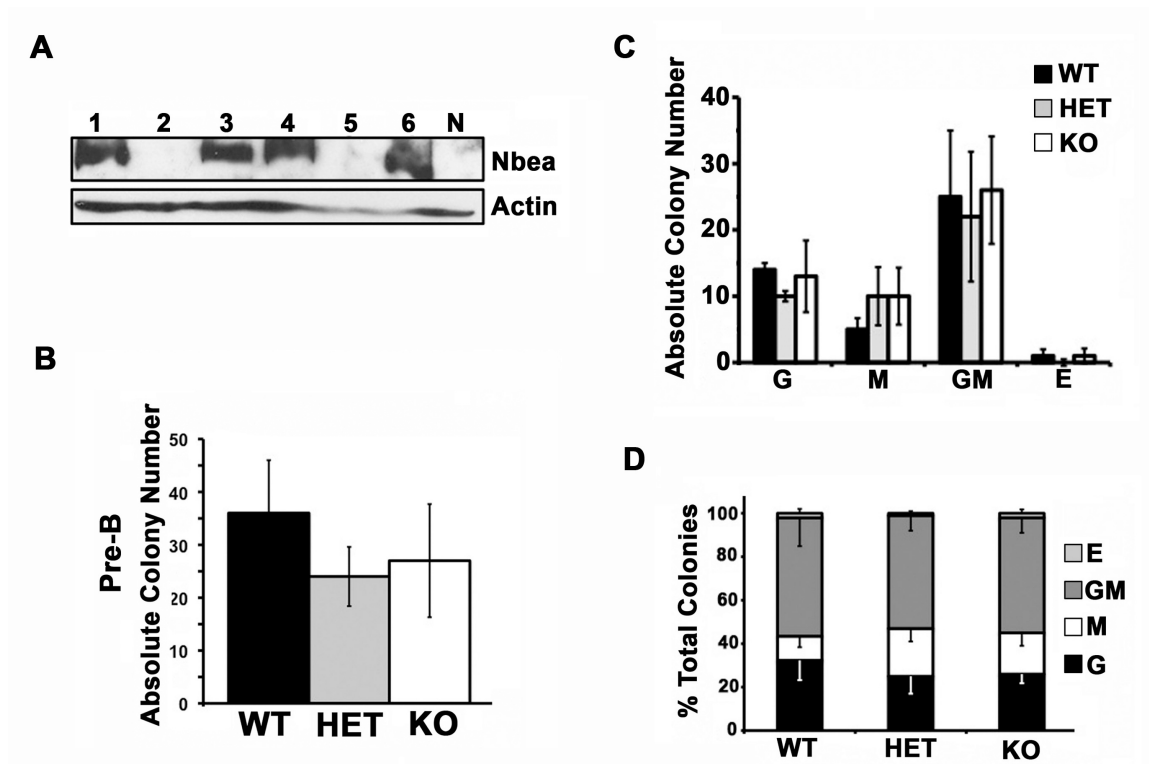
Figure 5. *Nbea* is not required for myeloid or Pre-B cell colony formation

A. Western Blot analysis of lysates isolated from fetal brains. Brains from each fetus are numbered. N; negative control lysates from a separate fetal liver brain known to be null for Nbea. **B**. Cells were plated into M3630 that supports pre B cells. WT, HET or KO fetal liver cells were plated in methocellulose in triplicate. WT (n=1), HET (n=2), KO (n=3). Data from same genotypes were pooled. Error bars are standard deviation of averages of each well scored. **C**. WT, HET or KO fetal liver cells were plated in methocellulose containing myeloid (M3434) cytokines. Absolute colony numbers of G, M, MG or E colonies are plotted. WT (n=1), HET (n=2), KO (n=3). Cells were plated in triplicate. Data from same

genotypes were pooled. Error bars are standard deviation of averages of each well scored. **D**. Percentage of total colonies counted in C**.**

Figure 6

A
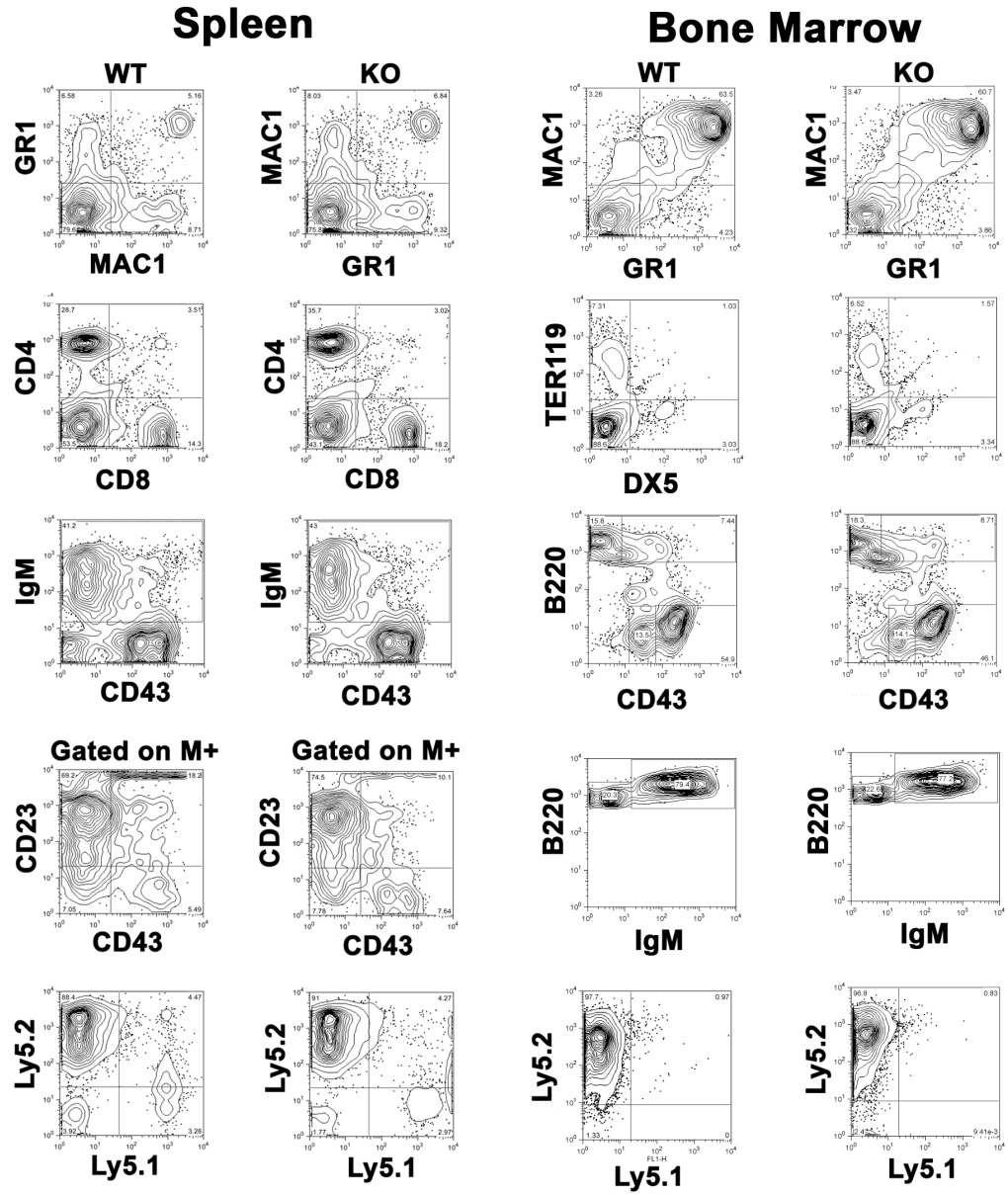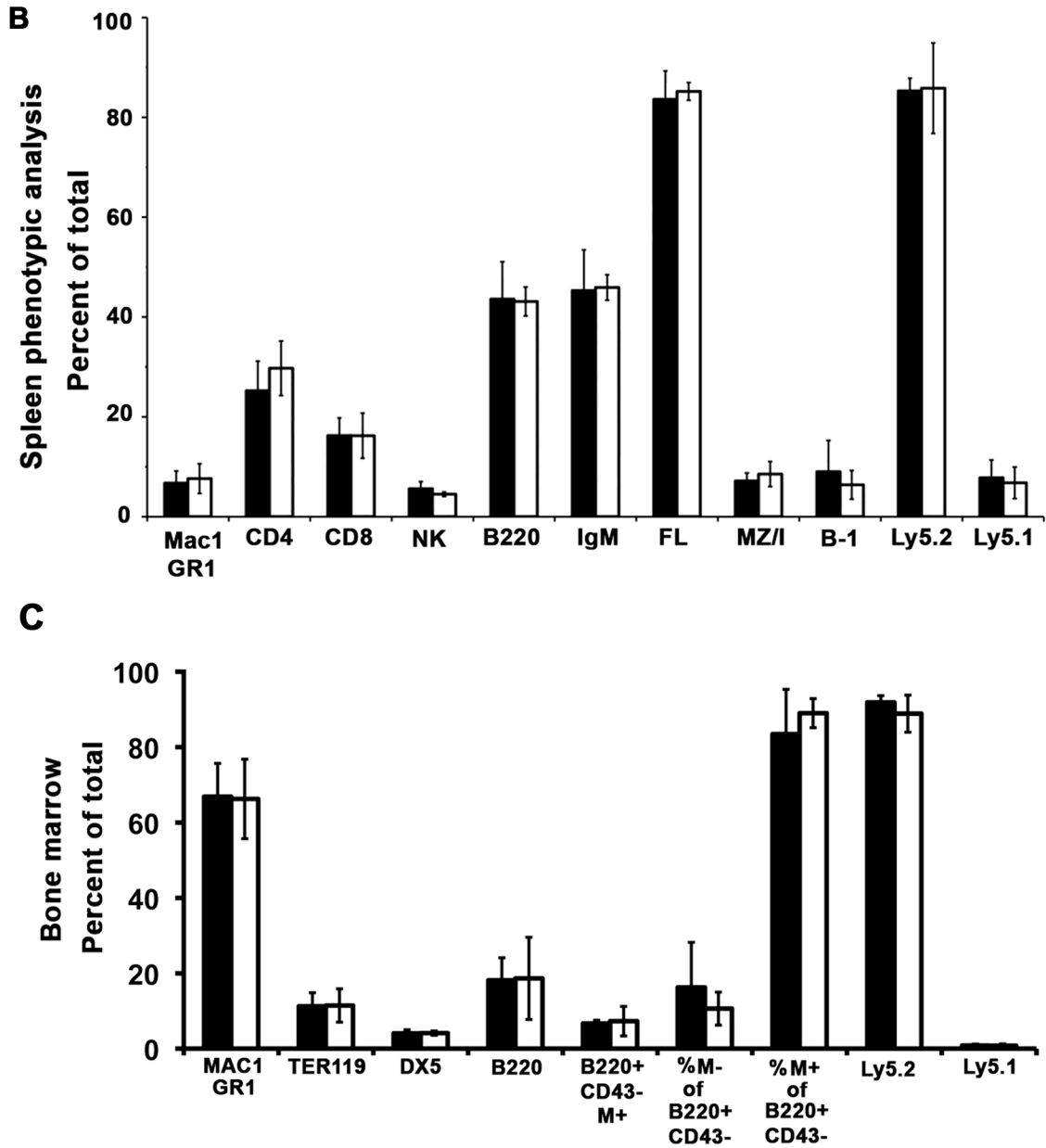
Spleen

Bone Marrow

Figure 6. *Nbea* **is dispensable for broad reconstitution of major hematopoietic lineages following transplantation**

A. FACS analysis of spleen (left) and bone marrow (right) of recipient mice transplanted with either Nbea$^{+/+}$ or *Nbea*$^{-/-}$ fetal liver donor cells. **B and C.** Summary of Spleen FACS analysis shown in A. of wild type (black bars) and knockout (white bars) recipient mice. Data are presented as mean of four mice

per group. Error bars are standard deviation. MZ/I: Presented as percentage of IgM+ cells that were CD23-CD43-. Follicular: Presented as percentage of IgM+ cells that were CD23+. B-1 cells: Presented as percentage of IgM+ cells that were CD23-, CD43+. MZ: marginal zone; I: immature; FL: Follicular, NK: natural killer.

Chapter 5

Summary and Future Directions

5.1 Summary

Numeric or structural chromosomal abnormalities are detected in nearly all patients with plasma cell dyscrasias, including primary amyloidosis, monoclonal gammopathy of undetermined significance (MGUS) and multiple myeloma (MM) [1]. Chromosome 13 deletions, most frequently monosomy 13, are detected in 10-20% of MM cases by routine cytogenetics or metaphase fluorescent in situ hybridization (FISH) and are a significant predictor of shortened survival [2-4]. Previous efforts to map somatically acquired chromosome 13 localized DNA copy number losses have been hampered by their relatively low-resolution approaches [5-14]. The goal of this thesis was to identify chromosome 13 genes affected by copy number loss in primary patient samples isolated from patients with plasma cell dyscrasias. Our analysis (using unprecedented high-resolution techniques and appropriate controls), identified two distinct minimally deleted regions on chromosome 13, each defined by deletions affecting one gene: *NBEA* at 13q13 and *RB1* at 13q14.2.

5.2 Hypothesis 1: *Rb1* haploinsufficiency contributes to myelomagenesis

Our aCGH, cytogenetic, and FISH analysis of chromosome 13 in primary patient samples revealed that one copy of *RB1* is a target of deletions in MM, yet in most patient samples (7/8 in our set) the other copy is retained in MGUS and MM (**Chapter 2**). No exonic *RB1* mutations were detected in our sequence analysis performed on DNA isolated from CD138 purified plasma cells from 41 MM or

MGUS primary patient samples, suggesting *RB1* alleles in MGUS and myeloma are wild-type (**Chapter 3**). We, and others [4,12,13] showed transcripts expressed from retained *RB1* alleles are expressed at reduced levels in patient samples harboring monosomy 13 *versus* samples with two *RB1* alleles (**Chapter 3**). This suggests in myeloma and MGUS cells, retained *RB1* alleles express transcripts that produce wild type RB1 protein. To address the hypothesis RB1 protein would be inactivated by hyper-phosphorylation, we performed immunohistochemistry (IHC) analysis on paraffin-embedded bone marrow biopsies isolated from 25 patients with MGUS (1), SMM (1) MM (22) or PCL (1). We found hyper-phosphorylation of RB1 protein was a rare event in all samples tested. Together, these data suggest unmutated, hypo-phosphorylated RB1 protein is expressed at reduced levels in MGUS and MM patient samples harboring monosomy 13. Since deletions affecting *RB1* are detected early in myelomagenesis, when rapid cell cycle does not occur, this suggests the contribution of reduced RB1 protein dose in myeloma is not via conventional uncontrolled proliferation found in other tumor types [15]. We hypothesize haploinsuffiency of *RB1* contributes to myelomagenesis.

Analysis of 8-9 week old $Rb1^{+/+}$ versus $Rb1^{+/-}$ mice (backcrossed to generation 10 C57BL/6) revealed no significant differences in steady state hematopoeisis or plasma cell induction after stimulation with sheep red blood cells (SRBCs; **Chapter 3**). However, in *Rb1* null retina cells, the *Rb1* family member, p107 compensates for Rb1 [16]. In hematopoeisis, p107 sometimes, [17] but not

always, [18] compensates for loss of *Rb1*. To avoid the issue of p107 compensation completely, *Rb1$^{+/-}$* mice are currently being bred to *p107$^{-/-}$* mice to generate *Rb1$^{+/+}$p107$^{-/-}$* and *Rb1$^{+/-}$p107$^{-/-}$* mice. To determine whether haploinsufficiency of *Rb1* is sufficient to alter the plasma cell compartment, serum will be analyzed every three months for detection of monoclonal protein by performing serum electrophoresis and immunofixation analysis. Total levels of serum protein will be assessed using serum protein electrophoresis (SPEP) analysis. We will assess for detection of increased plasma cell percentages in bone marrow using flow cytometry (B220/CD138 and PNA/B220). To stimulate formation of germinal centers and plasma cell maturation, these mice will be challenged with antigen (sheep red blood cells [19] or nitrophenyl-conjugated chicken gammaglobulin (NP-CGG;) [20] and the plasma cell compartment will be assessed as just described.

Preliminary data suggests Rb1$^{+/-}$p107$^{-/-}$ are born at reduced frequencies than expected from Mendelian ratios (**Table 1**). Specifically, when *Rb1$^{+/+}$p107$^{-/-}$* were mated to *Rb1$^{+/-}$p107$^{+/-}$* mice, zero *Rb1$^{+/-}$p107$^{-/-}$* mice were born. The expected frequency is 25% (of 27 pups total, expected 6 *Rb1$^{+/-}$p107$^{-/-}$* mice). When Rb1$^{+/-}$p107$^{+/-}$ mice were mated to Rb1$^{+/-}$p107$^{+/-}$, the expected frequency of Rb1$^{+/-}$p107$^{-/-}$ pups is 12.5%, but only 2 mice (of 83 pups total, 2.4%) were born. Also, *Rb1$^{+/-}$* mice succumb to pituitary tumors at 8 months [21]. We are therefore generating mice with conditional deletion of *Rb1* in plasma cells by mating *Rb1$^{flox/flox}$* [22] mice (provided by Tyler Jacks) to mice that express Cre recombinase only when

transcription of Cγ1 (IgG1) heavy chain occurs in germinal centers upon stimulation with T cell dependent antigens [23] (provided by Klaus Rajewsky). These mice will have *Rb1* deletions in most germinal center B cells. We will mate these mice to *p107$^{-/-}$* mice to generate C*γ1*Cre*Rb1$^{+/+}$p107$^{-/-}$ and* C*γ1*CreRb1$^{Flox/+}$*p107$^{-/-}$* mice. These mice will be assessed as above, for alterations in the plasma cell compartments. If haploinsufficiency of *Rb1* contributes to myelomagenesis, then we predict plasma cell development will be affected in the *Cγ1CreRb1$^{Flox/+}$p107$^{-/-}$* mice but not in the Cγ1Cre*Rb1$^{+/+}$p107$^{-/-}$* mice.

If true, we may anticipate that patients with hereditary retinoblastoma that harbor germline loss of one copy of *RB1* allele have an increased propensity for development of MGUS. Currently, there are no reports of increased incidence of MM in retinoblastoma patients. Since MGUS is asymptomatic, however, it remains a formal possibility that retinoblastoma patients have increased propensity for development of MGUS that has yet to be described. To address this hypothesis, serum samples of surviving retinoblastoma patients will be subject to serum SPEP and immunofixation analysis to examine for elevated and monoclonal serum antibodies, respectively. If true, this supports the hypothesis *RB1* haploinsufficiency contributes to alteration of PC's in humans. If not, it suggests in humans, development of MGUS may require additional mutations.

5.3 Hypothesis 2: *NBEA* is targeted by mutations in MM

Array CGH analysis revealed NBEA was a deletion target in MGUS and MM patient samples (**Chapter 2**). Our large-scale microarray expression analysis using published databases to examine *NBEA* transcripts in 262 patient samples revealed *NBEA* levels were decreased in primary patient samples harboring monosomy chromosome 13 *versus* patient samples that retained both alleles, (**Chapter 4**) suggesting NBEA could function as a tumor suppressor. However, further analysis using Q-RT-PCR and Western blotting, revealed a subset of primary patient samples harbored high levels of NBEA. Mutations in the p53 tumor suppressor gene lead to elevated P53 levels, and expression of functionally inactive protein [24]. To determine if the *NBEA* gene is a target of mutations in myeloma, complete sequencing of *NBEA* on DNA isolated from purified CD138 patient plasma cells will be performed at the Washington University Genome Sequencing Center.

5.4 Hypothesis 3: Expression of NBEA contributes to myelomagenesis

A subset of MM patient samples harbored robust expression of NBEA and SiRNA-mediated knockdown of NBEA in OPM2 cells led to growth reduction (**Chapter 4**), suggesting expressed NBEA provides a survival signal. We have undertaken the task of subcloning the entire *NBEA* cDNA for use in overexpression studies. We initially planned on using a retroviral-mediated high-level expression and bone marrow transplantation system to express NBEA in

murine hematopoietic cells, but the large size of *NBEA* is too big for efficient packaging into retrovirus.

A DNA construct is currently being generated that is predicted to direct expression of NBEA to B cells using the Eμ regulatory sequences in a transgenic mouse model. To determine whether expression of NBEA alters plasma cell development, serum will be analyzed every three months for detection of monoclonal protein by performing serum electrophoresis and immunofixation analysis. Total levels of serum protein will be assessed using serum protein electrophoresis (SPEP) analysis. We will assess for detection of increased plasma cell numbers in bone marrow using flow cytometry (B220/CD138 and PNA/B220). To stimulate formation of germinal centers and assess for altered plasma cell function, these mice will be challenged with antigen (sheep red blood cells [19] or or nitrophenyl-conjugated chicken gammaglobulin (NP-CGG;) [20] and the plasma cell compartment will be assessed as just described.

The original NBEA cDNA that we amplified from a primary patient sample revealed an unexpected insertion of intron 1 (296 base pairs). We are currently PCR amplifying NBEA 5' regions from first strand cDNA generated from RNA isolated from a normal human brain sample (kindly provided by William Schmidt, WUSM). PCR products will be subcloned and DNA sequenced to determine if transcription of intron 1 is tumor-associated.

Our aCGH analysis revealed two of the patient samples in our study harbored interstitial deletions affecting part of the *NBEA* locus (**Chapter 2**). In sample 95295, copy number decrease affected exons 3-19 and in sample 64511, exons 1-9 were affected. First strand cDNA will be generated from RNA templates from each of these patient samples and amplified products will be analyzed by sequence analysis. If shortened transcripts are detected, they will be subcloned into an expression vector and expression of altered protein will be determined. Altered NBEA could behave as a 'dominant negative' leading to an effective NBEA null state, or alternatively, confer a gain of function. If truncated proteins are detected, we will generate mice expressing these tumor-associated forms of *NBEA* in B cells under the Eμ regulatory sequences. They will be analyzed for MGUS or myeloma development as described above. If however, truncated NBEA is not expressed in these samples, it remains a future interest to determine why elevated levels of NBEA transcripts are detected in these patient samples from the other NBEA allele.

5.5 Hypothesis 4: High expression of NBEA cooperates with *Rb1* haploinsufficiency in myeloma development

A central finding of our aCGH analysis was that all patient samples with interstitial deletions affecting *RB1* also harbored interstitial deletions affecting *NBEA*, and that a subset of patient samples even with monosomy 13, harbored elevated NBEA expression (**Chapter 2**), suggesting alteration of these two genes

cooperate in myelomagenesis. To determine if NBEA expression cooperates with *Rb1* haploinsufficiency in plasma cells, we will mate our Cγ1Cre*Rb1*^{Flox/Flox}p107^{-/-} mice to Eμ*NBEA* mice that express *NBEA* in the B cell compartment to generate Eμ*NBEA*Cγ1Cre*Rb1*^{Flox/+}p107^{-/-} and Eμ*NBEA*Cγ1Cre*Rb1*^{+/+}p107^{-/-} mice. These mice will be assessed for abnormalities in plasma cells as described above.

5.6 Determine spleen cell subtype that expresses *Nbea*

We showed *Nbea* was dispensable for engraftment and development of adult steady state hematopoeisis using a fetal liver transplant system (**Chapter 4).** This was somewhat surprising since we found Nbea was expressed in spleen and thymus (**Chapter 4**). A report modeling lymphoid tumors with plasmablast/post germinal phenotypes revealed Nbea was upregulated over six fold when compared to a related model with a more immature/pre germinal center phenotype, suggesting Nbea could be developmentally regulated [25]. Combined with its relatively low level in spleen, its dysregulation in plasma cell dyscrasias, and expression in another secretory cell type (neurons), we posit Nbea could be expressed in normal plasma cells. To determine if Nbea is expressed in antigen stimulated plasma cells, mice will be challenged with sheep red blood cells and plasma cells will be sorted using cell surface markers PNA/B220 one week post injection when formation of spleen GCs are maximal [19]. Q-RT-PCR will be used to quantitively assess Nbea expression in these cells.

To determine the spleen localization of Nbea we will perform IHC staining for Nbea in murine spleen sections. We are currently testing a rabbit polyclonal Nbea antibody we have had made (Dan Crimmins, Cortex) for this purpose. Additionally, experiments are underway to sort spleen cell subsets based on cell surface expression of cell type specific markers (GR-1, B220, CD4, CD8, DX5) followed by Q-RT-PCR to determine in what spleen cell type *Nbea* transcripts are expressed in basal conditions.

5.7 Hypothesis 5: *Nbea* is required for plasma cell functions

If NBEA functions in vesicle traffic or PKA mediated regulation of AID in class switch recombination (CSR) or secretion, *Nbea* null plasma cells may have deficiencies in antibody formation and/or secretion. To assess this, we will use our fetal liver transplantation system to generate mice with null or wild type *Nbea* hematopoietic systems (**Chapter 4).** *In vivo* analysis of basal CSR will be assessed by performing ELISA assays on serum and levels of IgM, IgG1, IgG2a, IgG2B, IgG3 and IgA will be determined [26]. If Nbea null chimeras are deficient in CSR, it predicts detection of IgM (which does not undergo CSR), but not the other isotypes. If there are secretion defects, detection of all antibody isotypes is predicted to be low/undetectable.

To assess CSR in an antigen stimulated system, mice will be injected with SRBC and serum will be subject to ELISA for IgM and IgG1. *In vitro* assessment of class switch recombination will be performed by isolating splenocytes (CD43

depletion) from engrafted mice (*Nbea*$^{+/+}$ and *Nbea*$^{-/-}$) by stimulating purified B cell splenocytes with LPS, LPS and Il-4, pr LPS and TGFβ and then quantitating antibody isotypes in culture supernatents by ELISA as described above [26-28].

5.8 Hypothesis for cellular function of NBEA in PC Diseases

Our data implicate a role for NBEA in plasma cell dyscrasias, but its role in normal plasma cell and/pr malignant plasma cell development remains unclear. Below are three hypotheses for cellular functions NBEA could play a role in altering that may (or may not) contribute to diseased plasma cells.

5.8A NBEA may facilitate PKA-mediated alteration of class switch recombination (CSR)

NBEA domains provide clues to potential mechanistic roles for NBEA in plasma cell dyscrasias. NBEA transcript encodes a PKA binding domain, and murine Nbea binds to two PKA regulatory subunits (RIIα (Kd: 10nM) and RIIβ (Kd: 30nM); [28]. Since the core region responsible for PKA binding is absolutely conserved between mouse and human, human NBEA likely also binds these subunits. Recent data has illustrated phosphorylation of Serine 38 of the activation induced cytidine deaminase (AID) protein is mediated by the catalytic subunit of PKA (PKAcα) [27]. AID is the enzyme responsible for generating double stranded breaks required for class switch recombination (CSR) and somatic hypermutation (SHM) processes in antibody maturation. PKA enzymes are regulated by localization via binding to anchoring proteins (AKAPs) that

ensure PKA only phosphorylates appropriate targets at specific cellular locations. The AKAP that targets PKA to sites of CSR has not been identified.

In the context of PC dyscrasias, expressed NBEA may inappropriately target PKA to sites of CSR, leading to increased AID phosphorylation and activation, resulting in extra formation of double strand breaks that would otherwise not occur. This is consistent with the model that it is during recombination events in antibody production where aneuploidy in MM occurs. NBEA could affect PKA localization via a number of mechanisms, depending on whether it is wild type or mutated in myeloma. NBEA in rat neurons is localized near the nucleus and within the golgi network [28], however in MGUS and MM cells, NBEA may be mislocalized to the nucleus, resulting in extra pools of PKA localized to sites of AID activation. Alternatively, if NBEA normally binds PKA in the cytoplasm/golgi, where pools of PKA are found, mutations in NBEA may result in decreased binding, resulting in increased amounts of PKA localizing to sites of CSR. Localization studies are required to determine where NBEA and PKA are localized in normal, MGUS and MM plasma cells.

AID is required for mature plasma cell cancers in a model of Myc/BCL6 over-expression in mice [25], and Nbea expression was increased in tumor cells isolated from this model with plasma cell characteristics compared to tumors of an earlier B stage [25]. Generating mice with plasma cell specific deletions of *Nbea* (Cγ1Cre *Nbea*[Flox/Flox]) could be used to determine if it is required in this

model. If Nbea promotes formation of monoclonal antibody or aneuploidy due to double stranded breaks via regulation of PKA mediated CSR, it predicts monoclonal antibody production and disease phenotypes in this mouse model would revert to a functionally less mature stage, just like they do when the MYC/BCL6 mice are mated to Aid (*Aicda*) null mice [25].

5.8B NBEA alters vesicle formation, function, or trafficking

Because other proteins with BEACH/WD40 domains are implicated in vesicle formation or trafficking [28-30], and because subcellular localization studies of Nbea that revealed it localizes in perinuclear clusters near the trans side of golgi complexes and small tubulovesicular structures [28], perhaps NBEA (mutated or normal) in MM alters normal vesicle function, formation, or trafficking. Plasma cells (normal and diseased) generate, produce, and secrete large amounts of antibody via the secretory pathway. Nbea may enhance vesicle formation leading to enhanced secretion of immunoglobulin molecules. Alternatively, altered Nbea may result in inappropriate vesicle trafficking such that signaling molecules are misdirected in the cell i.e. such that proper lysosomal degradation of vesicles and/or cargo does not occur, resulting in increased signaling. Electron microscopy of vesicle structure and Nbea localization in MGUS and MM plasma cells can be used to address the hypothesis that Nbea alters vesicle traffic.

5.8C NBEA may provide a survival signal mediated by NFκB

NBEA may provide a survival signal in a general context by altering the NFκB pathway via its PKA domain. This is consistent with chromosome 13 deletions being detected early in MM stages including MGUS, and that during much of MM, plasma cells cycle slow, but avoid apoptosis. As stated above, human NBEA likely binds to PKA regulatory subunits. The catalytic subunits of PKA can phosphorylate the p65 member of the canonical NFκB family [32]. NFκB activating mutations affecting the non-canonical pathway are detected in MM samples [33], leading to constitutive activation. Perhaps NBEA activates, via PKA, the canonical NFκB pathway, in a mutually exclusive fashion to cells with non-canonical NFκB mutations. Although there is evidence for two separate "pools" of PKA catalytic subunits, [31] (one pool bound to IκB subunits and the other to PKA regulatory subunits), binding of PKA to NBEA (or not, if it is mutated) may alters this pool, such that more PKA catalytic subunits are free to phosphorylate downstream targets. Dysregulation of NBEA may be necessary but not sufficient to transform a normal PC to MGUS or MM via its ability to confer survival signals.

Although much needs to be done, we have provided a useful framework for pursuing the role of *RB1* and *NBEA* may play in normal and altered plasma cell development and have developed important reagents that will facilitate future experiments.

5.10 References

1. Zandecki M. Multiple Myeloma: Almost all patients are cytogenetically abnormal. British Journal of Hematology. 1996; 94: 217-227.

2. Chiecchio L, Protheror RKM, Ibrahim AH. et al. Deletion of chromosome 13 detected by conventional cytogenetics is a critical prognostic factor in myeloma. Leukemia. 2006; 1-8.

3. Shaughnessy J, Jr, Tian E, Sawyer J, et al. Prognostic impact of cytogenetic and interphase fluorescence in situ hybridization-defined chromosome 13 deletion in multiple myeloma: early results of total therapy II. British Journal of Haematology. 2003;120: 44-52.

4. Shaughnessy J, Jacobson J, and McCoy J. Continuous absence of metaphase-defined cytogenetic abnormalities, especially of chromosome 13 and hypodiploidy, ensures long-term survival in multiple myeloma treated with Total Therapy I: interpretation in the context of global gene expression. Blood. 2003; 101: 3849-56.

5. Aalto Y, Nordling S, Kivioja AH, Karaharju et al. Among numerous DNA copy number changes, losses of chromosome 13 are highly recurrent in plasmacytoma. Genes, Chromosomes and Cancer. 1999; 25:104-107.

6. Avet-Loiseau H, Andree-Ashley LE, Moore D, 2nd, et al. Molecular cytogenetic abnormalitiesin multiple myeloma and plasma cell leukemia measured using comparative genomic hybridization. Genes, Chromosomes and Cancer. 1997;19:124-133.

7. Nomdedeu JF, Lasa A, Ubeda J, et al. Interstitial deletions at the long arm of chromosome 13 may be as common as monosomies in multiple myeloma. A genotypic study. Haematologica. 2002; 87:828-835.

8. Fonseca R, Oken MM, Harrington D, et al. Deletions of chromosome 13 in multiple myeloma identified by interphase FISH usually denote large deletions of the q arm or monosomy. Leukemia. 2001; 15: 981-986.

9. Konigsberg R, Ackermann J, Kaufmann H, et al. Deletions of chromosome 13q in monoclonal gammopathy of undetermined significance. Leukemia. 2000;14:1975-79.

10. Shaughnessy J, Tian E, Sawyer J, et al. High incidence of chromosome 13 deletion inmultiple myeloma detected by multiprobe interphase FISH. Blood. 2000; 96:1505-11.

11. Elnenaei MO., Hamoudi RA., Swansbury J., et al. Delineation of the minimal region of loss at 13q14 in multiple myeloma. Genes, Chromosomes and Cancer. 2003: 36:99-106.

12. Agnelli L, Bicciato, S, Fabris S, et al. Integrative genomic analysis reveals distinct transcriptional and genetic features associated with chromosome 13 deletion in multiple myeloma. Haematologica. 2007; 92: 56-65.

13. Carrasco DR, Tonon G, Huang Y, et al. High-resolution genomic profiles define distinct clinico-pathogenetic subgroups of multiple myeloma patients. Cancer Cell. 2006; 9: 313-25.

14. Walker BA, Leone PE, Jenner MW, et al. Integration of global SNP-based mapping and expression arrays reveals key regions, mechanisms, and genes important in the pathogenesis of multiple myeloma Blood. 2006; 108: 1733-43.

15. Sherr CJ and McCormick F The RB and P53 pathways in cancer. Cancer Cell. 2002; 2: 103-112.

16. Donovan SL, Schweers B, Martins R, et al. Compensation by tumor suppressor genes during retinal development in mice and humans. BMC Biology. 2006; 4: 14.

17 Viatour, P, Somervaille TC, Venkatasubrahmanyan S et al. Hematopoeitic stem cell quiescence is maintained by compound contributions of the retinoblastoma gene family. Cell Stem Cell. 2008; 3: 416-428.

18 Walkley CR, Shea JM, Sims NA et al. Rb Regulates Interactions between Hematopoeitic Stem Cells and their Bone Marrow Microenvironment. Cell. 2007; 129: 1081-95.

19. Shinall SM, Gonzalez-Fernandez M, Noelle RJ, Waldschmidt TJ. Identification of murine germinal center B cell subsets defined by the expression of surface isotypes and differentiation antigens. J Immunol. 2000;164:5729-5738.

20. Kumazaki K, Tirosh B, Maehr R, et al. AID-/-mus-/- mice are gammaglobulinemic and fail to maintain B220-CD138+ plasma cells. Journal of Immunology. 2007; 178: 2192-303.

21. Jacks T, Fazeli A, Schmitt EM, Bronson RT, Goodell MA, Weinberg RA. Effects of an Rb mutation in the mouse. Nature. 1992;359:295-300.

22. Sage, J., A. L. Miller, P. A. Pérez-Mancera, J. M. Wysocki, and T. Jacks. 2003. Acute mutation of retinoblastoma gene function is sufficient for cell cycle re-entry. Nature 424:223-228.

23. Casola S, Cattoretti G, Uytterspro N, et al. Tracking germinal center B cells expressing germ-line immunoglobulin -1 transcripts by conditional gene targeting. PNAS. 2006; 103: 7396-7401.

24. Levine AJ, Momand J, and Finlay CA. The P53 tumour suppressor gene. Nature.1991; 351: 453-56.

25. Laura Pasqualucci, Govind Bhagat, Mila Jankovic, et al. AID is required for germinal center–derived lymphomagenesis. Nature Genetics. 2008; 40, 108-112.

26. Muramatsu M, Kinoshita K, Fagarasan S, et al. Class switch recombination and hypermutation require activation-induced cytidine deaminase (AID), a potential RNA editing enzyme. Cell. 2000; 102: 553-63.

27. Vuong BQ, Lee M, Kabir, S et al. Specific recruitment of protein kinase A to the immunoglobulin locus regulates class-switch recombination. Nature Immunology. 2009; 10: 420-26.

28. Wang X, Herberg FW, Laue MM et al. Neurobeachin: a protein kinase A anchoring beige/Chediak-higashi protein homolog implicated in neuronal membrane traffic. Journal of Neuroscience. 2000; 20: 8551-65.

29. Wang JW, Howson J, Haller E et al. Identification of a novel lipopolysaccharide-inducable gene with key features of both A kinase anchor proteins and chs2/beige proteins. Journal of Immunology. 2001; 166:4586-95.

30. Mohlig H, Mathieu S, Thon L et al. The WD repeat protein FAN regulates lysosome size independent from abnormal downregulation/membrane recruitment of protein kinase C. Exp. Cell Research. 2007; 313: 2703-18.

31. Perou CM, Moore KJ, Nagle DL et al. Identification of the murine *beige* gene by YAC complementation and positional cloning. Nature Genetics. 1996; 13: 303-08.

32. Zhong H. Yang HS, Erdjument-Bromage, et al. The transcriptional activity of NF-κB is regulated by the IκB-associated PKAc subunit through a cyclic AMP-independent mechanism. Cell. 1997; 89: 413-24.

5.11 Table

Table 1 Predicted and Actual Genotypes in Rb1 X p107 Breeding

Parents: Rb+/-107+/- X Rb+/+107-/-
Total number of pups: 27

	RB+/+p107+/-	RB1+/+p107-/-	Rb1+/-/p107+/-	Rb1+/-p107-/-
Expected %	25%	25%	25%	25%
Actual % (#pups)	44% (12)	15% (4)	41% (11)	0% (0)

Parents: Rb1+/-p107+/- X Rb1+/-p107+/-
Total number of pups: 83

	Rb1+/+107+/+	RB1+/+p107+/-	Rb1+/+p107-/-	Rb1+/-p107+/+	Rb1+/-p107+/-	Rb1+/-107-/-
Expected %	6%	13%	6%	6%	25%	13%
Actual % (#pups)	13% (11)	28% (23)	17% (14)	11% (9)	29% (24)	2% (2)

Rb1-/- do not live, so not included in chart